# E Scattering of Sound

E.1 Plane Wave Scattering at Cylinders

▶ *See also:* Mechel, Vol. I, Ch. 6 (1989)

See ⊙ *Sect. E.2* for a survey of formulas for cylinders and spheres.

The cylinder with diameter 2a is either bulk reacting, i.e. it consists of a homogeneous material with characteristic propagation constant Γ_a and wave impedance Z_a, or it consists of a similar material with same characteristic values, but locally reacting either in the axial direction or locally reacting in all directions. Local reaction is obtained either by a high flow resistivity Ξ of the porous material or by thin partitions at mutual distances smaller than about $\lambda_0/4$. Sound incidence of the plane wave with unit amplitude is in the x,z plane.

bulk reacting   axially local   omnidirectional local
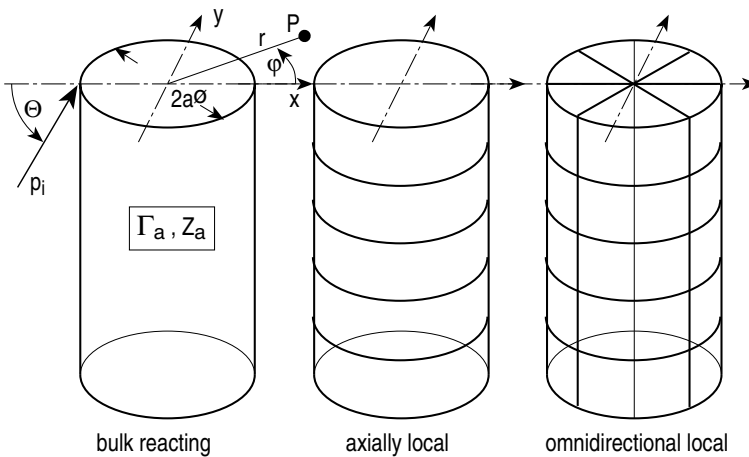
The field formulation will be given below for the bulk reacting cylinder; the fields for the other cylinders follow from that by simplifications.

Notations: • $\Gamma_{an} = \Gamma_a/k_0$; $Z_{an} = Z_a/Z_0$ normalised characteristic values;
  • p_i = incident plane wave;
  • p_s = scattered wave;
  • $p = p_i + p_s$ = total exterior field;
  • p_a = interior field in the absorbing cylinder.

Expansion of the incident plane wave in Bessel functions:

$$p_i(r, \varphi, z) = e^{-j\,k_0 z \cdot \sin\Theta} \sum_{m \geq 0} \delta_m(-j)^m$$
$$\cdot \cos(m\varphi) \cdot J_m(k_0 r \cdot \cos\Theta); \quad \delta_m = \begin{cases} 1\,; \ m = 0 \\ 2\,; \ m > 0 \end{cases} \tag{1}$$

Formulation of the scattered field:

$$p_s(r, \varphi, z) = e^{-j\,k_0 z \cdot \sin\Theta} \sum_{m \geq 0} D_m \cdot \delta_m(-j)^m \cdot \cos(m\varphi) \cdot H_m^{(2)}(k_0 r \cdot \cos\Theta). \tag{2}$$

Formulation of the interior field:

$$p_a(r, \varphi, z) = e^{-j\,k_0 z \cdot \sin\Theta} \sum_{m \geq 0} E_m \cdot \delta_m \cdot \cos(m\varphi)$$
$$\cdot I_m(\Gamma_a r \cdot \cos\Theta_1); \quad I_m(z) = (-j)^m J_m(jz), \tag{3}$$

with Bessel functions $J_m(z)$, Hankel functions of the second kind $H_m^{(2)}(z)$, modified Bessel functions $I_m(z)$.

From the boundary conditions of matching pressure and radial particle velocity:

$$j\,k_0 \cdot \sin\Theta = \Gamma_a \cdot \sin\Theta_1; \quad \Gamma_{an} \cdot \cos\Theta_1 = \sqrt{1 + \Gamma_{an}^2 - \cos^2\Theta} \tag{4}$$

(Θ_1 is the refracted angle), and

$$D_m = -\frac{J_m(\alpha) + j\,W_m \cdot J_m'(\alpha)}{H_m^{(2)}(\alpha) + j\,W_m \cdot H_m'^{(2)}(\alpha)} = -\frac{\left(\dfrac{\cos\Theta}{j\,W_m} + \dfrac{m}{k_0 a}\right) \cdot J_m(\alpha) - \cos\Theta \cdot J_{m+1}(\alpha)}{\left(\dfrac{\cos\Theta}{j\,W_m} + \dfrac{m}{k_0 a}\right) \cdot H_m^{(2)}(\alpha) - \cos\Theta \cdot H_{m+1}^{(2)}(\alpha)} \tag{5}$$

$$E_m = \frac{J_m(\alpha) + D_m \cdot H_m^{(2)}(\alpha)}{J_m(\beta)}$$

with the abbreviations $\quad \alpha = k_0 a \cdot \cos\Theta; \quad \beta = j\,k_0 a \cdot \Gamma_{an} \cdot \cos\Theta_1 \tag{6}$

and the modal normalised surface impedances

$$W_m = Z_{an} \frac{\cos\Theta}{\cos\Theta_1} \frac{I_m(\Gamma_a a \cdot \cos\Theta_1)}{I_m'(\Gamma_a a \cdot \cos\Theta_1)} = -j\,Z_{an} \frac{\cos\Theta}{\cos\Theta_1} \frac{J_m(y)}{J_m'(y)}$$

$$\frac{\cos\Theta}{j\,W_m} = -\frac{\Gamma_{an} \cdot \cos\Theta_1}{\Gamma_{an} Z_{an}} \left[\frac{J_{m+1}(y)}{J_m(y)} - \frac{m}{y}\right]. \tag{7}$$

For the cylinder which is locally reacting in the axial direction:
• Set $\Theta_1 = 0$.
For the cylinder which is locally reacting in all directions:
• Retain in p_a only the term $m = 0$;
• Set $\Theta_1 = 0$;

- Replace everywhere $W_m \to W_0$, in which case:

$$\frac{\cos \Theta}{j\,W_m} \to \frac{\cos \Theta}{j\,W_0} = -\frac{1}{Z_{an}} \frac{J_1(j\,k_0 a \cdot \Gamma_{an})}{J_0(j\,k_0 a \cdot \Gamma_{an})}. \tag{8}$$

The result then describes the scattering of a cylinder consisting of a (porous) material and made locally reacting.

For a cylinder which is locally reacting in all directions and described by a normalised surface admittance G:
- Neglect p_a;
- Replace everywhere $W_m \to W_0 = 1/G$, in which case:

$$\frac{\cos \Theta}{j\,W_m} \to \frac{\cos \Theta}{j\,W_0} = -j\,G \cdot \cos \Theta. \tag{9}$$

The incident plane wave is temporarily assumed to have an amplitude p_0 (which above was set at $p_0 = 1$). The integrals $\oint$ below are taken at the cylinder surface ($r = a$). A star * indicates the complex conjugate.

Scattering cross section(ratio of scattered power to incident intensity):

$$Q_s = \oint \text{Re} \left\{ \frac{p_s}{p_0} \cdot \frac{v_{rs}^*}{p_0/Z_0} \right\} dS \xrightarrow[p_0=1]{} \oint \text{Re}\{p_s \cdot Z_0 v_{rs}^*\}\, dS, \tag{10}$$

$$\frac{Q_s}{2a} = \frac{2}{k_0 a} \sum_{m \geq 0} \delta_m \cdot |D_m|^2. \tag{11}$$

Absorption cross section (ratio of absorbed power to incident intensity):

$$Q_a = -\oint \text{Re}\{p \cdot Z_0 v_r^*\}\, dS, \tag{12}$$

$$\frac{Q_a}{2a} = \frac{-2}{k_0 a} \sum_{m \geq 0} \delta_m \cdot \left(\text{Re}\{D_m\} + |D_m|^2 \right). \tag{13}$$

Extinction cross section:

$$Q_e = Q_s + Q_a = -\oint \text{Re}\{p_i^* \cdot v_r + p \cdot v_{ri}^*\}\, dS, \tag{14}$$

$$\frac{Q_e}{2a} = \frac{-2}{k_0 a} \sum_{m \geq 0} \delta_m \cdot \text{Re}\{D_m\}. \tag{15}$$

With the always possible separation of the scattered far field into an angular and a radial factor:

$$p_s(r, \vartheta, \varphi) \xrightarrow[k_0 r \gg 1]{} \Phi(\vartheta, \varphi) \cdot \frac{e^{-j k_0 r}}{r} + O(r^{-2}) \tag{16}$$

the extinction cross section is (extinction theorem)

$$Q_e = -\frac{4\pi}{k_0} \text{Im}\{\Phi(\vartheta_0, \varphi_0)\}, \tag{17}$$

where a radius with the angles ϑ_0, φ_0 points in the forward direction of the incident wave.

Backscattering cross section (measures the strength of the backscattering to the source):

$$Q_r = 2\pi r \frac{|p_s(r, \vartheta_0 + \pi, \varphi_0 + \pi)|^2}{p_0^2} \quad ; \quad k_0 r \gg 1. \tag{18}$$

Absorption cross section for diffuse sound incidence:

There exist several definitions in the literature (differing from each other in the reference intensity). Π_a = absorbed power; I_i = intensity of an incident plane wave

First definition:
$$Q_{a1} = \Pi_a / I_i \ ,$$
$$Q_{a1} = 4\pi \int_0^{\pi/2} Q_a(\Theta) \cdot \cos\Theta \ d\Theta \ . \tag{19}$$

Second definition:
$$Q_{a2} = \Pi_a / I_{i,\text{dif}} \quad ; \quad I_{i,\text{dif}} = \pi \cdot I_i \ ,$$
$$Q_{a2} = \frac{Q_{a1}}{\pi} = 4 \int_0^{\pi/2} Q_a(\Theta) \cdot \cos\Theta \ d\Theta \ . \tag{20}$$

Third definition:
with $\Pi_{i,\text{dif}}$ = incident power in a diffuse field on a cylinder of unit length and diameter

$$Q_{a3} = \Pi_a / \Pi_{i,\text{dif}} \quad ; \quad \Pi_{i,\text{dif}} = 4\pi \cdot I_i$$
$$Q_{a3} = \frac{Q_{a1}}{4\pi} = \frac{Q_{a2}}{4} = \int_0^{\pi/2} Q_a(\Theta) \cdot \cos\Theta \ d\Theta \tag{21}$$

E.2　Plane Wave Scattering at Cylinders and Spheres

▶ *See also:* Mechel, Vol. I, Ch. 6 (1989)

See previous ◉ *Sect. E.1* for an oblique plane wave incident on a cylinder. This section briefly gives the fundamental relations for a plane wave incident on a sphere and then collects equations for both spheres and cylinders (with normal incidence on the cylinder axis). In the case of a bulk reacting sphere, it consists of a homogeneous material with characteristic propagation constant Γ_a and wave impedance Z_a.
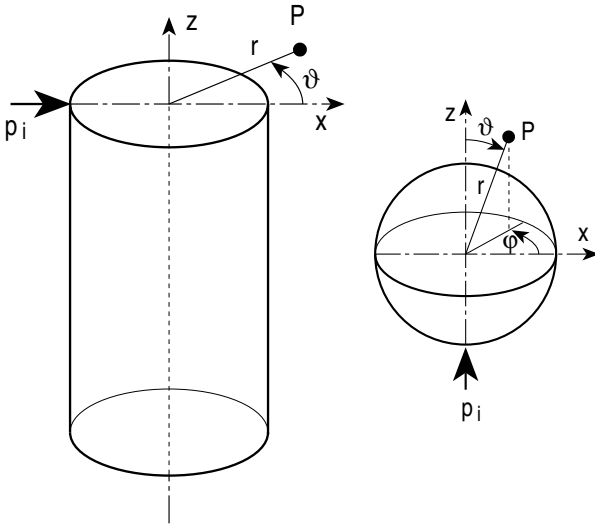
Diameter 2a; incident plane wave p_i; field point P

Notations:
- $\Gamma_{an} = \Gamma_a/k_0$; $Z_{an} = Z_a/Z_0$ normalised characteristic values;
- p_i = incident plane wave (with amplitude $p_0 = 1$);
- p_s = scattered wave;
- $p = p_i + p_s$ = total exterior field;
- p_a = interior field in the absorbing cylinder or sphere.

Sound field formulations for a sphere:

Incident plane wave:

$$p_i(r, \vartheta) = e^{-j\,k_0 r \cdot \cos\vartheta} = \sum_{m \geq 0} (2m + 1)\,(-j)^m \cdot P_m(\cos\vartheta) \cdot j_m(k_0 r). \tag{1}$$

Scattered wave:

$$p_s(r, \vartheta) = \sum_{m \geq 0} D_m \cdot (2m + 1)\,(-j)^m \cdot P_m(\cos\vartheta) \cdot h_m^{(2)}(k_0 r). \tag{2}$$

Total exterior field: $p = p_i + p_s$,
where $P_m(z)$ = Legendre polynomial, $j_m(z)$ = spherical Bessel function, $h_m^{(2)}(z)$ = spherical Hankel function of the second kind.

The following table contains corresponding quantities for cylinders and spheres, of diameter 2a, which are *locally reacting* with a normalised surface admittance G. Hankel functions of the second kind are written as $H_m(z)$. The argument $k_0 a$ of Bessel and Hankel functions is dropped. In some equations $W = 1/G = R + j \cdot X$ will be used.

The amplitude factors C_m are $C_m = 2D_m - 1$.

Quantity	Symbol	Cylinder	Sphere
Factors	$D_m =$	$-\dfrac{(-j\,G + m/k_0 a)\;J_m - J_{m+1}}{(-j\,G + m/k_0 a)\;H_m - H_{m+1}}$	$-\dfrac{(-j\,G + m/k_0 a)\;j_m - j_{m+1}}{(-j\,G + m/k_0 a)\;h_m - h_{m+1}}$
	$C_m =$	$-\dfrac{(-j\,G + m/k_0 a)\;H_m^* - H_{m+1}^*}{(-j\,G + m/k_0 a)\;H_m - H_{m+1}}$	$-\dfrac{(-j\,G + m/k_0 a)\;h_m^* - h_{m+1}^*}{(-j\,G + m/k_0 a)\;h_m - h_{m+1}}$
	$T_m =$	$\cos(m\vartheta)$	$P_m(\cos\vartheta)$
	$\delta_m =$	$\begin{cases} 1\;;\; m = 0 \\ 2\;;\; m > 0 \end{cases}$	$2m+1$
Cross section	$S =$	$2a$	πa^2
Incident wave	$p_i(r, \vartheta) =$	$e^{-j\,k_0 r \cdot \cos\vartheta}$	
		$\displaystyle\sum_{m \geq 0} \delta_m (-j)^m \cdot T_m \cdot J_m(k_0 r)$	$\displaystyle\sum_{m \geq 0} \delta_m (-j)^m \cdot T_m \cdot j_m(k_0 r)$
Scattered wave	$p_s(r, \vartheta) =$	$\displaystyle\sum_{m \geq 0} D_m \delta_m (-j)^m T_m J_m(k_0 r)$	$\displaystyle\sum_{m \geq 0} D_m \delta_m (-j)^m T_m j_m(k_0 r)$
Scattered far field	$p_s(r, \vartheta) \rightarrow$	$\sqrt{\dfrac{2j}{\pi}}\dfrac{e^{-j\,k_0 r}}{\sqrt{k_0 r}}\displaystyle\sum_{m \geq 0} D_m \delta_m T_m$	$j\dfrac{e^{-j\,k_0 r}}{k_0 r}\displaystyle\sum_{m \geq 0} D_m \delta_m T_m$
	$\rightarrow$	$\sqrt{\dfrac{2j}{\pi}}\,\Phi(\vartheta)\dfrac{e^{-j\,k_0 r}}{\sqrt{k_0 r}}$	$\Phi(\vartheta)\dfrac{e^{-j\,k_0 r}}{k_0 r}$
Total field	$p(r, \vartheta) =$	$\displaystyle\sum_{m \geq 0} \delta_m (-j)^m T_m$ $\cdot \left[J_m(k_0 r) + D_m H_m(k_0 r)\right]$	$\displaystyle\sum_{m \geq 0} \delta_m (-j)^m T_m$ $\cdot \left[j_m(k_0 r) + D_m h_m(k_0 r)\right]$
Scattering cross section	$Q_s =$	$\displaystyle\oint \mathrm{Re}\{p_s \cdot v_{rs}^*\}\,dS$	
	$Q_s/S =$	$\dfrac{2}{k_0 a}\displaystyle\sum_{m \geq 0} \delta_m |D_m|^2$	$\dfrac{4}{(k_0 a)^2}\displaystyle\sum_{m \geq 0} \delta_m |D_m|^2$
	$=$	$\dfrac{2}{k_0 a}\displaystyle\sum_{m \geq 0} \delta_m |1 - C_m|^2$	$\dfrac{4}{(k_0 a)^2}\displaystyle\sum_{m \geq 0} \delta_m |1 - C_m|^2$

Table continued:

Quantity	Symbol	Cylinder	Sphere
		Scattering cross section; approximations	
$k_0 a \gg 1$; $R = 0$ or $= \infty$	$Q_s/S =$	2	2
$k_0 a \ll 1$; $G = 0$	$Q_s/S =$	$\dfrac{3\pi^2}{8}(k_0 a)^3$	$\dfrac{7}{9}(k_0 a)^4$
$k_0 a \ll 1$; $|G| \to \infty$	$Q_s/S =$	$\dfrac{\pi^2}{2\,k_0 a\,\ln^2(1/k_0 a)}$	4
$k_0 a \ll 1$; $G = $ else	$Q_s/S =$	$5\,k_0 a|G|^2$	$4\,(k_0 a)^2|G|^2$
Absorption cross section	$Q_a =$	$-\oint \mathrm{Re}\{p \cdot v_r^*\}\,dS$	
	$Q_a/S =$	$\dfrac{-2}{k_0 a}\displaystyle\sum_{m\geq 0}\delta_m\left(\mathrm{Re}\{D_m\} + |D_m|^2\right)$	$\dfrac{-4}{(k_0 a)^2}\displaystyle\sum_{m}\delta_m\left(\mathrm{Re}\{D_m\} + |D_m|^2\right)$
	$=$	$\dfrac{1}{2\,k_0 a}\displaystyle\sum_{m\geq 0}\delta_m\left(1 - |C_m|^2\right)$	$\dfrac{1}{(k_0 a)^2}\displaystyle\sum_{m\geq 0}\delta_m\left(1 - |C_m|^2\right)$
		Absorption cross section; approximations	
$k_0 a \ll 1$; $|X| \ll R$	$Q_a/S =$	$\dfrac{\pi}{R}$	$\dfrac{4}{R}$
$k_0 a \ll 1$; $R < |X|/2$	$Q_a/S =$	$\dfrac{\pi R}{X^2}$	$\dfrac{4R}{X^2}$
Extinction cross section	$Q_e =$	$-\oint \mathrm{Re}\{p_i^* \cdot v_r^* + p \cdot v_{ri}^*\}\,dS$	
with scattered far field	$Q_e/S =$	$\dfrac{-2}{k_0 a}\displaystyle\sum_{m\geq 0}\delta_m T_m(0) \cdot \mathrm{Re}\{D_m\}$	$\dfrac{-4}{(k_0 a)^2}\displaystyle\sum_{m\geq 0}\delta_m T_m(0) \cdot \mathrm{Re}\{D_m\}$
	$p_s \to$	$\sqrt{2j/\pi} \cdot \Phi(\vartheta) \cdot \dfrac{e^{-j k_0 r}}{\sqrt{k_0 r}}$	$j \cdot \Phi(\vartheta) \cdot \dfrac{e^{-j k_0 r}}{k_0 r}$
	$Q_e/S =$	$\dfrac{-2}{k_0 a}\mathrm{Re}\{\Phi(0)\}$	$\dfrac{-4}{(k_0 a)^2}\mathrm{Re}\{\Phi(0)\}$

Table continued:

Quantity	Symbol	Cylinder	Sphere
Backscatter cross section	$Q_r =$	$2\pi r \cdot |p_s(r,\pi)|^2$	$4\pi r^2 \cdot |p_s(r,\pi)|^2$
Backscatter cross-section; approximations			
$k_0 a \gg 1$; $|G| \to 0$ or ∞	$Q_r/S =$	$\pi/2$	1
$k_0 a \ll 1$; $|G| \to \infty$	$Q_r/S =$	$\dfrac{2\pi^2}{k_0 a \left(\pi^2 + 4\ln^2(1.123/k_0 a)\right)}$	4
$k_0 a <$ first resonance; G else	$Q_r/S =$	$\dfrac{\pi^2}{2} k_0 a |G|^2$	$4\,k_0 a |G|^2$
Reactance at m-th resonance $k_0 a < 1$ $ß = 1.123$	$X_0 =$	$-k_0 a \cdot \ln \dfrac{ß}{k_0 a}$ $\cdot \dfrac{1 - \frac{1}{2}(k_0 a)^2 \ln \frac{ß}{k_0 a}}{1 - \frac{1}{2}(k_0 a)^2 \ln \frac{ß}{k_0 a}}$	$\dfrac{-k_0 a}{1 + (k_0 a)^2}$
	$X_1 =$	$-k_0 a \cdot \dfrac{1 + 2.14(k_0 a)^2 \ln \frac{ß}{k_0 a}}{1 - (k_0 a)^2 \ln \frac{ß}{k_0 a}}$	$-k_0 a \dfrac{1 + 2(k_0 a)^2}{1 + (k_0 a)^2}$
	$X_m =$	$-\dfrac{k_0 a}{m} \cdot \dfrac{1 + \frac{(k_0 a)^2}{4(m-1)}}{1 + \frac{(m-2)(k_0 a)^2}{4m(m-1)}}$	$-\dfrac{k_0 a}{m} \cdot \dfrac{1}{1 - \frac{(k_0 a)^2}{2m^2}}$
Q_s at lowest resonance; $R = 0; X = X_0$	$Q_s/S =$	$\dfrac{2}{k_0 a}$	$\dfrac{4}{(k_0 a)^2}$
Frequency of lowest back-scatter minimum	$k_0 a =$	$\dfrac{2\,|X|}{2 + 3\,|X|^2}$ $|X|_{max} = \sqrt{2/3}$ $(k_0 a)_{max} = 1/\sqrt{6}$	$\dfrac{6\,|X|}{3 + 5\,|X|^2}$ $|X|_{max} = (k_0 a)_{max} = \sqrt{3/10}$

The next table contains corresponding values for cylinders and spheres, with diameter 2a, consisting of a *homogeneous (bulk reacting) material* with characteristic propagation constant Γ_a and wave impedance Z_a. Hankel functions of the second kind are written as $H_m(z)$ and spherical Hankel functions of the second kind as $h_m(z)$; the arguments $k_0 a$ of Bessel and Hankel functions are dropped. The abbreviation $z = j \cdot \Gamma_a a$ will be used, and $\Gamma_{an} = \Gamma_a / k_0$, $Z_{an} = Z_a / Z_0$. A prime at functions indicates the derivative; a prime or double prime at Γ_{an} or Z_{an} indicates the real or imaginary part, respectively. An asterisk indicates the complex conjugate.

Quantity	Symbol	Cylinder	Sphere
Factors	$D_m =$	$-\dfrac{(-j\,G_m + m/k_0 a)\ J_m - J_{m+1}}{(-j\,G_m + m/k_0 a)\ H_m - H_{m+1}}$	$-\dfrac{(-j\,G_m + m/k_0 a)\ j_m - j_{m+1}}{(-j\,G_m + m/k_0 a)\ h_m - h_{m+1}}$
	$C_m =$	$-\dfrac{(-j\,G_m + m/k_0 a)\ H_m^* - H_{m+1}^*}{(-j\,G_m + m/k_0 a)\ H_m - H_{m+1}}$	$-\dfrac{(-j\,G_m + m/k_0 a)\ h_m^* - h_{m+1}^*}{(-j\,G_m + m/k_0 a)\ h_m - h_{m+1}}$
	$T_m =$	$\cos(m\vartheta)$	$P_m(\cos\vartheta)$
	$\delta_m =$	$\begin{cases} 1 \ ;\ m = 0 \\ 2 \ ;\ m > 0 \end{cases}$	$2m+1$
Cross section	$S =$	$2a$	πa^2
Modal admittance	$G_m =$ $(z = j \cdot \Gamma_a a)$	$j\,\dfrac{Z_0}{Z_a}\dfrac{J_m'(z)}{J_m(z)}$	$j\,\dfrac{Z_0}{Z_a}\dfrac{j_m'(z)}{j_m(z)}$
Incident wave	$p_i(r,\vartheta) =$	$e^{-j k_0 r \cdot \cos\vartheta}$	
		$\displaystyle\sum_{m\geq0} \delta_m (-j)^m \cdot T_m \cdot J_m(k_0 r)$	$\displaystyle\sum_{m\geq0} \delta_m (-j)^m \cdot T_m \cdot j_m(k_0 r)$
Scattered wave	$p_s(r,\vartheta) =$	$\displaystyle\sum_{m\geq0} D_m \cdot \delta_m (-j)^m \cdot T_m \cdot H_m(k_0 r)$	$\displaystyle\sum_{m\geq0} D_m \cdot \delta_m (-j)^m \cdot T_m \cdot h_m(k_0 r)$
Scattered far field	$p_s(r,\vartheta) \rightarrow$	$-\sqrt{\dfrac{2j}{\pi k_0 r}}\,e^{-j k_0 r}\displaystyle\sum_{m\geq0} C_m \cdot \delta_m T_m$	$\dfrac{j}{k_0 r}e^{-j k_0 r}\displaystyle\sum_{m\geq0} C_m \cdot \delta_m T_m$ $=: \dfrac{e^{-j k_0 r}}{k_0 r}\cdot \Phi(\vartheta)$
Total ext. field	$p(r,\vartheta) =$	$\displaystyle\sum_{m\geq0} \delta_m (-j)^m T_m$ $\cdot \big(J_m(k_0 r) + D_m H_m(k_0 r)\big)$	$\displaystyle\sum_{m\geq0} \delta_m (-j)^m T_m$ $\cdot \big(j_m(k_0 r) + D_m h_m(k_0 r)\big)$

Table continued:

| Quantity	Symbol	Cylinder	Sphere
Scattering cross section	$\dfrac{Q_s}{S} =$	$\dfrac{1}{2\,k_0 a} \sum_m \delta_m \cdot |1 - C_m|^2$	$\dfrac{1}{(k_0 a)^2} \sum_m \delta_m \cdot |1 - C_m|^2$
Absorption cross section	$\dfrac{Q_a}{S} =$	$\dfrac{1}{2\,k_0 a} \sum_m \delta_m \cdot \left(1 - |C_m|^2\right)$	$\dfrac{1}{(k_0 a)^2} \sum_m \delta_m \cdot \left(1 - |C_m|^2\right)$
		Approximations: $k_0 a \ll 1$	
Modal admittance	$G_0 =$	$\dfrac{k_0 a}{2}\, \dfrac{\Gamma_{an}}{Z_{an}}$	$\dfrac{k_0 a}{3}\, \dfrac{\Gamma_{an}}{Z_{an}}$
Scattering cross section	$\dfrac{Q_s}{S} =$	$\dfrac{1}{2\,k_0 a} \sum_m \delta_m \cdot |1 - C_0|^2$ $= \dfrac{\pi^2 (k_0 a)^3}{16}$ $\cdot \left[1 + \left(\left(\dfrac{\Gamma_{an}}{Z_{an}}\right)' - \left(\dfrac{\Gamma_{an}}{Z_{an}}\right)''\right)^2\right]$	$\dfrac{1}{(k_0 a)^2} \sum_m \delta_m \cdot |1 - C_0|^2$ $= \dfrac{4(k_0 a)^4}{9} \cdot \left[\left|1 + j\,\dfrac{\Gamma_{an}}{Z_{an}}\right|^2 + 3\left|\dfrac{1 + j\,\Gamma_{an} Z_{an}}{1 - 2j\,\Gamma_{an} Z_{an}}\right|^2\right]$
Absorption cross section, cylinder	$\dfrac{Q_a}{S} =$	$\dfrac{(1 - |C_0|^2)}{2k_0 a} = \dfrac{\pi\,k_0 a}{2} \cdot \left(\dfrac{\Gamma_{an}}{Z_{an}}\right)'$ $\cdot \dfrac{1 + k_0 a \cdot \ln\,(0.890\,k_0 a)}{\left[1 + k_0 a \cdot \ln\,(0.890\,k_0 a)\left(1 + \dfrac{(k_0 a)^2}{2}\left(\dfrac{\Gamma_{an}}{Z_{an}}\right)''\right)\right]^2}$	
Absorption cross section, sphere	$\dfrac{Q_a}{S} =$	$\dfrac{(1 - |C_0|^2)}{(k_0 a)^2} = -\dfrac{4\,k_0 a}{3} \cdot \mathrm{Im}\left\{1 + j\,\dfrac{\Gamma_{an}}{Z_{an}} + 3\,\dfrac{1 + j\,\Gamma_{an} Z_{an}}{1 - 2j\,\Gamma_{an} Z_{an}}\right\}$	

Table continued:

Quantity	Symbol	Cylinder	Sphere
		Approximations: $k_0 a \ll 1$	
Total ext. field at surface, sphere	$p(a, \vartheta) =$	$1 - j\,k_0 a \dfrac{3\,\Gamma_{an} Z_{an}}{j + 2\,\Gamma_{an} Z_{an}} \cdot \cos(\vartheta)$	
Radial particle velocity at surface, sphere	$v_r(a,\vartheta) =$	$\dfrac{-k_0 a}{3} \dfrac{\Gamma_{an}}{Z_{an}} + \dfrac{3\,j}{j + 2\,\Gamma_{an} Z_{an}} \cdot \cos(\vartheta)$	
Scattered field directivity in the far field, cylinder	$\Phi(\vartheta) =$	$\sqrt{\dfrac{-j\,\pi}{8\,k_0}}(k_0 a)^3 \left[-\left(1 + j\dfrac{\Gamma_{an}}{Z_{an}}\right) + 2\dfrac{\Gamma_{an} Z_{an} - j}{\Gamma_{an} Z_{an} + j} \cdot \cos(\vartheta) \right]^{*)}$	
Scattered field directivity in the far field, cylinder	$\Phi(\vartheta) =$	$\dfrac{k_0^2 a^3}{3} \left[-\left(1 + j\dfrac{\Gamma_{an}}{Z_{an}}\right) + 2\dfrac{\Gamma_{an} Z_{an} - j}{\Gamma_{an} Z_{an} + j} \cdot \cos(\vartheta) \right]^{*)}$	

Some numerical examples will illustrate the quantities and relations given above.


[*)] See Preface to the 2nd Edition.
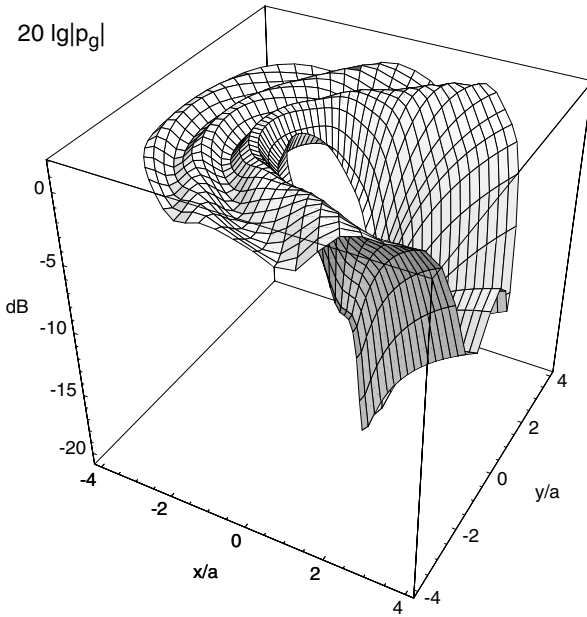
Total sound pressure level around a cylinder of homogeneous, bulk reacting, porous glass fibre material. Sound incidence from the left-hand side. $f = 1000$ [Hz]; $a = 0.25$ [m]; $\Theta = 45°$; $\Xi = 10000$ [Pa s/m^2]; $m_{hi} = 32$ (upper summation limit)
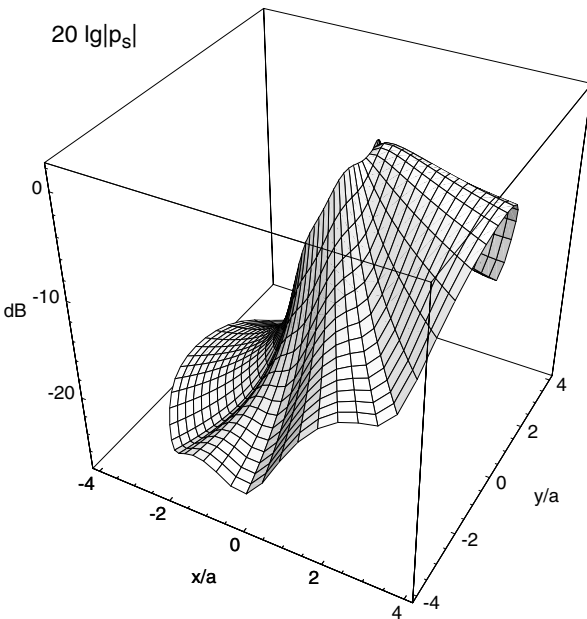

Scattered sound pressure level around a cylinder of homogeneous, bulk reacting, porous glass fibre material. Sound incidence from the left-hand side. $f = 1000$ [Hz]; $a = 0.25$ [m]; $\Theta = 45°$; $\Xi = 10000$ [Pa s/m^2]; $m_{hi} = 32$ (upper summation limit)
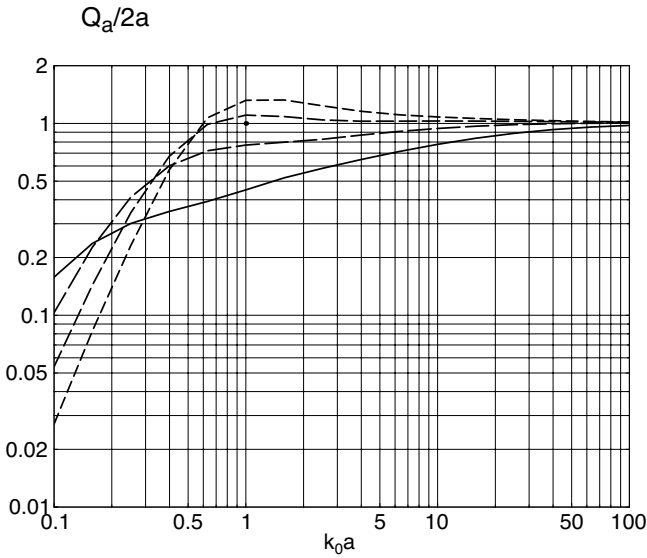
$Q_a/2a$

Normalised absorption cross section $Q_a/2a$ of a cylinder of homogeneous, bulk reacting, porous glass fibre material. $\Theta = 0°$; $m_{hi} = 32$ (upper sum limit); parameter values of curves: $R = \Xi \cdot a/Z_0$: R={0.2, 0.5, 1., 2.} (dashes are shorter in that order)
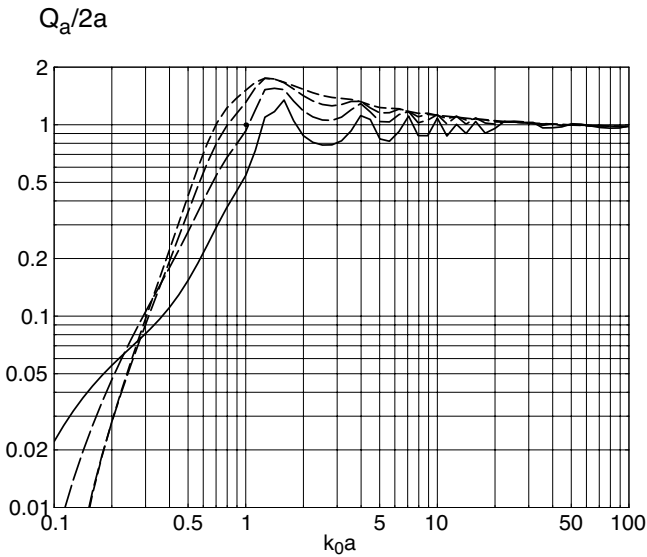
$Q_a/2a$

Normalised absorption cross section $Q_a/2a$ of a cylinder of homogeneous, porous glass fibre material, made fully locally reacting $\Theta = 0°$; $m_{hi} = 32$ (upper sum limit); parameter values of curves: $R = \Xi \cdot a/Z_0$: R={0.2, 0.5, 1., 2.} (dashes are shorter in that order)

Qs/2a, fully loc.cyl., G=var.
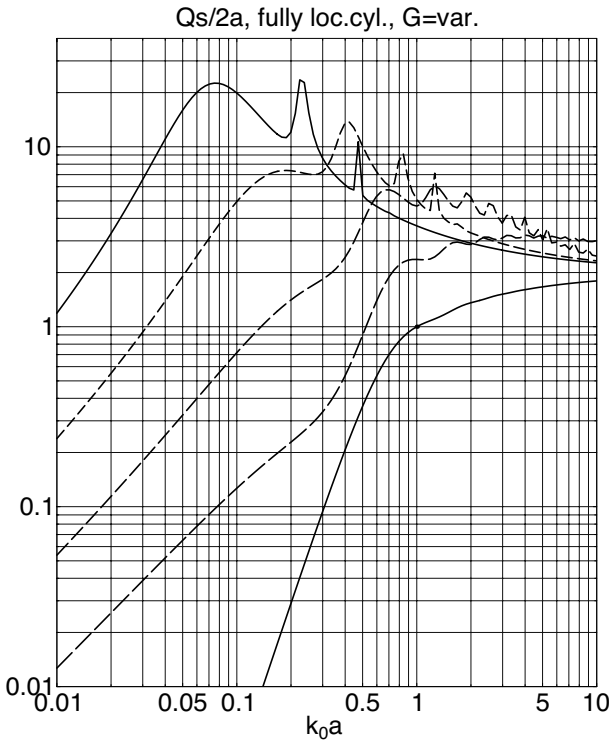
Normalised scattering cross section of a locally reacting cylinder with given values of the normalised surface adimittance G={0, 0.5j, 1j, 2j, 4j} (curves from low to high in that order). The graph illustrates the scattering resonances (the exterior vibrating mass resonates with the resilience of the surface)

E.3   Multiple Scattering at Cylinders and Spheres

▶ *See also:* Mechel, Vol. II, Ch. 14 (1995)

Consider an "artificial medium" consisting of an arrangement (preferably random) of hard scatterers (cylindrical or spherical) with a root mean square average radius a and mutual distances such that the "massivity" μ of the arrangement (fraction of the space occupied by the scatterers) holds. A sound wave propagates through that medium with an effective (complex) wave number k_{eff} and wave impedance Z_{eff} given by

$$\frac{k_{eff}^2}{k_0^2} = \frac{\rho_{eff}}{\rho_0} \cdot \frac{C_{eff}}{C_0} \quad ; \quad \frac{Z_{eff}^2}{Z_0^2} = \frac{\rho_{eff}}{\rho_0} \Big/ \frac{C_{eff}}{C_0}, \tag{1}$$

with the effective density ρ_{eff} and compressibility C_{eff}

$$\frac{\rho_{eff}}{\rho_0} = 1 + j \frac{8\mu}{\pi(k_0 a)^2} \sum_{n=1,3,5...} D_n \quad ; \quad \frac{C_{eff}}{C_0} = 1 + j \frac{8\mu}{\pi(k_0 a)^2} \cdot \left[0.5 D_0 + \sum_{n=2,4,6...} D_n \right], \tag{2}$$

where the coefficients D_n are taken from the table in ▶ *Sect. E.2*, and $C_0 = 1/(\rho_0 c_0^2)$. (3)

E.4   Cylindrical Wave Scattering at Cylinders

A line source at Q is parallel to the axis of a locally reacting cylinder with radius a and (normalised) surface admittance G. The field point is at P. The source distance r_q defines two radial zones (a),(b).

The sound field is composed of the sum of the source free field p_Q and the scattered field p_s:

$$p(r, \vartheta) = p_Q(r') + p_s(r, \vartheta). \tag{1}$$
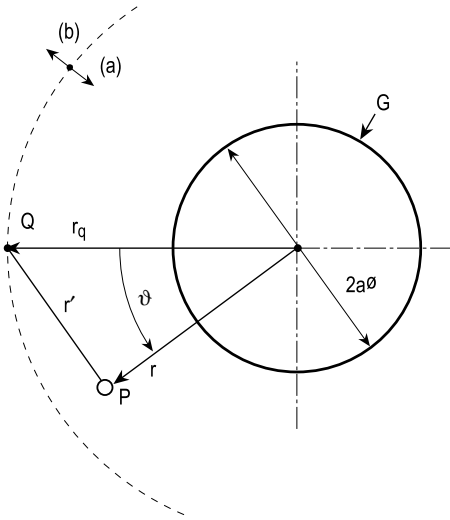
The source free field p_Q is transformed with the addition theorem for Hankel functions to the co-ordinates (r,ϑ):

$$p_Q(r') = P_0 \cdot H_0^{(2)}(k_0 r') = P_0 \cdot \begin{cases} \sum_{m\geq 0} \delta_m \cdot J_m(k_0 r) \cdot H_m^{(2)}(k_0 r_q) \cdot \cos(m\vartheta); & \text{in (a),} \\[2mm] \sum_{m\geq 0} \delta_m \cdot J_m(k_0 r_q) \cdot H_m^{(2)}(k_0 r) \cdot \cos(m\vartheta); & \text{in (b),} \end{cases} \tag{2}$$

with $\quad \delta_m = \begin{cases} 1 & ; \quad m = 0, \\ 2 & ; \quad m > 0. \end{cases}$ \hfill (3)

Formulation of the scattered field:

$$p_s(r, \vartheta) = P_0 \cdot \sum_{m\geq 0} a_m \cdot \delta_m \cdot J_m(k_0 r_q) \cdot H_m^{(2)}(k_0 r) \cdot \cos(m\vartheta). \tag{4}$$

The boundary condition $-Z_0 \left(v_{Q_r} + v_{sr}\right) \overset{!}{=} G \cdot \left(p_Q + p_s\right)$ gives the amplitudes

$$a_m = -\frac{j \cdot J'_m(k_0 a) + G \cdot J_m(k_0 a)}{j \cdot H_m'^{(2)}(k_0 a) + G \cdot H_m^{(2)}(k_0 a)} \cdot \frac{H_m^{(2)}(k_0 r_q)}{J_m(k_0 r_q)}$$

$$\xrightarrow[G \to 0]{} -\frac{J'_m(k_0 a) \cdot H_m^{(2)}(k_0 r_q)}{J_m(k_0 r_q) \cdot H_m'^{(2)}(k_0 a)} = a_{hm} \tag{5}$$

$$\xrightarrow[|G| \to \infty]{} -\frac{J_m(k_0 a) \cdot H_m^{(2)}(k_0 r_q)}{J_m(k_0 r_q) \cdot H_m^{(2)}(k_0 a)} = a_{sm}$$

with the special cases $G \to 0$ (hard) and $|G| \to \infty$ (soft).

In a different notation, the scattered field is

$$p_s(r, \vartheta) = -P_0 \cdot \sum_{m \geq 0} \delta_m \cdot c_m \cdot H_m^{(2)}(k_0 r_q) \cdot H_m^{(2)}(k_0 r) \cdot \cos(m\vartheta),$$

$$c_m = \frac{\left(G + \dfrac{m}{k_0 a}\right) \cdot J_m(k_0 a) - j \cdot J_{m+1}(k_0 a)}{\left(G + \dfrac{m}{k_0 a}\right) \cdot H_m^{(2)}(k_0 a) - j \cdot H_{m+1}^{(2)}(k_0 a)}. \tag{6}$$

$|p_g/P_0|$; exact
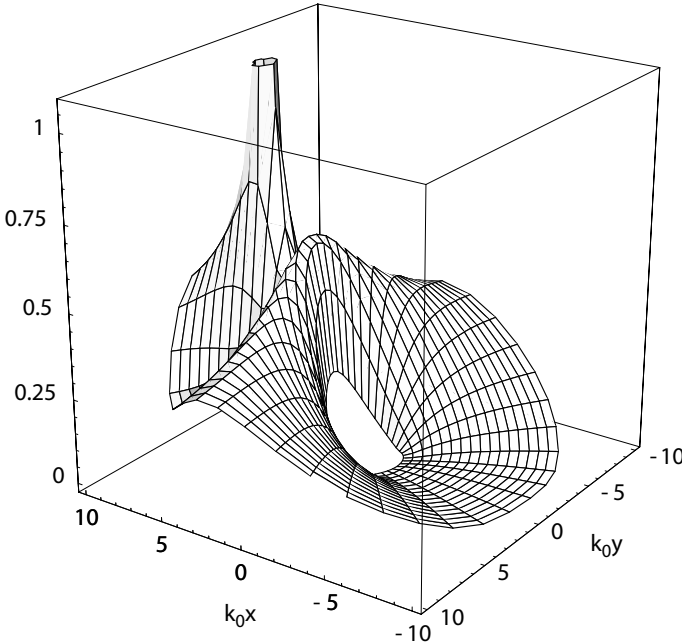
Sound pressure magnitude from a line source around a locally absorbing cylinder. $G = 0.5 - 2 \cdot j$; $k_0 a = 2$; $k_0 r_q = 6.1$; upper summation limit $m_{hi} = 8$

E.5 Cylindrical or Plane Wave Scattering at a Corner Surrounded by a Cylinder

▶ *See also:* Mechel, Improvement of Corner Shielding by an Absorbing Cylinder (1999)

The apex line of a corner with hard flanks at $\vartheta = 0$ and $\vartheta = \vartheta_0 \leq 2\pi$ is surrounded by a locally reacting cylinder of radius a and (normalised) surface admittance G. The line source at Q has the co-ordinates (r_q, ϑ_q).

The sound field is formulated as a mode sum:

$$p(r, \vartheta, z) = Z(k_z z) \sum_\eta R_\eta(kr) \cdot T(\eta\vartheta). \tag{1}$$

The factor $Z(k_z z)$ may be any of the functions $e^{\pm j k_z z}$, $\cos(k_z z)$, $\sin(k_z z)$ or a linear combination thereof. If $k_z \neq 0$, set $k^2 = k_0^2 - k_z^2$.

Below it will be supposed (for simplicity) that $k_z = 0$, $Z(k_z z) = 1$.
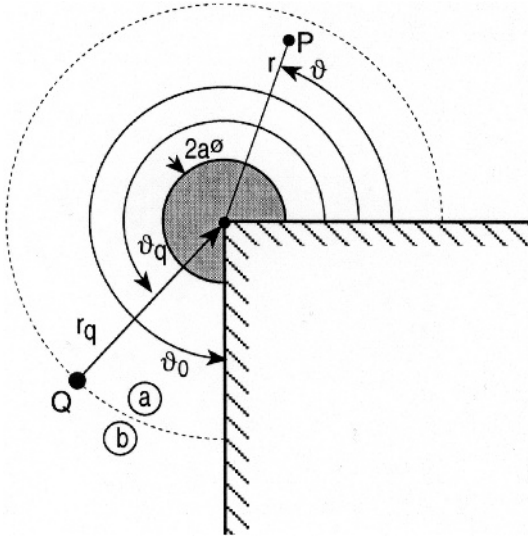
The azimuthal functions are $T(\eta\vartheta) = \cos(\eta\vartheta)$, and the azimuthal wave numbers satisfy the characteristic equation

$$(\eta_n \vartheta_0) \cdot \tan(\eta_n \vartheta_0) = 0 \tag{2}$$

with the solutions $\eta_n \vartheta_0 = n \cdot \pi$; $n = 0, 1, 2, \ldots$. Field formulations in the two radial zones (a),(b):

$$p_a(r, \vartheta) = \sum_{n\geq 0} A_n \cdot H_{\eta_n}^{(2)}(kr_q) \cdot \left[H_{\eta_n}^{(1)}(kr) + r_n \cdot H_{\eta_n}^{(2)}(kr) \right] \cdot \cos(\eta_n \vartheta); \quad a \leq r \leq r_q$$

$$p_b(r, \vartheta) = \sum_{n\geq 0} A_n \cdot \left[H_{\eta_n}^{(1)}(kr_q) + r_n \cdot H_{\eta_n}^{(2)}(kr_q) \right] \cdot H_{\eta_n}^{(2)}(kr) \cdot \cos(\eta_n \vartheta); \quad r_q \leq r < \infty \tag{3}$$

with the modal reflection factors at the cylinder:

$$r_n = -\frac{G \cdot H_{\eta_n}^{(1)}(ka) + j\frac{k}{k_0}H_{\eta_n}^{\prime(1)}(ka)}{G \cdot H_{\eta_n}^{(2)}(ka) + j\frac{k}{k_0}H_{\eta_n}^{\prime(2)}(ka)}. \tag{4}$$

The mode amplitudes A_n follow from the source condition:

$$A_n = \frac{\pi}{4}k_0 r_q \frac{Z_0 q}{\vartheta_0 N_n} \cos(\eta_n \vartheta_q) = \frac{\pi}{\vartheta_0 N_n} \frac{p_Q(0)}{H_0^{(2)}(kr_q)} \cos(\eta_n \vartheta_q). \tag{5}$$

In the second form the source strength is given by the free field source pressure $p_Q(0)$ in the corner apex line. The terms N_n are the mode norms:

$$N_n = \frac{1}{\vartheta_0} \int_0^{\vartheta_0} \cos^2(\eta_n \vartheta) \, d\vartheta = \frac{1}{2}\left(1 + \frac{\sin(2\eta_n \vartheta_0)}{2\eta_n \vartheta_0}\right) = \begin{cases} 1 & ; & n = 0 \\ 1/2; & n > 0 \end{cases}. \tag{6}$$

An alternative formulation, showing separately the contributions of the corner alone and of the cylinder with radius a, is

$$p_a(r, \vartheta) = p_{a,\text{Corner}} + p_{a,\text{Cyl}}$$

$$= \frac{2\pi}{\vartheta_0} \frac{p_Q(0)}{H_0^{(2)}(kr_q)} \sum_{n \geq 0} \frac{\cos(\eta_n \vartheta_q)}{N_n} \cdot H_{\eta_n}^{(2)}(kr_q) \cdot J_{\eta_n}(kr) \cdot \cos(\eta_n \vartheta)$$

$$- \frac{2\pi}{\vartheta_0} \frac{p_Q(0)}{H_0^{(2)}(kr_q)} \sum_{n \geq 0} C_n \cdot \frac{\cos(\eta_n \vartheta_q)}{N_n} \cdot H_{\eta_n}^{(2)}(kr_q) \cdot H_{\eta_n}^{(2)}(kr) \cdot \cos(\eta_n \vartheta), \tag{7}$$

$$p_b(r, \vartheta) = p_{b,\text{Corner}} + p_{b,\text{Cyl}}$$

$$= \frac{2\pi}{\vartheta_0} \frac{p_Q(0)}{H_0^{(2)}(kr_q)} \sum_{n \geq 0} \frac{\cos(\eta_n \vartheta_q)}{N_n} \cdot J_{\eta_n}(kr_q) \cdot H_{\eta_n}^{(2)}(kr) \cdot \cos(\eta_n \vartheta)$$

$$- \frac{2\pi}{\vartheta_0} \frac{p_Q(0)}{H_0^{(2)}(kr_q)} \sum_{n \geq 0} C_n \cdot \frac{\cos(\eta_n \vartheta_q)}{N_n} \cdot H_{\eta_n}^{(2)}(kr_q) \cdot H_{\eta_n}^{(2)}(kr) \cdot \cos(\eta_n \vartheta). \tag{8}$$

with the following coefficients:

$$C_n = \frac{G \cdot J_{\eta_n}(ka) + j\frac{k}{k_0}J_{\eta_n}'(ka)}{G \cdot H_{\eta_n}^{(2)}(ka) + j\frac{k}{k_0}H_{\eta_n}^{\prime(2)}(ka)}; \tag{9}$$

$$C_n \xrightarrow[G \to 0]{} \frac{J_{\eta_n}'(ka)}{H_{\eta_n}^{\prime(2)}(ka)}; \quad C_n \xrightarrow[|G| \to \infty]{} \frac{J_{\eta_n}(ka)}{H_{\eta_n}^{(2)}(ka)}; \quad C_n \xrightarrow[ka \to 0]{} 0.$$
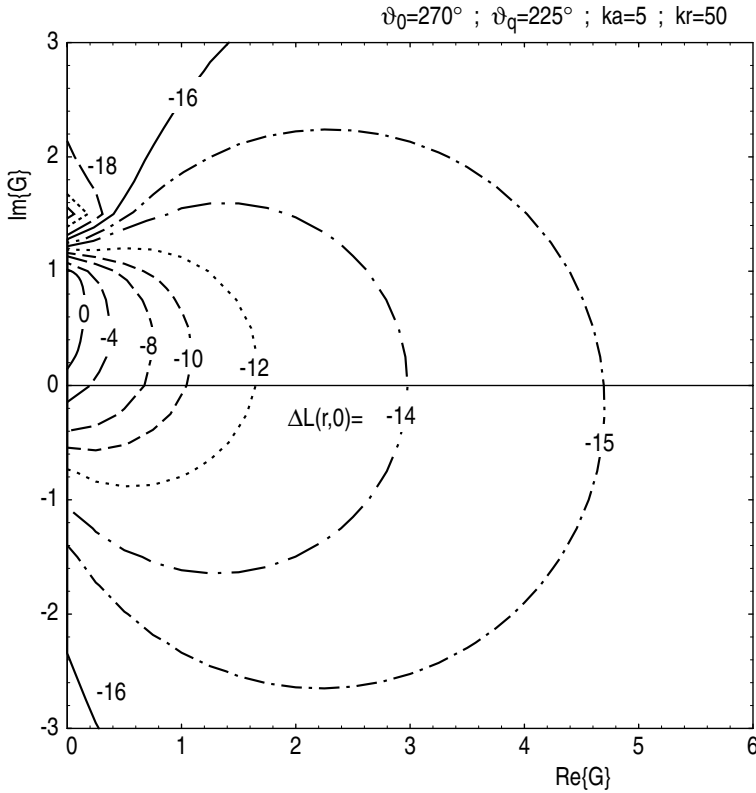
Level reduction in the zones i = a, b by the cylinder:

$$\Delta L_i(r, \vartheta) = 20 \cdot \lg\left|1 + p_{i,\text{Cyl}}/p_{i,\text{Corner}}\right|; \quad i = a, b. \tag{10}$$

Plane wave incidence from the direction ϑ_q:

$$p(r, \vartheta) = p_{Corner} + p_{Cyl}$$

$$= \frac{2\pi}{\vartheta_0} p_Q(0) \sum_{n \geq 0} \frac{e^{j \eta_n \pi/2}}{N_n} \cdot J_{\eta_n}(kr) \cdot \cos(\eta_n \vartheta_q) \cdot \cos(\eta_n \vartheta) \tag{11}$$

$$- \frac{2\pi}{\vartheta_0} p_Q(0) \sum_{n \geq 0} C_n \cdot \frac{e^{j \eta_n \pi/2}}{N_n} \cdot H_{\eta_n}^{(2)}(kr) \cdot \cos(\eta_n \vartheta_q) \cdot \cos(\eta_n \vartheta).$$

A special case of a thin screen is obtained with $\vartheta_0 = 2\pi$ and $\eta_n = n/2; n = 0, 1, 2, \ldots$

Contour lines in the complex plane of G of the sound pressure level reduction $\Delta L(r, 0)$ by an absorbent cylinder, at the shadowed flank $\vartheta = 0$ at a distance $kr = 50$, for a plane wave incident under $\vartheta_q = 225°$, on a rectangular convex corner ($\vartheta_0 = 270°$), with a cylinder radius given by $ka = 5$

Below it is assumed that no cylinder exists at the corner line. The sound field in the shadow zone of a corner decays monotonously with the distance to the corner and on approaching the shadowed flank. If the distance between two consecutive convex corners

is not too small, the sound field at the later corner can approximately be assumed to be generated by a line source situated at the earlier corner. Thus the sound shielding by buildings can be evaluated by iteration over the surrounded corners.

The required intermediate values $L(kr, \vartheta = 0) = 20 \cdot \lg|p(kr, 0)/p_Q(0)|$ can be evaluated by regression over kr for corner parameters ϑ_0 (r = distance between earlier and later corner):

$$L(kr, 0) = a_0 + a_1 \cdot x + a_2 \cdot x^2 + \ldots \quad ; \quad x = \lg(kr)$$

$$a_i = \begin{cases} a_i(\vartheta_0, kr_q, \vartheta_q) \\ \\ a_i(\vartheta_0, \vartheta_q) \end{cases} ; \quad i = \begin{cases} 0, 1, 2 ; \quad \text{line source} \\ \\ 0, 1, 2, 3; \quad \text{plane wave} \end{cases} \tag{12}$$

In the case of a line source at (r_q, ϑ_q), the coefficients a_i are expanded as follows:

For $\vartheta_0 \neq 2\pi$:

$$a_i(kr_q, \vartheta_q) = b_{0,0} + b_{1,0} \cdot z + b_{2,0} \cdot z^2 + b_{3,0} \cdot z^3 + b_{0,1} \cdot y + b_{0,2} \cdot y^2$$

$$+ b_{1,1} \cdot z \cdot y + b_{1,2} \cdot z \cdot y^2 + b_{2,1} \cdot z^2 \cdot y + b_{2,2} \cdot z^2 \cdot y^2 \tag{13}$$

$$z = \lg(kr_q); \quad y = (\vartheta_0 - \vartheta_q)_{rad}; \quad i = 0, 1, 2 ; \quad \text{line source}$$

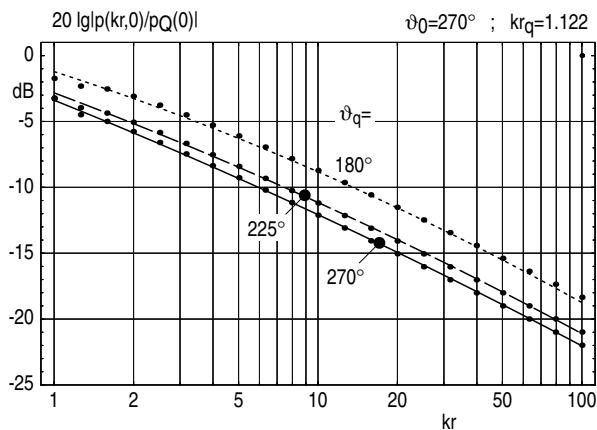$$b_{m,n} = b_{m,n}(\vartheta_0, i); \quad \vartheta_0 \neq 2\pi$$

For $\vartheta_0 = 2\pi$ (note change in sign of y):

$$a_i(kr_q, \vartheta_q) = b_{0,0} + b_{1,0} \cdot z + b_{2,0} \cdot z^2 + b_{3,0} \cdot z^3$$

$$+ b_{0,1} \cdot y + b_{0,2} \cdot y^2 + b_{0,3} \cdot y^3$$

$$+ b_{1,1} \cdot z \cdot y + b_{1,2} \cdot z \cdot y^2 + b_{1,3} \cdot z \cdot y^3 \tag{14}$$

$$+ b_{2,1} \cdot z^2 \cdot y + b_{2,2} \cdot z^2 \cdot y^2 + b_{2,3} \cdot z^2 \cdot y^3$$
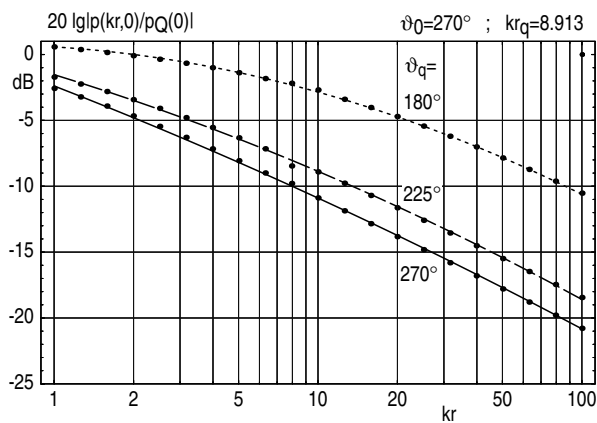
$$z = \lg(kr_q) \quad ; \quad y = (\vartheta_q - \vartheta_0)_{rad} \quad ; \quad i = 0, 1, 2; \quad \text{line source}$$

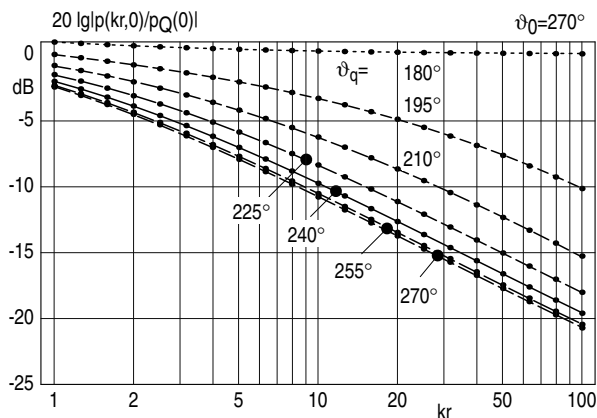$$b_{m,n} = b_{m,n}(\vartheta_0, i) \quad ; \quad \vartheta_0 = 2\pi$$

The following diagrams show the sound pressure level at the shadowed flank ($\vartheta = 0$), evaluated with mode sums (points) and from the above regressions (lines).

20 lg|p(kr,0)/p_Q(0)| $\vartheta_0=270°$; $kr_q=1.122$

A line source at a small distance $kr_q = 1.122$

20 lg|p(kr,0)/p_Q(0)| $\vartheta_0=270°$; $kr_q=8.913$

A line source at a medium distance $kr_q = 8.913$

20 lg|p(kr,0)/p_Q(0)| $\vartheta_0=270°$

Plane wave incidence from different directions ϑ_q

In the case of a plane wave from ϑ_q, the coefficients a_i are expanded similarly. The coefficients are:

Line source; $\vartheta_0 = 270°$.

$$
\begin{aligned}
a_0 =\ & -3.508914089 + 2.522196950 \cdot z - 1.883348105 \cdot z^2 + 0.4967954203 \cdot z^3 \\
& + 0.02544989020 \cdot y + 0.8345544874 \cdot y^2 \\
& + 0.3679533261 \cdot z \cdot y + 0.3777085214 \cdot z \cdot y^2 \\
& - 0.09024391927 \cdot z^2 \cdot y - 0.1947245060 \cdot z^2 \cdot y^2 \\[4pt]
a_1 =\ & -8.048512868 - 0.009541528038 \cdot z + 0.5769454995 \cdot z^2 - 0.3051673769 \cdot z^3 \\
& + 0.3821548481 \cdot y + 0.2651097458 \cdot y^2 \\
& - 0.6159740550 \cdot z \cdot y + 3.292101514 \cdot z \cdot y^2 \\
& + 0.2958236606 \cdot z^2 \cdot y - 0.8724895618 \cdot z^2 \cdot y^2 \\[4pt]
a_2 =\ & -0.6310612470 - 0.1423972091 \cdot z + 0.01678228228 \cdot z^2 + 0.04756468413 \cdot z^3 \\
& - 0.1407494337 \cdot y - 0.08464913202 \cdot y^2 \\
& + 0.5043646313 \cdot z \cdot y - 1.107819931 \cdot z \cdot y^2 \\
& - 0.7181971540 \cdot z^2 \cdot y + 0.8256508092 \cdot z^2 \cdot y^2
\end{aligned}
\tag{15}
$$

Line source; $\vartheta_0 = 225°$:

$$
\begin{aligned}
a_0 =\ & -0.09540693872 + 3.1825983742 \cdot z - 2.211437627 \cdot z^2 + 0.5797754874 \cdot z^3 \\
& - 1.521470673 \cdot y + 2.965063818 \cdot y^2 \\
& + 3.512579747 \cdot z \cdot y - 4.438049225 \cdot z \cdot y^2 \\
& - 1.739392722 \cdot z^2 \cdot y + 2.146307680 \cdot z^2 \cdot y^2 \\[4pt]
a_1 =\ & -7.323833505 + 3.020507185 \cdot z - 0.08553799890 \cdot z^2 - 0.4849823570 \cdot z^3 \\
& + 3.284316693 \cdot y - 4.259941774 \cdot y^2 \\
& - 7.601695001 \cdot z \cdot y + 16.521364584 \cdot z \cdot y^2 \\
& + 4.276159321 \cdot z^2 \cdot y - 7.413341455 \cdot z^2 \cdot y^2 \\[4pt]
a_2 =\ & -0.8765745279 - 1.203362984 \cdot z + 0.3513458955 \cdot z^2 + 0.03401430131 \cdot z^3 \\
& - 1.529012091 \cdot y + 1.973388860 \cdot y^2 \\
& + 4.011726713 \cdot z \cdot y - 7.347839244 \cdot z \cdot y^2 \\
& - 2.352498508 \cdot z^2 \cdot y + 4.809651759 \cdot z^2 \cdot y^2
\end{aligned}
\tag{16}
$$

Line source; $\vartheta_0 = 360°$ $(y = (\vartheta_q - \vartheta_0)_{rad})$:

$$
\begin{aligned}
a_0 \ = \ & -9.074649329 + 1.352053882 \cdot z - 1.152752755 \cdot z^2 + 0.3306858082 \cdot z^3 \\
& - 0.1455294858 \cdot y + 0.5960196681 \cdot y^2 - 0.008012063348 \cdot y^3 \\
& + 0.6291707040 \cdot z \cdot y + 0.8532798218 \cdot z \cdot y^2 + 0.1325783868 \cdot z \cdot y^3 \\
& - 0.2481813528 \cdot z^2 \cdot y - 0.3078462069 \cdot z^2 \cdot y^2 - 0.04647002117 \cdot z^2 \cdot y^3 \\[4pt]
a_1 \ = \ & -8.796878642 - 0.4605118745 \cdot z + 0.2689865167 \cdot z^2 - 0.03586357874 \cdot z^3 \\
& + 0.6092864775 \cdot y + 0.8416378006 \cdot y^2 + 0.1356184578 \cdot y^3 \\
& - 1.530126829 \cdot z \cdot y - 1.589422436 \cdot z \cdot y^2 - 0.6606164056 \cdot z \cdot y^3 \\
& + 0.7158176859 \cdot z^2 \cdot y + 0.6233222389 \cdot z^2 \cdot y^2 + 0.2175905849 \cdot z^2 \cdot y^3 \\[4pt]
a_2 \ = \ & -0.4550505284 + 0.1300965967 \cdot z - 0.06995829336 \cdot z^2 - 0.03107882535 \cdot z^3 \\
& - 0.2438201115 \cdot y - 0.3079336093 \cdot y^2 - 0.05023497076 \cdot y^3 \\
& + 0.7849193467 \cdot z \cdot y + 0.7181240230 \cdot z \cdot y^2 + 0.2441835343 \cdot z \cdot y^3 \\
& - 0.7782697727 \cdot z^2 \cdot y - 0.7604596554 \cdot z^2 \cdot y^2 - 0.2139967639 \cdot z^2 \cdot y^3
\end{aligned}
\tag{17}
$$

The corresponding expansions for plane wave incidence are as follows:

Plane wave; $\vartheta_0 = 270°$:

$$
\begin{aligned}
a_0 \ = \ & -2.389774901 - 0.1395262072 \cdot y + 2.414652403 \cdot y^2 - 2.082638349 \cdot y^3 \\
& + 1.727712526 \cdot y^4 - 0.5024423058 \cdot y^5 \\[4pt]
a_1 \ = \ & -6.387181695 + 1.429899038 \cdot y - 6.294135235 \cdot y^2 + 22.1143696537 \cdot y^3 \\
& -19.7690393085 \cdot y^4 + 5.565221750 \cdot y^5 \\[4pt]
a_2 \ = \ & -2.552124597 - 2.342005059 \cdot y + 14.7867785184 \cdot y^2 - 38.0273605653 \cdot y^3 \\
& + 36.1731866937 \cdot y^4 - 10.7284415031 \cdot y^5 \\[4pt]
a_3 \ = \ & 0.5883191145 + 0.7953788225 \cdot y - 5.524362056 \cdot y^2 + 13.7842093181 \cdot y^3 \\
& - 13.6837211307 \cdot y^4 + 4.349290260 \cdot y^5
\end{aligned}
\tag{18}
$$

Plane wave; $\vartheta_0 = 225°$:

$$
\begin{aligned}
a_0 \ = \ & 1.568078212 + 0.04605330206 \cdot y + 0.9901780451 \cdot y^2 + 1.888227817 \cdot y^3 \\
& -1.204873300 \cdot y^4 - 0.5572513587 \cdot y^5 \\[4pt]
a_1 \ = \ & -3.081659731 - 0.5413285417 \cdot y + 8.6690503927 \cdot y^2 - 24.2944777516 \cdot y^3 \\
& + 19.7879485353 \cdot y^4 + 0.7720284647 \cdot y^5 \\[4pt]
a_2 \ = \ & -3.729226627 + 1.080888001 \cdot y - 4.076862638 \cdot y^2 + 52.4234791286 \cdot y^3 \\
& - 59.9341011899 \cdot y^4 + 11.3285552296 \cdot y^5 \\[4pt]
a_3 \ = \ & 0.6710694247 - 0.5457149106 \cdot y + 3.322227192 \cdot y^2 - 28.5329448742 \cdot y^3 \\
& + 41.1343130200 \cdot y^4 - 13.8714159690 \cdot y^5
\end{aligned}
\tag{19}
$$

Plane wave; $\vartheta_0 = 360°$ ($y = \vartheta_0 - \vartheta_q$ rad):

$$a_0 = -8.619029147 - 0.04914242523 \cdot y + 0.98893551678 \cdot y^2 - 0.09677973083 \cdot y^3$$
$$+0.04314542296 \cdot y^4 - 0.007092745198 \cdot y^5$$

$$a_1 = -8.495414675 + 0.6349841469 \cdot y - 0.9414382840 \cdot y^2 + 0.9074414634 \cdot y^3$$
$$-0.03120088534 \cdot y^4 - 0.03111306942 \cdot y^5$$

$$a_2 = -1.051533957 - 2.397034644 \cdot y + 6.111232667 \cdot y^2 - 5.903508575 \cdot y^3$$
$$+2.008747402 \cdot y^4 - 0.2088099622 \cdot y^5$$

$$a_3 = 0.2143116375 + 1.396801316 \cdot y - 3.902386481 \cdot y^2 + 3.949226446 \cdot y^3$$
$$-1.549939902 \cdot y^4 + 0.2033883155 \cdot y^5$$

(20)

E.6 Plane Wave Scattering at a Hard Screen

The hard screen is a special case with $\vartheta_0 = 2\pi$ of ▶ *Sect. E.5;* ▶ *Sect. E.7.*

A plane wave is incident in the direction ϑ_q. Its sound pressure at the screen corner is $p_Q(0)$. The radial wave number component is k (see ▶ *Sect. E.5*).
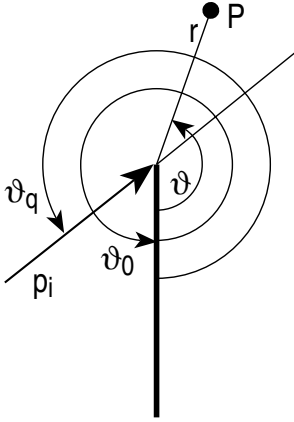
The sound pressure around the screen is

$$p(r, \vartheta) = p_Q(0)\frac{1+j}{2}\left\{e^{j\,kr\,\cos(\vartheta-\vartheta_q)}\left[\frac{1-j}{2} + C\left(\sqrt{2kr}\,\cos\frac{\vartheta-\vartheta_q}{2}\right)\right.\right.$$
$$\left. - jS\left(\sqrt{2kr}\,\cos\frac{\vartheta-\vartheta_q}{2}\right)\right]$$
$$+ e^{j\,kr\,\cos(\vartheta+\vartheta_q)}\left[\frac{1-j}{2} + C\left(\sqrt{2kr}\,\cos\frac{\vartheta+\vartheta_q}{2}\right)\right.$$
$$\left.\left. - jS\left(\sqrt{2kr}\,\cos\frac{\vartheta+\vartheta_q}{2}\right)\right]\right\}$$

(1)

with the Fresnel integrals defined by

$$S(x) = \sqrt{\frac{2}{\pi}} \int_0^x \sin(t^2)\, dt \quad ; \quad C(x) = \sqrt{\frac{2}{\pi}} \int_0^x \cos(t^2)\, dt. \tag{2}$$

E.7 Cylindrical or Plane Wave Scattering at a Screen with an Elliptical Cylinder Atop

▶ *See also:* Mechel (1997) for notation, formulas and evaluation of Mathieu functions.

A hard, thin screen of height h has a locally absorbing, elliptical cylinder at its top; the surface admittance of the cylinder is G; its long and short axes are 2a, 2b. The eccentricity of the ellipse is c.

A line source parallel to the axis of the ellipse is at Qu with the elliptical co-ordinates (ρ_q, φ_q). For $\rho_q \to \infty$; a plane wave incidence prevails.

First, the height h is taken as $h \to \infty$; then the arrangement is mirror-reflected at $y = -h$, and the scattering of the field from the mirror-reflected source is evaluated, then both fields are superposed.
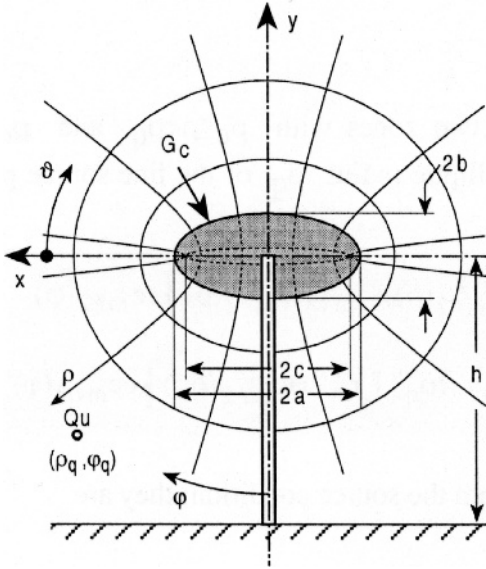
Transformation between Cartesian (x, y) and elliptic-hyperbolic (ρ, ϑ) co-ordinates:

$$x = c \cdot \cosh\rho \cdot \cos\vartheta \quad ; \quad y = c \cdot \sinh\rho \cdot \sin\vartheta \quad ; \quad z = z;$$
$$x \pm jy = c \cdot \cosh(\rho \pm j\vartheta). \tag{1}$$

Also used are the co-ordinates (ρ, φ) with

$$\varphi = \vartheta + \pi/2 \quad ; \quad \cos\vartheta = \sin\varphi \quad ; \quad \sin\vartheta = -\cos\varphi. \tag{2}$$

Geometrical parameters (with ρ_c on the elliptical cylinder):

$$\frac{a}{c} = \cosh \rho_c \;\; ; \;\; \frac{b}{c} = \sinh \rho_c \;\; ; \;\; \frac{b}{a} = \tanh \rho_c \;\; ; \;\; c = \frac{a}{\cosh \rho_c}. \tag{3}$$

With a separation $p(\rho, \vartheta, z) = R(\rho) \cdot T(\vartheta) \cdot Z(z)$ and an axial factor $Z(z)$ proportional to either one or a linear combination of the functions $Z(z) = e^{\pm jk_z z}$; $\cos(k_z)$; $\sin(k_z z)$ given by a wave with a wave number k_z leading to the wave number k in the plane normal to the axis with $k^2 = k_0^2 - k_z^2$, the axial factor $Z(z)$ can be dropped; only $p(\rho, \vartheta)$ will be given.

Sound field from a line source

The line source is placed at (ρ_q, ϑ_q) or (ρ_q, φ_q). Its polar distance to the origin is r_q with

$$r_q^2 = x_q^2 + y_q^2 = c^2 \cdot \left[\cosh^2 \rho_q \cdot \sin^2 \varphi_q + \sinh^2 \rho_q \cdot \cos^2 \varphi_q \right]. \tag{4}$$

When it has a volume flow q (per unit length), then it will produce the sound pressure in free space at the position of the origin:

$$p_Q(0) = \frac{1}{4} Z_0 k_0 r_q \cdot q \cdot H_0^{(2)}(k r_q). \tag{5}$$

General field formulations in the two zones with $\rho_c \le \rho < \rho_q$ and $\rho_q < \rho < \infty$, respectively, separated from each other by the elliptic radius ρ_q of the line source position, are (integer summation index m)

$$p_1(\rho, \varphi) = \sum_{m \ge 0} a_m \cdot Hc_{m/2}^{(2)}(\rho_q) \cdot \left[Hc_{m/2}^{(1)}(\rho) + r_m \cdot Hc_{m/2}^{(2)}(\rho) \right] \cdot ce_{m/2}(\varphi),$$

$$p_2(\rho, \varphi) = \sum_{m \ge 0} a_m \cdot Hc_{m/2}^{(2)}(\rho) \cdot \left[Hc_{m/2}^{(1)}(\rho_q) + r_m \cdot Hc_{m/2}^{(2)}(\rho_q) \right] \cdot ce_{m/2}(\varphi). \tag{6}$$

The term amplitudes a_m follow from the source condition; they are

$$a_m = \frac{Z_0 q \cdot k_0 c}{2} \sum_{n \ge 0} ce_{n/2}(\varphi_q) \cdot Ic_{m,n}(\rho_q) \tag{7}$$

with the integrals (about which see below)

$$Ic_{m,n}(\rho) := \frac{1}{2\pi} \int_0^{2\pi} \sqrt{\sinh^2 \rho + \cos^2 \varphi} \cdot ce_{m/2}(\varphi) \cdot ce_{n/2}(\varphi) \, d\varphi. \tag{8}$$

The modal reflection factors r_m (at the cylinder surface) are obtained from the boundary condition at the cylinder with the form $b_m = r_m \cdot a_m$ from the system of equations (with explicitly known a_m):

$$\sum_{m \ge 0} b_m \cdot Hc_{m/2}^{(2)}(\rho_q) \cdot \left[G_c \cdot Hc_{m/2}^{(2)}(\rho_c) \cdot Ic_{m,n}(\rho_c) + \delta_{m,n} \cdot \frac{j}{2k_0 c} Hc_{m/2}^{\prime(2)}(\rho_c) \right]$$

$$= - \sum_{m \ge 0} a_m \cdot Hc_{m/2}^{(2)}(\rho_q) \cdot \left[G_c \cdot Hc_{m/2}^{(1)}(\rho_c) \cdot Ic_{m,n}(\rho_c) + \delta_{m,n} \cdot \frac{j}{2k_0 c} Hc_{m/2}^{\prime(1)}(\rho_c) \right] \tag{9}$$

($\delta_{m,n}$ the Kronecker symbol).

First special case: In the first special case, the cylinder is supposed to be rigid, $G_c = 0$. The system of equations for the r_m simplifies to

$$b_m = r_m \cdot a_m = -a_m \cdot \frac{Hc_{m/2}^{\prime(1)}(\rho_c)}{Hc_{m/2}^{\prime(2)}(\rho_c)}. \tag{10}$$

Second special case: In the second special case with $\rho_c = 0$, in which the cylinder degenerates to an absorbing strip of width 2c, the equations formally remain unchanged, but the integrals $Ic_{m,n}(\rho_c)$ simplify drastically, as will be seen below.

Third special case: The third special case is a combination of the first and second: $G_c = 0$ and $\rho_c = 0$; the cylinder changes to a rigid strip. Then

$$b_m = r_m \cdot a_m = -a_m \cdot \frac{Hc_{m/2}^{\prime(1)}(0)}{Hc_{m/2}^{\prime(2)}(0)}. \tag{11}$$

There still remain the integrals $Ic_{m,n}(\rho)$ to be evaluated. They can be expressed in terms of the Fourier coefficients A_ν of the even azimuthal Mathieu functions $ce_\mu(\varphi)$, B_ν of the odd azimuthal Mathieu functions $se_\mu(\varphi)$, which are needed at any rate for the evaluation of such Mathieu functions.

When μ and ν are integers and both even, then:

$$Ic_{m.n}(\rho) = \frac{(-1)^{(\mu+\nu)/2}}{4\pi} \sum_{s,\sigma \geq 0} (-1)^{s+\sigma} A_{2s}(\mu) \cdot A_{2\sigma}(\nu) \cdot \left[I_{|s-\sigma|}(\rho) + I_{s+\sigma}(\rho) \right] \tag{12}$$

with

$$\begin{aligned} I_i(\rho) &= \int_0^{2\pi} \cos(2i\varphi) \cdot \sqrt{\sinh^2 \rho + \cos^2 \varphi} \, d\varphi \\ &= 4 \int_0^{\pi/2} \cos(2i\varphi) \cdot \sqrt{\sinh^2 \rho + \cos^2 \varphi} \, d\varphi \quad ; \quad 2i = \text{even} \\ &= 0 \quad ; \quad 2i = \text{odd} \end{aligned} \tag{13}$$

and the values

$$I_i(\rho) = 2\pi(-1)^{i+1} \cdot \cosh\rho \sum_{k\geq0} \frac{(2(i+k)-3)!! \cdot (2(i+k)-1)!!}{k! \cdot (2i+k)!} \frac{1}{(2\cosh\rho)^{2(i+k)}} ; \tag{14}$$

$$i \geq 1 \quad ; \quad \rho > 0 \quad ; \quad (0)!! = (-1)!! = 1 \quad ; \quad (2n+1)!! = 1 \cdot 3 \cdot 5 \cdot \ldots \cdot (2n+1)$$

with the special value $I_0(\rho) = 4 \cosh\rho \cdot E(1/\cosh\rho)$, ($E(z)$ the exponential integral), and for $\rho = 0$:

$$I_i(0) = \begin{cases} \pi & ; \quad 2i+1 = 0; \\ 2\left[\dfrac{\sin(2i-1)\pi/2}{2i-1} + \dfrac{\sin(2i+1)\pi/2}{2i+1} \right] & ; \quad 2i = \text{even}; \\ 0 & ; \quad 2i = \text{odd} \neq 1. \end{cases} \tag{15}$$

When μ and ν are integers and both odd, then

$$I_{cm,n}(\rho) = \frac{(-1)^{(\mu+\nu-2)/2}}{4\pi} \sum_{s,\sigma \geq 0} (-1)^{s+\sigma} B_{2s+1}(\mu) \cdot B_{2\sigma+1}(\nu) \cdot \left[I_{|s-\sigma|}(\rho) + I_{s+\sigma+1}(\rho) \right]. \tag{16}$$

When μ and ν are integers, one even the other odd, then $I_{cm,n}(\rho) = 0$.

When μ is half-valued, ν is an integer, or inversely, then $I_{cm,n}(\rho) = 0$.

When μ, ν are both half-valued, with $\mu = \mu' + 1/2$, $\nu = \nu' + 1/2$, and both μ', ν' even or odd:

$$I_{cm,n}(\rho) = \frac{1}{4\pi} \sum_{s,\sigma=-\infty}^{+\infty} (-1)^{s+\sigma} C_{2s}(\mu) \cdot C_{2\sigma}(\nu) \cdot I_{|(\mu'-\nu')/2+s-\sigma|}(\rho). \tag{17}$$

When μ, ν are both half-valued, with μ' even, ν' odd, or inversely:

$$I_{cm,n}(\rho) = \frac{1}{4\pi} \sum_{s,\sigma=-\infty}^{+\infty} (-1)^{s+\sigma} C_{2s}(\mu) \cdot C_{2\sigma}(\nu) \cdot I_{|(\mu'+\nu'+1)/2+s+\sigma|}(\rho). \tag{18}$$

One gets in the limit $\rho \to \infty$ with　$\sqrt{\sinh^2 \rho + \cos^2 \varphi} = \sqrt{\cosh^2 \rho - \sin^2 \varphi} \to \cosh\rho$: (19)

$$I_i(\rho) \to 4\cosh\rho \int_0^{\pi/2} \cos(2i\varphi)\, d\varphi = \begin{cases} 2\pi \cosh\rho; & i = 0; \\ 0; & i \neq 0, \quad \text{integer;} \\ 2\pi \cosh\rho \cdot \sin(i\pi)/(i\pi); & \text{else.} \end{cases} \tag{20}$$

This gives in the above cases of non-zero $I_{cm,n}(\rho)$

$$I_{cm,n}(\rho) \to \frac{1}{2}(-1)^{(\mu+\nu)/2} \cosh\rho \cdot \left[\sum_{s,\sigma \geq 0; s=\sigma} A_{2s}(\mu) \cdot A_{2\sigma}(\nu) + A_0(\mu) \cdot A_0(\nu) \right],$$

$$I_{cm,n}(\rho) \to \frac{1}{2}(-1)^{(\mu+\nu)/2-1} \cosh\rho \cdot \sum_{s,\sigma \geq 0; s=\sigma} B_{2s+1}(\mu) \cdot B_{2\sigma+1}(\nu),$$

$$I_{cm,n}(\rho) = \frac{1}{2} \cosh\rho \cdot \sum_{\substack{s,\sigma=-\infty \\ (\mu'-\nu')/2+s-\sigma=0}}^{\infty} (-1)^{s+\sigma} C_{2s}(\mu) \cdot C_{2\sigma}(\nu),$$

$$I_{cm,n}(\rho) = \frac{1}{2} \cosh\rho \cdot \sum_{\substack{s,\sigma=-\infty \\ (\mu'+\nu'+1)/2+s+\sigma=0}}^{\infty} (-1)^{s+\sigma} C_{2s}(\mu) \cdot C_{2\sigma}(\nu). \tag{21}$$

Sound field from a plane wave

This case is treated as the limit $\rho_q \to \infty$. The polar radius r_q of the source position approaches $r_q \to c \cdot \cosh\rho_q$, whence $2\sqrt{q} \cosh\rho_q \to kr_q$. One further replaces

$$Z_0 q = \frac{4\, p_Q(0)}{k_0 r_q \cdot H_0^{(2)}(kr_q)}. \tag{22}$$

Finally, one replaces above

$$a_m \cdot Hc^{(2)}_{m/2}(\rho_q) \xrightarrow[\rho_q \to \infty]{} 2p_Q(0) \cdot e^{jm\pi/4} \cdot \sum_{n \geq 0} ce_{n/2}(\varphi_q) \cdot Ic'_{m,n}, \tag{23}$$

and in $\quad b_m \cdot Hc^{(2)}_{m/2}(\rho_q) = r_m \cdot a_m \cdot Hc^{(2)}_{m/2}(\rho_q). \tag{24}$

Rigid screen with a mushroom-like hat

The cylindrical body atop the screen has a semielliptical shape; its surface is curved and rigid on the upper side and flat and absorbing on its lower side with the admittance G_c.
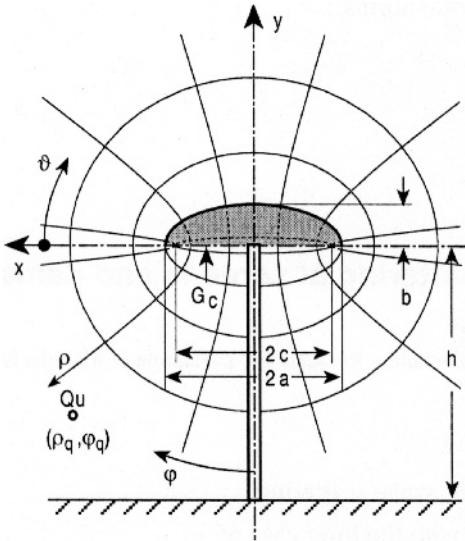
The boundary condition at the cylinder is

$$G_c = \begin{cases} 0; & \pi/2 \leq \varphi \leq 3\pi/2 \,, \\ \\ G_c; & \text{else}\,, \end{cases}$$

$$\rho_c = \begin{cases} \rho_c; & \pi/2 \leq \varphi \leq 3\pi/2 \,, \\ \\ 0; & \text{else}\,, \end{cases} \tag{25}$$

i.e.:

$$\frac{j}{k_0 c \sqrt{\sinh^2 \rho + \cos^2 \varphi}} \frac{\partial p_1}{\partial \rho} = \begin{cases} 0 & ; \quad \rho = \rho_c \; ; \quad \pi/2 \leq \varphi \leq 3\pi/2, \\ \\ -G_c \cdot p_1 & ; \quad \rho = 0 \quad ; \quad \text{else}. \end{cases} \tag{26}$$

The term amplitudes a_m remain as above; the system of equations for the $b_m = r_m \cdot a_m$ changes to

$$
\sum_{m \geq 0} b_m \cdot Hc^{(2)}_{m/2}(\rho_q)
$$

$$
\cdot \left[\left(Hc'^{(2)}_{m/2}(\rho_c) - Hc'^{(2)}_{m/2}(0) \right) \frac{1}{2\pi} \int\limits_{\pi/2}^{3\pi/2} ce_{m/2}(\varphi) \cdot ce_{n/2}(\varphi) \, d\varphi \right.
$$

$$
- j\,k_0 c \cdot G_c \cdot Hc^{(2)}_{m/2}(0) \frac{1}{2\pi} \int\limits_{else} |\cos\varphi| \cdot ce_{m/2}(\varphi) \cdot ce_{n/2}(\varphi) \, d\varphi
$$

$$
\left. + \delta_{m,n} N_m Hc'^{(2)}_{m/2}(0) \right]
$$

$$
= - \sum_{m \geq 0} a_m \cdot Hc^{(2)}_{m/2}(\rho_q)
$$

$$
\cdot \left[\left(Hc'^{(1)}_{m/2}(\rho_c) - Hc'^{(1)}_{m/2}(0) \right) \frac{1}{2\pi} \int\limits_{\pi/2}^{3\pi/2} ce_{m/2}(\varphi) \cdot ce_{n/2}(\varphi) \, d\varphi \right.
$$

$$
- j\,k_0 c \cdot G_c \cdot Hc^{(1)}_{m/2}(0) \frac{1}{2\pi} \int\limits_{else} |\cos\varphi| \cdot ce_{m/2}(\varphi) \cdot ce_{n/2}(\varphi) \, d\varphi
$$

$$
\left. + \delta_{m,n} N_m Hc'^{(1)}_{m/2}(0) \right].
$$

(27)

The N_m are the azimuthal mode norms:

$$
N_m = \frac{1}{2\pi} \int\limits_0^{2\pi} ce^2_{m/2}(\varphi) \, d\varphi.
$$

(28)

E.8   Uniform Scattering at Screens and Dams

▶ *See also:* Mechel, A Uniform Theory of Sound Screens and Dams (1997), see Mechel, Mathieu Functions (1997) for notation, formulas and evaluation of Mathieu functions

This section describes the plane wave scattering
- at a "high" absorbent dam, with the limit case of
  - a thin absorbent screen;
- at a "flat" absorbent dam, with the limit case of
  - a flat absorbent strip in a rigid baffle wall.

A semicircular absorbent dam could also be treated as a limiting case of this uniform theory (it will, however, be discussed separately in ▶ *Sect. 10*). All objects are situated on a hard ground. All absorbent objects are locally reacting with a normalised surface admittance G.

The distinction between "high" and "flat" dam is necessary because of the orientation of the axes and co-ordinates of the elliptical cylinder, with which the objects are modelled.
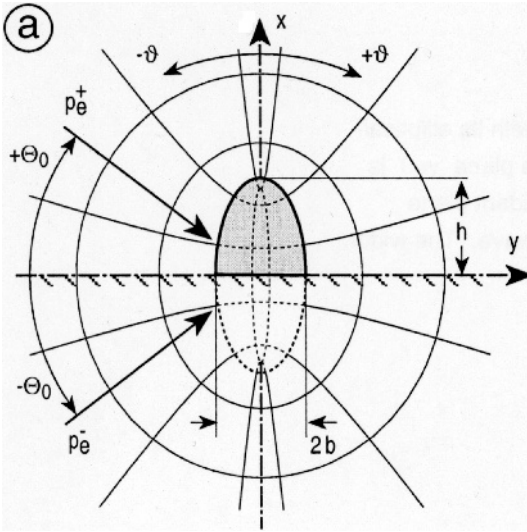
A high dam with its elliptical-hyperbolic co-ordinate system. The plane $x = 0$ is the hard ground. p_e^+ is the incident plane wave; p_e^- is the mirror-reflected wave. The height of the dam is h; its width at ground level is 2b
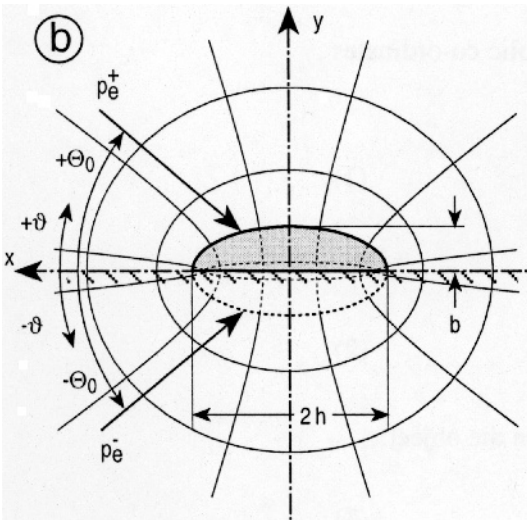
A flat dam with its elliptical-hyperbolic co-ordinate system. The plane $y = 0$ is the hard ground. p_e^+ is the incident plane wave; p_e^- is the mirror-reflected wave. The height of the dam is b; its width at ground level is 2h
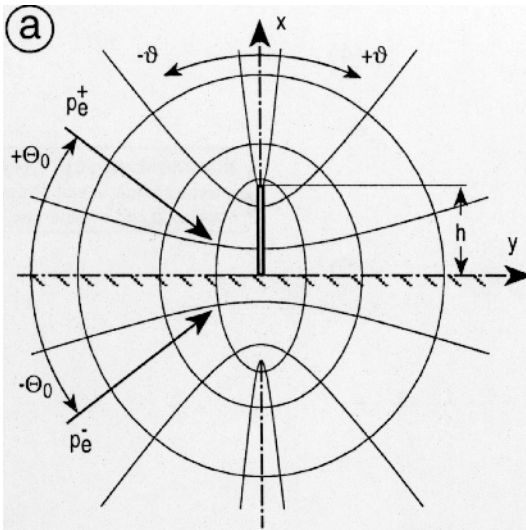
Limit cases are:

A thin, absorbent screen with its elliptical-hyperbolic co-ordinate system. The plane $x = 0$ is the hard ground. p_e^+ is the incident plane wave; p_e^- is the mirror-reflected wave. The height of the screen is h
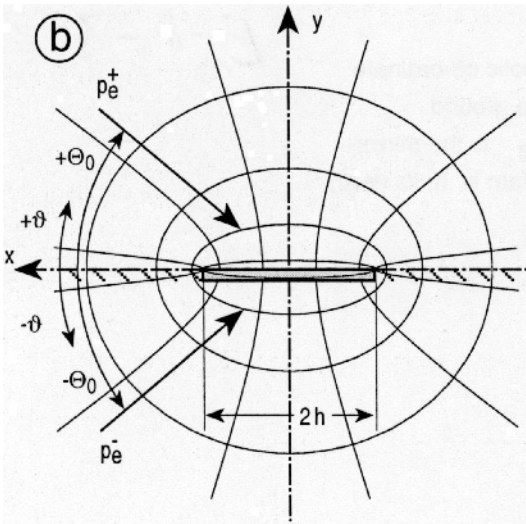

An absorbent strip in a hard baffle with its elliptical-hyperbolic co-ordinate system. The plane $y = 0$ is the hard baffle wall. p_e^+ is the incident plane wave; p_e^- is the mirror-reflected wave. The width of the strip is 2h

The co-ordinate transformation between Cartesian (x,y) and elliptic-hyperbolic co-ordinates $(\rho\vartheta)$ is, with the eccentricity of the ellipses c,

$$\left.\begin{array}{l} x = c \cdot \cosh\rho \cdot \cos\vartheta \\ \\ y = c \cdot \sinh\rho \cdot \sin\vartheta \end{array}\right\} \quad ; \quad 0 \le \rho < \infty \quad ; -\pi \le \vartheta \le +\pi \tag{1}$$

and in the backward direction:

$$\rho + j\vartheta = \text{area } \cosh(\xi + j\eta) = \ln\left(\xi + jn \pm \sqrt{(\xi + j\eta)^2 - 1}\right), \tag{2}$$

with $\xi = x/c$, $\eta = y/c$. Geometrical parameters are with the elliptical radius ρ_c on the object:

$$\left.\begin{array}{l} h/c = \cosh\rho_c \\ b/c = \sinh\rho_c \end{array}\right\} \quad ; \quad b/h = \tanh\rho_c; \quad c = \frac{h}{\cosh\rho_c}. \tag{3}$$

The geometrical shadow limit for plane wave incidence with an angle Θ_0 is given by

$$h/c - \text{tg}\Theta_0 \cdot \sinh\rho \cdot \sin\vartheta = \cosh p \cdot \cos\vartheta . \tag{4}$$
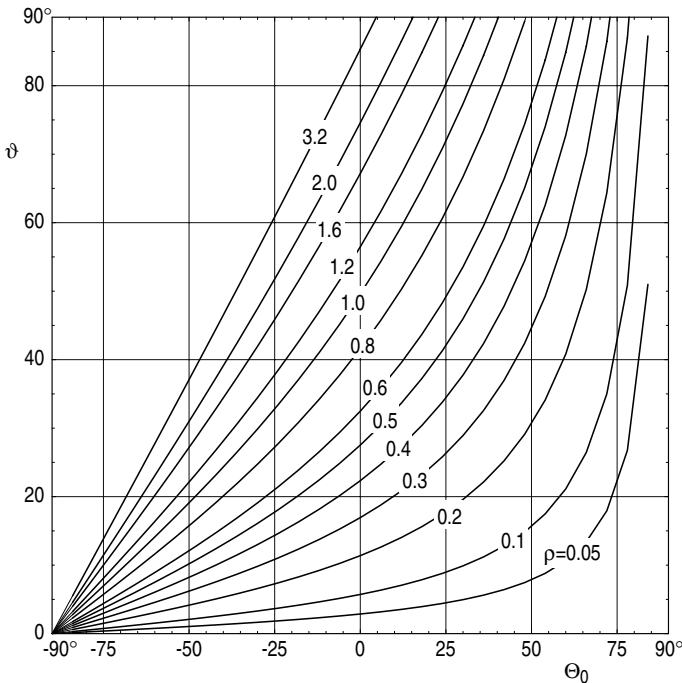
Geometrical shadow limits for $h/c = 1$

With the special cases

$$\rho = 0: \quad \vartheta = \arccos(h/c) \xrightarrow[h/c \to 1]{} 0,$$

$$\Theta_0 = 0: \quad \vartheta = \arccos \frac{h/c}{\cosh \rho}, \tag{5}$$

$$\rho \gg 1: \quad \vartheta \approx -\arctan \frac{h/c}{\tan \Theta_0 \tanh \rho}.$$

Let $p_e^{\pm}$ be the incident wave and the mirror-reflected wave at the ground. $p_e = p_e^+ + p_e^-$ then is the "exciting" wave with hard ground, and $p_e = p_e^+ + \underline{r} \cdot p_e^-$ the exciting wave with absorbing ground having a reflection factor $\underline{r}$. The total field is composed of the sum $p = p_e + p_{rs}$ of the exciting wave p_e and a "reflected plus scattered" wave p_{rs}.

The following description uses the second principle of superposition from ⊳ *Sect. B.10*, i.e. the task is subdivided in two subtasks (ß) = (h), (w), in which the plane of symmetry through the scattering object (where it is sound transmissive) is considered first as hard (h), second as soft (w). The reflected plus scattered wave is marked and decomposed in both subtasks as $p_{rs}^{(\beta)} = p_r^{(\beta)} + p_s^{(\beta)}$, where $p_r^{(\beta)}$ is the reflected wave at the plane of symmetry, with hard reflection for (ß) = (h) and soft reflection for (ß) = (w), respectively, i.e. $p_r^{(w)}(y) = -p_r^{(h)}(y)$. The component $p_s^{(\beta)}$ is the "truly" scattered wave. At the high dam, the co-ordinate normal to the plane of symmetry is $y \to \vartheta$. According to the principle of superposition the sound field on the front side (side of sound incidence) is

$$p_{\text{front}}(\vartheta < 0) = p_e(\vartheta) + \frac{1}{2}\left[p_s^{(h)}(\vartheta) + p_s^{(w)}(\vartheta)\right]$$

$$= \frac{1}{2}\left[\left(p_e(\vartheta) + p_r^{(h)}(\vartheta)\right) + p_s^{(h)}(\vartheta) + \left(p_e(\vartheta) + p_r^{(w)}(\vartheta)\right) + p_s^{(w)}(\vartheta)\right] \tag{6}$$

and the transmitted sound field on the back side is:

$$p_{\text{back}}(\vartheta > 0) = p_e(\vartheta) + \frac{1}{2}\left[p_s^{(h)}(-\vartheta) - p_s^{(w)}(-\vartheta)\right]$$

$$= \frac{1}{2}\left[\left(p_e(-\vartheta) + p_r^{(h)}(-\vartheta)\right)\right. \tag{7}$$

$$\left. + p_s^{(h)}(-\vartheta) - \left(p_e(-\vartheta) + p_r^{(w)}(-\vartheta)\right) - p_s^{(w)}(-\vartheta)\right].$$

The basis for the field analysis is the decomposition of a plane wave in Mathieu functions:

$$u(x, y) = e^{-j k_0(x \cos \alpha + y \sin \alpha)}$$

$$= 2 \sum_{m=0}^{\infty} (-j)^m ce_m(\alpha) \cdot ce_m(\vartheta) \cdot Jc_m(\rho) \tag{8}$$

$$+ 2 \sum_{m=1}^{\infty} (-j)^m se_m(\alpha) \cdot se_m(\vartheta) \cdot Js_m(\rho)$$

(α is the angle between the wave number vector and the positive x axis), and the decomposition of the Hankel function of the second kind in Mathieu functions:

$$H_0^{(2)}(k_0 R) = 2 \left[\sum_{m \geq 0} ce_m(\vartheta_0) \cdot ce_m(\vartheta) \cdot \begin{cases} Jc_m(\rho_0) Hc_m^{(2)}(\rho) & ; \quad \rho > \rho_0 \\\\ Jc_m(\rho) Hc_m^{(2)}(\rho_0) & ; \quad \rho < \rho_0 \end{cases} \right.$$

$$\left. + \sum_{m \geq 1} se_m(\vartheta_0) \cdot se_m(\vartheta) \cdot \begin{cases} Js_m(\rho_0) Hs_m^{(2)}(\rho) & ; \quad \rho > \rho_0 \\\\ Js_m(\rho) Hs_m^{(2)}(\rho_0) & ; \quad \rho < \rho_0 \end{cases} \right] \tag{9}$$

with the source of the Hankel function in the elliptical co-ordinates (ρ_0, ϑ_0). The parameter of the Mathieu differential equation is $q = (k_0 c)^2 / 4$; $ce_m(\vartheta)$, $se_m(\vartheta)$ are even and odd azimuthal Mathieu functions; $Jc_m(\rho)$, $Yc_m(\rho)$, $Hc_m^{(2)}(\rho) = Jc_m(\rho) - j \cdot Yc_m(\rho)$ and $Js_m(\rho)$, $Ys_m(\rho)$, $Hs_m^{(2)}(\rho) = Js_m(\rho) - j \cdot Ys_m(\rho)$ are the associated radial Mathieu-Bessel, Mathieu-Neumann and Mathieu-Hankel functions.

High dam

Let the incident wave be a plane wave with $\alpha^\pm = \pi/2 \pm \Theta_0$. The exciting wave on hard ground is:

$$p_e = p_e^+ + p_e^- = P_e e^{-jk_y y} (e^{+jk_x x} + e^{-jk_x x}) = 2P_e \cos k_x x \cdot e^{-jk_y y}, \tag{10}$$

and with absorbing ground:

$$p_e = p_e^+ + \underline{r} \cdot p_e^- = P_e e^{-jk_y y} (e^{+jk_x x} + \underline{r} \cdot e^{-jk_x x}) \tag{11}$$

with $\quad k_x = k_0 \sin \Theta_0 \quad ; \quad k_y = k_0 \cos \Theta_0$, $\tag{12}$

With hard ground, the exciting and reflected waves are in both subtasks h, w:

$$p_e + p_r^{(h)} = 8P_e \sum_{r \geq 0} (-j)^{2r} ce_{2r}(\alpha^+) \cdot ce_{2r}(\vartheta) \cdot Jc_{2r}(\rho), \tag{13}$$

$$p_e + p_r^{(w)} = 8P_e \sum_{r \geq 0} (-j)^{2r+1} se_{2r+1}(\alpha^+) \cdot se_{2r+1}(\vartheta) \cdot Js_{2r+1}(\rho). \tag{14}$$

The scattered waves are formulated as:

$$p_s^{(h)} = P_e \sum_{r \geq 0} C_r \cdot ce_{2r}(\vartheta) \cdot Hc_{2r}^{(2)}(\rho), \tag{15}$$

$$p_s^{(w)} = P_e \sum_{r \geq 0} S_r \cdot se_{2r+1}(\vartheta) \cdot Hs_{2r+1}^{(2)}(\rho) \tag{16}$$

with still undetermined term amplitudes C_r, S_r. They follow from the boundary condition at the elliptic cylinder:

$$-Z_0 \left(v_{e\rho} + v_{r\rho}^{(\text{ß})} + v_{s\rho}^{(\text{ß})} \right)_{\rho = \rho_c} \overset{!}{=} G \cdot \left(p_e + p_r^{(\text{ß})} + p_s^{(\text{ß})} \right)_{\rho = \rho_c} \tag{17}$$

using the integrals

$$Ic_{m,\mu}(u) := \int_0^\pi ce_m(t) \cdot ce_\mu(t) \cdot \sqrt{u^2 + \sin^2 t}\, dt \quad ; \quad u^2 = \sinh^2 \rho$$

$$(18)$$

$$Is_{m,\mu}(u) := \int_0^\pi se_m(t) \cdot se_\mu(t) \cdot \sqrt{u^2 + \sin^2 t}\, dt$$

and the orthogonality relation:

$$\int_0^\pi ce_m(t) \cdot ce_\mu(t)\, dt = \int_0^\pi se_m(t) \cdot se_\mu(t)\, dt = \delta_{m,\mu} \cdot \pi/2. \tag{19}$$

One gets the following systems of equations for the term amplitudes:

For (ß) = (h) by: $\displaystyle\int_0^\pi \ldots \cdot ce_{2s}(t) \cdot \sqrt{u^2 + \sin^2 t}\, dt \quad ; \quad s \geq 0$

$$\sum_{r\geq 0} C_r \cdot \left[\delta_{r,s} \frac{j\pi}{2\,k_0 c} Hc_{2r}^{\prime(2)}(\rho_c) + G \cdot Hc_{2r}^{(2)}(\rho_c) \cdot Ic_{2r,2s} \right]$$

$$(20)$$

$$= -8 \sum_{r\geq 0} (-j)^{2r} ce_{2r}(\alpha^+) \cdot \left[\delta_{r,s} \frac{j\pi}{2\,k_0 c} Jc_{2r}'(\rho_c) + G \cdot Jc_{2r}(\rho_c) \cdot Ic_{2r,2s} \right]; \quad s \geq 0.$$

For (ß) = (w) by: $\displaystyle\int_0^\pi \ldots \cdot se_{2s+1}(t) \cdot \sqrt{u^2 + \sin^2 t}\, dt \quad ; \quad s \geq 0$

$$\sum_{r\geq 0} S_r \cdot \left[\delta_{r,s} \frac{j\pi}{2\,k_0 c} Hs_{2r+1}^{\prime(2)}(\rho_c) + G \cdot Hs_{2r+1}^{(2)}(\rho_c) \cdot Is_{2r+1,2s+1} \right] = -8 \sum_{r\geq 0} (-j)^{2r} se_{2r+1}(\alpha^+)$$

$$(21)$$

$$\cdot \left[\delta_{r,s} \frac{j\pi}{2\,k_0 c} Js_{2r+1}'(\rho_c) + G \cdot Js_{2r+1}(\rho_c) \cdot Ic_{2r+1,2s+1} \right]; \quad s \geq 0.$$

With the Fourier coefficients $A_v(\mu)$ of the $ce_\mu(z)$ and $B_v(\mu)$ of the $se_\mu(z)$, the required integrals are

$$Ic_{m,\mu} = \sum_{n,v\geq 0} A_n(m) \cdot A_v(\mu) \cdot \int_0^\pi \cos(n\vartheta) \cos(v\vartheta) \sqrt{u^2 + \sin^2 \vartheta}\, d\vartheta$$

$$(22)$$

$$Is_{m,\mu} = \sum_{n,v\geq 1} B_n(m) \cdot B_v(\mu) \cdot \int_0^\pi \sin(n\vartheta) \sin(v\vartheta) \sqrt{u^2 + \sin^2 \vartheta}\, d\vartheta,$$

and

$$Ic_{m,\mu} = \frac{1}{2} \sum_{n,\nu \geq 0} A_n(m) \cdot A_\nu(\mu) \cdot [I_{(n-\nu)/2} + I_{(n+\nu)/2}],$$

$$Is_{m,\mu} = \frac{1}{2} \sum_{n,\nu \geq 0} B_n(m) \cdot B_\nu(\mu) \cdot [I_{(n-\nu)/2} - I_{(n+\nu)/2}],$$

(23)

where

$$I_i = I_i(u) := \int_0^\pi \cos(2i\vartheta)\sqrt{u^2 + \sin^2 \vartheta} \, d\vartheta.$$

(24)

Special case of a hard high dam, i.e. $G = 0$:

Has the explicit solutions:

$$C_r = -8(-1)^{2r} ce_{2r}(\alpha^+) \frac{Jc'_{2r}(\rho_W)}{Hc'^{(2)}_{2r}(\rho_W)} \quad ; \quad S_r = -8(-1)^{2r+1} se_{2r+1}(\alpha^+) \frac{Js'_{2r+1}(\rho_W)}{Hs'^{(2)}_{2r+1}(\rho_W)}.$$

(25)

Special case of a thin screen, i.e. $\rho_c \to 0$:

Has the special values:

$$Jc'_m(0) = 0 \quad ; \quad Js_m(0) = 0 \quad ; \quad Hc'^{(2)}_m(0) = -j\,Yc'_m(0) \quad ; \quad Hs^{(2)}_m(0) = -j\,Ys_m(0) \quad (26)$$

and if further $G = 0$, i.e. the screen is hard: $C_r = 0$.

With absorbent ground, having the reflection factor $\underline{r}$:

Exciting and reflected wave ($\alpha^\pm = \pi/2 \pm \Theta_0$):

$$p_e + p_r^{(h)} = 4P_e \sum_{m \geq 0} (-j)^m ce_m(\alpha^+)(1 + \underline{r} \cdot (-1)^m) \cdot ce_m(\vartheta) \cdot Jc_m(\rho),$$

$$p_e + p_r^{(w)} = 4P_e \sum_{m \geq 1} (-j)^m se_m(\alpha^+)(1 - \underline{r} \cdot (-1)^m) \cdot se_m(\vartheta) \cdot Js_m(\rho).$$

(27)

Formulation of the scattered waves for both subtasks h, w:

$$p_s^{(h)} = P_e \sum_{m \geq 0} C_m \cdot ce_m(\vartheta) \cdot Hc_m^{(2)}(\rho),$$

$$p_s^{(w)} = P_e \sum_{m \geq 1} S_m \cdot se_m(\vartheta) \cdot Hs_m^{(2)}(\rho).$$

(28)

The systems of equations for the term amplitudes C_m, S_m become

$$\sum_{m \geq 0} C_m \cdot \left[\delta_{m,\mu} \frac{j\pi}{2k_0c} Hc_m'^{(2)}(\rho_c) + Z_0 G \cdot Hc_m^{(2)}(\rho_c) \cdot Ic_{m,\mu} \right]$$

$$= -4 \sum_{m \geq 0} (-j)^m ce_m(\alpha^+)\, (1 + \underline{r} \cdot (-1)^m) \cdot \left[\delta_{m,\mu} \frac{j\pi}{2k_0c} Jc'_m(\rho_c) + Z_0 G \cdot Jc_m(\rho_c) \cdot Ic_{m,\mu} \right]; \quad (29)$$

$$\mu \geq 0$$

$$\sum_{m\geq1} S_m \cdot \left[\delta_{m,\mu}\frac{j\,\pi}{2\,k_0 c}Hs_m''^{(2)}(\rho_c) + Z_0 G \cdot Hs_m^{(2)}(\rho_c) \cdot Is_{m,\mu}\right]$$

$$=-4\sum_{m\geq1}(-j)^m se_m(\alpha^+)\,(1-\underline{r}\cdot(-1)^m)\cdot\left[\delta_{m,\mu}\frac{j\,\pi}{2\,k_0 c}Js_m'(\rho_c)+Z_0 G \cdot Js_m(\rho_c) \cdot Is_{m,\mu}\right];\quad \cdot\,(30)$$

$$\mu \geq 1$$

The orders m,µ in the integrals $Ic_{m,\mu}$, $Is_{m,\mu}$ have the same parity.

High dam and cylindrical incident wave

The original source (1) is at (ρ_0, ϑ_0). Some mirror sources (2)…(4) are used.

The original free field is

$$p_e^+ = p_1 = P_e \cdot H_0^{(2)}(k_0 R_1). \tag{31}$$
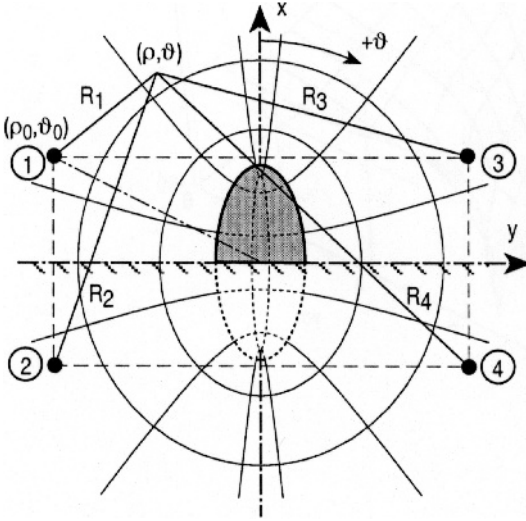
The exciting wave with hard ground is:

$$p_e = p_e^+ + p_e^- = P_e \cdot [H_0^{(2)}(k_0 R_1) + H_0^{(2)}(k_0 R_2)], \tag{32}$$

and with absorbent ground:

$$p_e = p_e^+ + \underline{r} \cdot p_e^- = P_e \cdot [H_0^{(2)}(k_0 R_1) + \underline{r} \cdot H_0^{(2)}(k_0 R_2)]. \tag{33}$$

In the range $\rho < \rho_0$, and especially $\rho = \rho_c$ one has with a hard ground:

$$p_e + p_r^{(h)} = 8P_e \sum_{r\geq0} ce_{2r}(\vartheta_0) \cdot ce_{2r}(\vartheta) \cdot Jc_{2r}(\rho) \cdot Hc_{2r}^{(2)}(\rho_0), \tag{34}$$

$$p_e + p_r^{(w)} = 8P_e \sum_{r\geq0} se_{2r+1}(\vartheta_0) \cdot se_{2r+1}(\vartheta) \cdot Js_{2r+1}(\rho) \cdot Hs_{2r+1}^{(2)}(\rho_0). \tag{35}$$

The formulations for the scattered waves of the subtasks (ß) = (h), (w) remain as above. The systems of equations for the term amplitudes are obtained from those above by the following substitutions ($\alpha^{\pm} = \pi/2 \pm \Theta_0$):

$$(\beta) = \begin{cases} \text{(h):} & (-j)^m \cdot ce_m(\alpha^+) \rightarrow ce_m(\vartheta_0) \cdot Hc_m^{(2)}(\rho_0), \\[2mm] \text{(w):} & (-j)^m \cdot se_m(\alpha^+) \rightarrow se_m(\vartheta_0) \cdot Hs_m^{(2)}(\rho_0). \end{cases} \tag{36}$$

An absorbent ground is introduced as above.

20 lg|p(x/h, y/h)/p_norm|
h=4 [m] ; b/h=0.5 ; f=500 [Hz] ; 2c/λ₀=10.091 ; G=0.25 – j1 ;
ρ₀=1.5 ; Θ₀=-87° ; Δr=8 ; Δϑ=6° ; Δρ=0.25
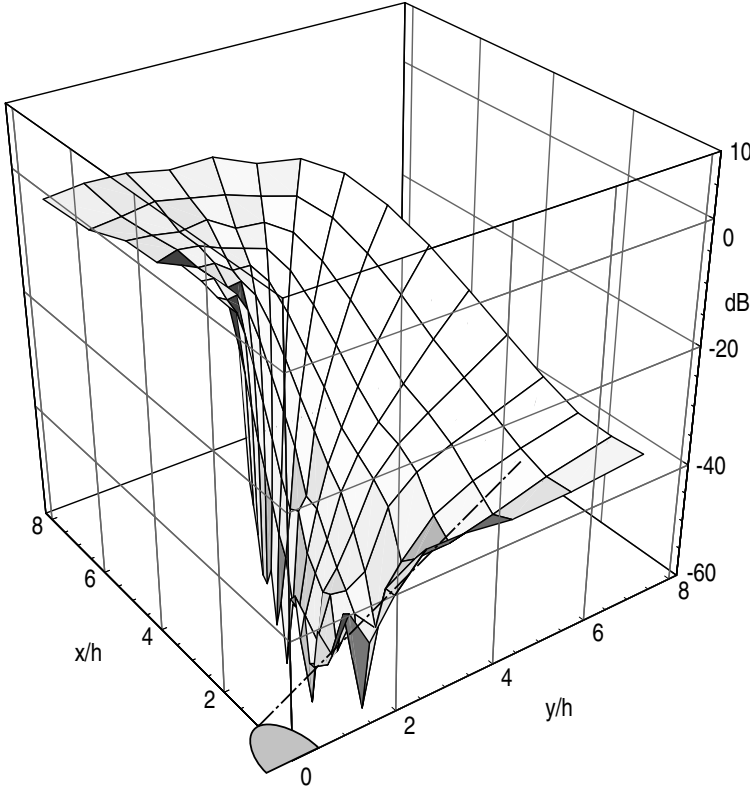
Sound pressure level on the shadow side behind a high dam; the line source is near the ground at $\rho_0 = 1.5; \Theta_0 = -87°$

E.9   Scattering at a Flat Dam

Scattering at a flat dam is contained in a separate section, because the formulas are different from those for a high dam. See the previous ⟩ *Sect. E.8* for the distinction between flat and high dams.

The sound field is again evaluated with the principle of superposition (see previous ▶ *Sect. E.8*). The exciting wave p_e, with the incident plane wave p_e^+ and the plane wave reflected at ground p_e^- (reflection factor $\underline{r}$ of the ground), is:

$$p_e = p_e^+ + \underline{r} \cdot p_e^- = P_e \cdot e^{jk_x x} \cdot \left(e^{jk_y y} + \underline{r} e^{-jk_y y} \right),$$

(1)

$$k_x = k_0 \cos \Theta_0 \quad ; \quad k_y = k_0 \sin \Theta_0.$$
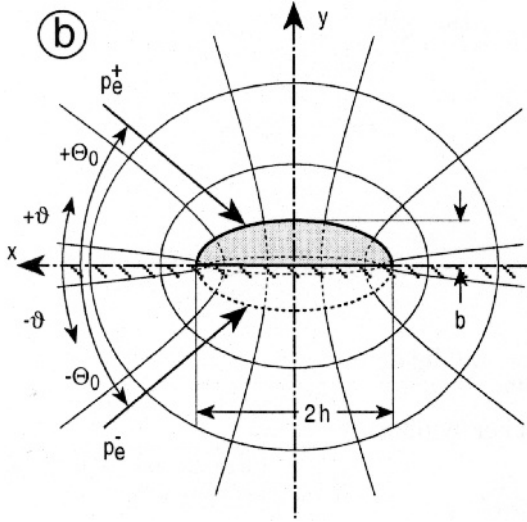
A flat dam with its elliptical-hyperbolic co-ordinate system. The plane $y = 0$ is the hard ground. p_e^+ is the incident plane wave; p_e^- is the mirror-reflected wave. The height of the dam is b; its width at ground level is $2h$. The angle Θ_0 of sound incidence is measured with respect to the ground. The dam is a semi-ellipse with eccentricity c. See the previous ▶ *Sect. E.8* for relations with other geometrical parameters

The sound fields in front of (side of incidence) and behind the dam are:

$$p_{front}(x > 0, y) = p_e(x, y) + \frac{1}{2}\left[p_s^{(h)}(x, y) + p_s^{(w)}(x, y) \right],$$

(2)

$$p_{back}(x < 0, y) = p_e(x, y) + \frac{1}{2}\left[p_s^{(h)}(-x, y) - p_s^{(w)}(-x, y) \right]$$

with $p_s^{(\text{ß})}(x, y)$ the scattered fields for the subtask $(\text{ß}) = (h)$ with hard plane $x = 0$ and the subtask $(\text{ß}) = (w)$ with soft plane $x = 0$. The field in $x \geq 0$ in the two subtasks is $p_e + p_r^{(\text{ß})} + p_s^{(\text{ß})}$, where $p_r^{(h)}$ is the exciting wave after hard reflection at the plane $x = 0$, and $p_r^{(w)}$ is the exciting wave after soft reflection at the plane $x = 0$. The sums $p_e + p_r^{(\text{ß})}$ are $(\alpha^{\pm} = \pi/2 \pm \Theta_0)$:

$$p_e + p_r^{(h)} = 4P_e(1 + \underline{r}) \sum_{r \geq 0} (-j)^{2r} ce_{2r}(\alpha^+) ce_{2r}(\vartheta) Jc_{2r}(\rho)$$

(3)

$$+ 4P_e(1 - \underline{r}) \sum_{r \geq 1} (-j)^{2r} se_{2r}(\alpha^+) se_{2r}(\vartheta) Js_{2r}(\rho),$$

$$p_e + p_r^{(w)} = 4P_e(1 + \underline{r}) \sum_{r\geq 0}(-j)^{2r+1} ce_{2r+1}(\alpha^+)ce_{2r+1}(\vartheta)Jc_{2r+1}(\rho)$$

$$+ 4P_e(1 - \underline{r}) \sum_{r\geq 0}(-j)^{2r+1} se_{2r+1}(\alpha^+)se_{2r+1}(\vartheta)Js_{2r+1}(\rho). \tag{4}$$

The formulations for the scattered fields are, with still unknown term amplitudes $C_r^{(ß)}$, $S_r^{(ß)}$:

$$p_s^{(h)} = P_e \left[\sum_{r\geq 0} C_r^{(h)} ce_{2r}(\vartheta)Hc_{2r}^{(2)}(\rho) + \sum_{r\geq 1} S_r^{(h)} se_{2r}(\vartheta)Hs_{2r}^{(2)}(\rho) \right], \tag{5}$$

$$p_s^{(w)} = P_e \left[\sum_{r\geq 0} C_r^{(w)} ce_{2r+1}(\vartheta)Hc_{2r+1}^{(2)}(\rho) + \sum_{r\geq 0} S_r^{(w)} se_{2r+1}(\vartheta)Hs_{2r+1}^{(2)}(\rho) \right]. \tag{6}$$

The boundary condition $-Z_0 \left(v_{e\rho} + v_{r\rho}^{(ß)} + v_{s\rho}^{(ß)} \right)_{\rho=\rho_c} \overset{!}{=} G \cdot \left(p_e + p_r^{(ß)} + p_s^{(ß)} \right)_{\rho=\rho_c}$ at the dam surface gives for $(ß) = (h)$ the following two systems of equations ($\delta_{r,s}$ = Kronecker symbol):

$$\sum_{r\geq 0} C_r^{(h)} \left[\delta_{r,s} \frac{j\pi}{2k_0c} Hc'_{2r}{}^{(2)}(\rho_c) + G \cdot Hc_{2r}^{(2)}(\rho_c) \cdot Ic_{2r,2s} \right]$$

$$= -4(1 + \underline{r}) \sum_{r\geq 0}(-j)^{2r} ce_{2r}(\alpha^+) \left[\delta_{r,s} \frac{j\pi}{2k_0c} Jc'_{2r}(\rho_c) + G \cdot Jc_{2r}(\rho_c) \cdot Ic_{2r,2s} \right]; \quad s \geq 0, \tag{7}$$

$$\sum_{r\geq 1} S_r^{(h)} \left[\delta_{r,s} \frac{j\pi}{2k_0c} Hs'_{2r}{}^{(2)}(\rho_c) + G \cdot Hs_{2r}^{(2)}(\rho_c) \cdot Is_{2r,2s} \right]$$

$$= -4(1 - \underline{r}) \sum_{r\geq 1}(-j)^{2r} se_{2r}(\alpha^+) \left[\delta_{r,s} \frac{j\pi}{2k_0c} Js'_{2r}(\rho_c) + G \cdot Js_{2r}(\rho_c) \cdot Ic_{2r,2s} \right]; \quad s \geq 1, \tag{8}$$

and for $(ß) = (w)$ two more systems of equations:

$$\sum_{r\geq 0} C_r^{(w)} \left[\delta_{r,s} \frac{j\pi}{2k_0c} Hc'^{(2)}_{2r+1}(\rho_c) + G \cdot Hc_{2r+1}^{(2)}(\rho_c) \cdot Ic_{2r+1,2s+1} \right]$$

$$= -4(1 + \underline{r}) \sum_{r\geq 0}(-j)^{2r+1} ce_{2r+1}(\alpha^+) \tag{9}$$

$$\left[\delta_{r,s} \frac{j\pi}{2k_0c} Jc'_{2r+1}(\rho_c) + G \cdot Jc_{2r+1}(\rho_c) \cdot Ic_{2r+1,2s+1} \right]; \quad s \geq 0$$

$$\sum_{r\geq0} S_r^{(w)}\left[\delta_{r,s}\frac{j\pi}{2k_0c}Hs'^{(2)}_{2r+1}(\rho_c) + G\cdot Hs^{(2)}_{2r+1}(\rho_c)\cdot Is_{2r+1,2s+1}\right]$$

$$= -4\,(1-\underline{r})\sum_{r\geq0}(-j)^{2r+1}se_{2r+1}(\alpha^+) \tag{10}$$

$$\left[\delta_{r,s}\frac{j\pi}{2k_0c}Js'_{2r+1}(\rho_c) + G\cdot Js_{2r+1}(\rho_c)\cdot Ic_{2r+1,2s+1}\right];\quad s\geq0$$

The integrals $Ic_{m,n}$, $Is_{m,n}$ are described in ❯ *Sect. E.8*. The sound field is known after solving for the $C_r^{(\text{ß})}$, $S_r^{(\text{ß})}$.

E.10 Scattering at a Semicircular Absorbing Dam on Absorbing Ground

▶ *See also:* Mechel, Vol. III, Ch. 22 (1998)

A semicircular, locally reacting dam, with radius a and normalised surface admittance G, sits on an absorbent ground plane with reflection factor $\underline{r}$.

A plane or cylindrical wave p_e^+ is incident at an angle Θ_0 with the ground plane. The ground plane produces the mirror-reflected wave p_e^-. A field point is at the cylindrical co-ordinates (ρ, ϑ).

The second diagram (b) shows the co-ordinates as they are generally used in scattering problems at cylinders, such as in ❯ *Sects. E.1 and E.2*.
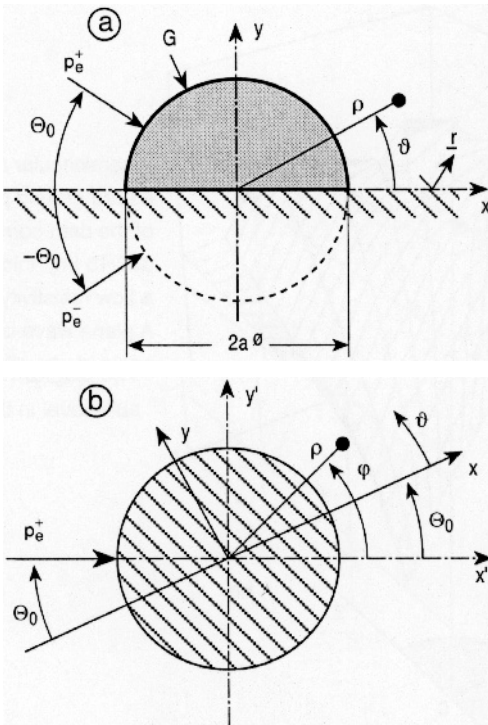
20 lg|p(ρ,ϑ)/2P$_e$|
h=4 [m] ; f=500 [Hz] ;   k$_0$h=36.60 ;
d=0.15 [m] ; Ξ=40 [kPa s/m ^{2}] ; G=0.272+j·0.232 ;
Θ$_0$=3°
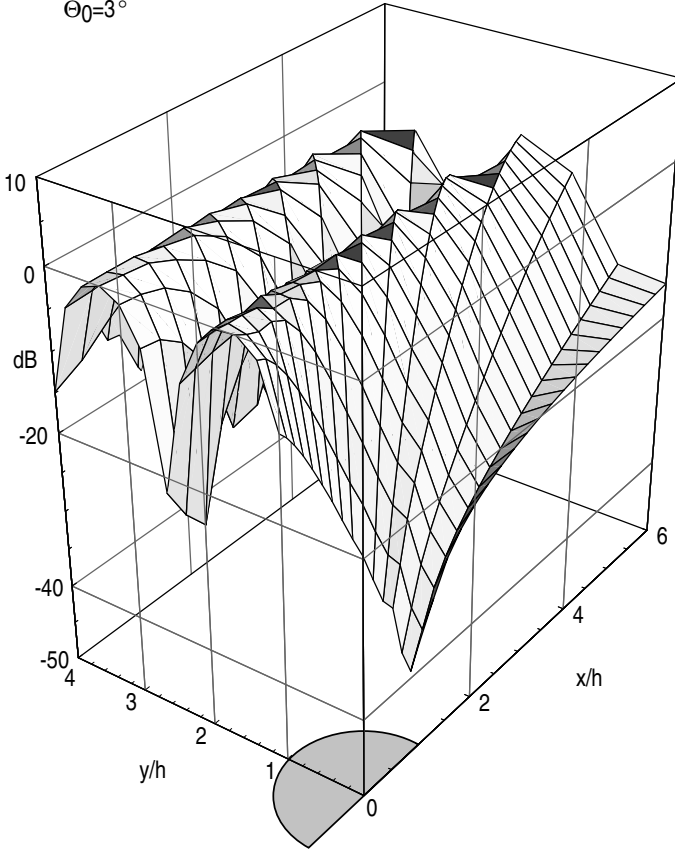
A semicircular absorbent dam on a hard ground plane. The absorption of the dam corresponds to that of a $d = 0.15$ [m] thick glass fibre layer with a flow resistivity of $\Xi = 40[kPa \cdot s/m^2]$. A plane wave is incident under an angle of elevation of $\Theta_0 = 3°$. The diagram shows the sound pressure level in the shadow area

The exciting wave is

$$p_e = p_e^+ + \underline{r} \cdot p_e^-. \tag{1}$$

Incident plane wave

The exciting wave expanded in Bessel functions:

$$p_e = P_e \cdot e^{-jk_x x} \left(e^{+jk_y y} + \underline{r} \cdot e^{-jk_y y} \right)$$

$$= P_e \sum_{m \geq 0} \delta_m (-j)^m \left[\cos(m(\delta + \Theta_0)) + \underline{r} \cdot \cos(m(\vartheta - \Theta_0)) \right] \cdot J_m(k_0 \rho) \tag{2}$$

with $\quad \delta_m = \begin{cases} 1; m = 0 \\ 2; m \neq 0 \end{cases} \quad ; \quad k_x = k_0 \cos \Theta_0; \quad k_y = k_0 \sin \Theta_0.$ (3)

Formulation of the scattered field with as yet undetermined term amplitudes D_m:

$$p_s = P_e \sum_{m \geq 0} \delta_m (-j)^m \cdot D_m \cdot [\cos(m(\vartheta + \Theta_0)) + \underline{r} \cdot \cos(m(\vartheta - \Theta_0))] \cdot H_m^{(2)}(k_0\rho).$$ (4)

The boundary condition at the cylinder gives for the term amplitudes:

$$\begin{aligned} D_m &= -\frac{J_m'(k_0h) - j Z_0 G \cdot J_m(k_0h)}{H_m'^{(2)}(k_0h) - j Z_0 G \cdot H_m^{(2)}(k_0h)} \\ &= -\frac{(m/k_0h - j Z_0 G) \cdot J_m(k_0h) - J_{m+1}(k_0h)}{(m/k_0h - j Z_0 G) \cdot H_m^{(2)}(k_0h) - H_{m+1}^{(2)}(k_0h)}. \end{aligned}$$ (5)

20 lg|p(ρ,ϑ)/2P$_e$|
h=4 [m] ; f=500 [Hz] ; k$_0$h=36.60 ;
d=0.15 [m] ; Ξ=40 [kPa s/m^2] ; G=0.272+j·0.232
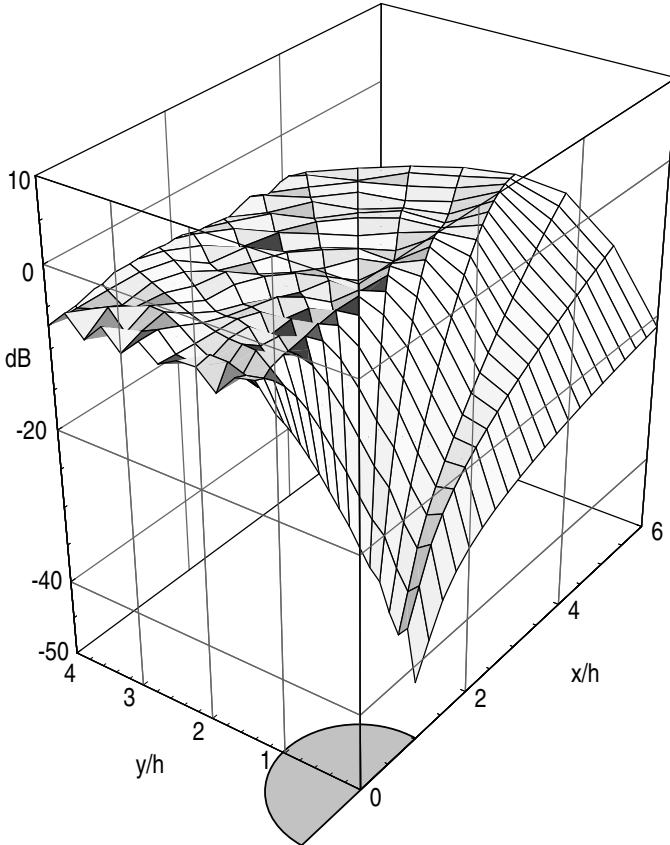
As above, but with a fully absorbent ground plane ($\underline{r} = 0$)

Incident cylindrical wave

Let the line source Q of the cylindrical wave be at a distance ρ_0 from the dam axis under an elevation angle Θ_0 with the ground plane. The ground plane with the reflection factor $\underline{r}$ produces the mirror-reflected wave p_e^- to the original incident wave p_e^+.

The exciting wave is in the radial range $\rho < \rho_0$:

$$p_e = P_e \left[H_0^{(2)}(k_0 R_1) + \underline{r} \cdot H_0^{(2)}(k_0 R_2) \right]$$

$$= P_e \sum_{m \geq 0} \delta_m (-1)^m \cdot H_m^{(2)}(k_0 \rho_0) \cdot J_m(k_0 \rho) \cdot [\cos (m(\vartheta + \Theta_0)) \tag{6}$$

$$+ \underline{r} \cdot \cos (m(\vartheta - \Theta_0))] \, .$$
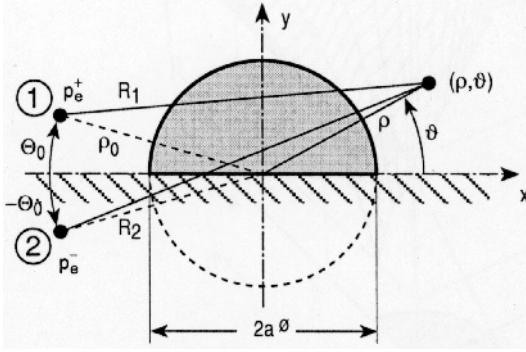
The total field is $p = p_e + p_s$ with the scattered field:

$$p_s = P_e \sum_{m \geq 0} \delta_m (-1)^m \cdot D_m \cdot H_m^{(2)}(k_0 \rho_0) \cdot H_m^{(2)}(k_0 \rho) \cdot [\cos (m(\vartheta + \Theta_0))$$

$$+ \underline{r} \cdot \cos (m(\vartheta - \Theta_0))] . \tag{7}$$

The term amplitudes D_m follow from the boundary condition at the dam surface $\rho = a$ as:

$$D_m = -\frac{J_m'(k_0 a) - j\, G \cdot J_m(k_0 a)}{H_m'^{(2)}(k_0 a) - j\, G \cdot H_m^{(2)}(k_0 a)} = -\frac{(m/k_0 a - j\, G) \cdot J_m(k_0 a) - J_{m+1}(k_0 a)}{(m/k_0 a - j\, G) \cdot H_m^{(2)}(k_0 a) - H_{m+1}^{(2)}(k_0 a)} . \tag{8}$$

The component form $p_e = P_e \left[H_0^{(2)}(k_0 R_1) + \underline{r} \cdot H_0^{(2)}(k_0 R_2) \right]$ is valid for all $\rho \geq a$, like p_s. The radii R_1, R_2 are given by

$$k_0 R_1 = k_0 \sqrt{(\rho \cos \vartheta + \rho_0 \cos \Theta_0)^2 + (\rho \sin \vartheta - \rho_0 \sin \Theta_0)^2},$$

$$\tag{9}$$

$$k_0 R_2 = k_0 \sqrt{(\rho \cos \vartheta + \rho_0 \cos \Theta_0)^2 + (\rho \sin \vartheta + \rho_0 \sin \Theta_0)^2}.$$

20 lg|p(ρ,ϑ)/p_norm|
h=4 [m] ; f=500 [Hz] ; k_0h=36.60 ; G=0.272+j·0.232 ;
ρ_0/h=4 ; Θ_0=3°
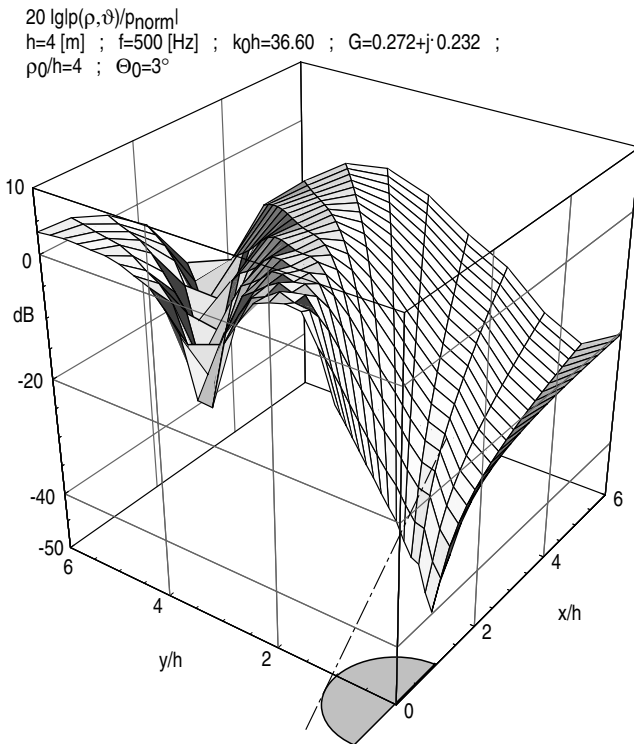
Sound pressure level in the shadow zone of a semicircular absorbing dam on a hard ground plane for a cylindrical incident wave from the source position $\rho_0/h = 4; \Theta_0 = 3°$

E.11   Scattering in Random Media, General

▶ *See also:* Mechel, Vol. II, Ch. 14 (1995)

This section presents general distinctions and concepts for the scattering of sound in random media. The composite medium consists of a fluid with randomly distributed scatterers.
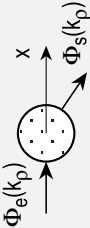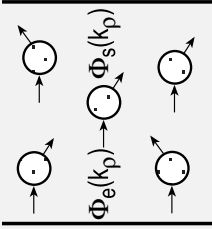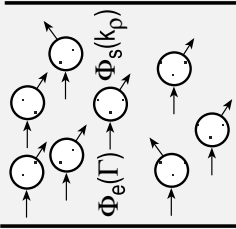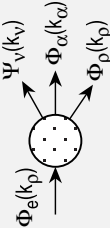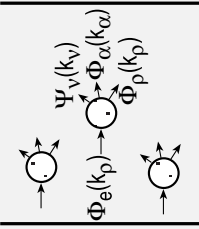
The fluid
- May have no losses,
- May have viscous and thermal losses.

The scatterers	• May be different with respect to their shape, e.g. below:
	• Spheres,
	• Cylinders,
	• May be different with respect to their consistency:
	• Rigid or soft,
	• Fluid, with or without losses,
	• Elastic,
	• May be different with respect to their dynamical behaviour:
	• Not moving (though oscillating at their surface),
	• Moving as a total under the influence of acoustical forces.
The composite medium	• May be disperse, i.e. multiple scattering negligible,
	• May be dense, i.e. multiple scattering not negligible.
The scattering	• May retain the wave type (monotype scattering),
	• May change the wave type into the triple of density, thermal, viscous waves (triple type scattering).

Table 1 on the next page gives a survey of some of the different scattering processes. The upper rows belong to monotype scattering: both the exciting wave Φ_e and the scattered wave Φ_s are of the same type. The lower rows describe triple-type scattering: the exciting wave Φ_e generates the triple of density (ρ), thermal (α) and viscous (ν) waves as scattered waves. The propagation of sound through the composite medium is composed of elementary scattering processes at single scatterers, which is indicated in the first column. In disperse media (second column) the multiple scattering (scattering of scattered fields) is neglected, i.e. the scattered waves propagate freely through the medium. In dense media (third column) multiple scattering must be taken into account. The exciting wave then is an "effective" wave Φ_E .

The scatterers will have a uniform random distribution in the composite medium. If there are inhomogeneities, e.g. holes or clusters, they are supposed to be randomly distributed as well and to form a subsystem of scatterers.

Table 1 Survey of scattering in random media

	Type of scattering	**1** Single scatterer	**2** Disperse medium	**3** Dense medium
1	**Monotype scattering**	$\Phi_e(k_\rho)$ x $\Phi_s(k_\rho)$	$\Phi_e(k_\rho) \longrightarrow \Phi_s(k_\rho)$	$\Phi_e(\Gamma) \longrightarrow \Phi_s(k_\rho)$
	Exciting wave	$\Phi_e(k_\rho x) = e^{-jk_\rho x}$	$\Phi_e(k_\rho) = e^{-jk_\rho x} + \sum_{j\neq i}\Phi_s(k_\rho r_j)$	$\Phi_E = e^{-\Gamma x} + \sum_{j\neq i}\Phi_s(k_\rho r_j)$
	Scattered wave	$\Phi_s(k_\rho r)$	$\Phi_s(k_\rho r)$	$\Phi_s(k_\rho r)$
	Triple-type scattering	$\Phi_e(k_\rho)$ $\Psi_v(k_v)$ $\Phi_\alpha(k_\alpha)$ $\Phi_\rho(k_\rho)$	$\Phi_e(k_\rho) \to \begin{array}{l}\Psi_v(k_v)\\ \Phi_\alpha(k_\alpha)\\ \Phi_\rho(k_\rho)\end{array}$	$\Phi_e(k_\rho) \to \begin{array}{l}\Psi_v(k_v)\\ \Phi_\alpha(k_\alpha)\\ \Phi_\rho(k_\rho)\end{array}$
2	Exciting wave	$\Phi_e(k_\rho x) = e^{-jk_\rho x}$	$\Phi_e(k_\rho x) = e^{-jk_\rho x} + \sum_{\beta,j\neq i}\Phi_s(k_\beta r_j)$	$\Phi_E = e^{-\Gamma x} + \sum_{\beta,j\neq i}\Phi_s(k_\beta r_j)$
	Scattered wave	$\Phi_s(k_\beta r) = \{\Phi_\rho(k_\rho r), \Phi_a(k_\alpha r), \Psi_v(k_v r)\}$	$\Phi_s(k_\beta r) = \{\Phi_\rho(k_\rho r), \Phi_a(k_\alpha r), \Psi_v(k_v r)\}$	$\Phi_s(k_\beta r) = \{\Phi_\rho(k_\rho r), \Phi_a(k_\alpha r), \Psi_v(k_v r)\}$

Reiche's experiment:

A simple experiment is the background of many theories for the determination of the characteristic propagation constant Γ and wave impedance Z_i inside a composite medium with random scatterers:

A plane wave Φ_e is incident on a layer of thickness D of the investigated material. A receiver on the front side "collects" the backscattered wave components from inside the layer as reflected wave Φ_r; a receiver on the back side "collects" the forward-scattered wave components from inside the layer as transmitted wave Φ_t. The characteristic values of the material are determined from the reflection and transmission factors $\underline{r}_e$, t_e on the front side and $\underline{r}_a$, t_a on the back side (reflection factors are underlined for distinction with the later used symbol r for radius and/or general co-ordinate). The forward and backward waves inside the layer are Φ_+, Φ_-, respectively. The fluid inside the layer (between the scatterers) equals the fluid outside the layer.
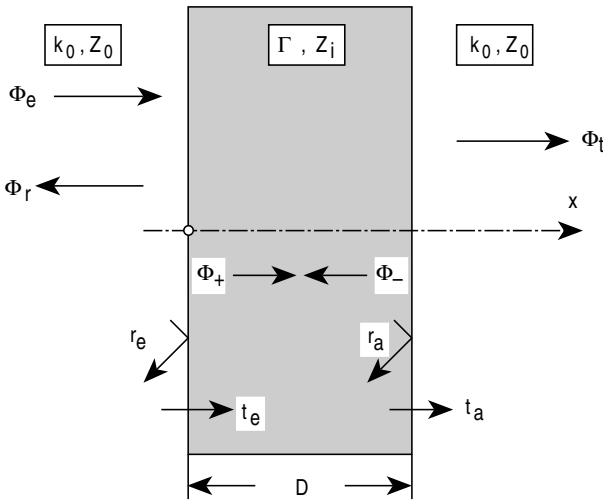
Monotype scattering:

$$\Phi_e(x) = e^{-j\,k_0 x} \quad ; \quad \Phi_r(x) = \underline{r}_e \cdot e^{+j\,k_0 x} \quad ; \quad \Phi_t(x) = t \cdot e^{-j\,k_0(x-D)}$$

$$\underline{r}_e = \Phi_r(0)/\Phi_e(0) \quad ; \quad \underline{r}_a = \Phi_-(D)/\Phi_+(D)$$

$$t_e = \Phi_+(0)/\Phi_e(0) \quad ; \quad t_a = \Phi_t(D)/\Phi_+(D) \tag{1}$$

$$t = \Phi_t(D)/\Phi_e(0)$$

For transmission with $y = \Gamma D$:

$$t_a = 1 + \underline{r}_a = \frac{2}{1 + Z_i/Z_0} \quad ; \quad t_e = \frac{1 - \underline{r}_a}{1 - \underline{r}_a^2 \cdot e^{-2y}}$$

$$t = \frac{1 - \underline{r}_a^2}{1 - \underline{r}_a^2 \cdot e^{-2y}} \cdot e^{-y} \quad ; \quad t = t_e\, t_a\, e^{-y} \tag{2}$$

For reflection with $y = \Gamma D$:

$$\underline{r}_a = \frac{1 - Z_i/Z_0}{1 + Z_i/Z_0} \quad ; \quad \underline{r}_e = -\underline{r}_a \cdot \frac{1 - e^{-2y}}{1 - \underline{r}_a^2 \cdot e^{-2y}}. \tag{3}$$

Field inside the layer:

$$\Phi_l(x) = \Phi_+(x) + \Phi_-(x) = t_e \cdot \left(e^{-\Gamma x} + \underline{r}_a \cdot e^{+\Gamma(x-2D)} \right). \tag{4}$$

Field at a field point $\mathbf{r}$ (which may be well outside the layer):

$$\Phi(\mathbf{r}) = \Phi_e(\mathbf{r}) + U(\mathbf{r}) \quad ; \quad U(\mathbf{r}) = \sum_s u_s(\mathbf{r} - \mathbf{r}_s), \tag{5}$$

where u_s is the scattered field of a single scatterer with running index s having its position at $\mathbf{r}_s$. This often-used elementary decomposition implicitly assumes that the exciting wave can reach the scatterers (even deeply inside the layer) without attenuation; this form therefore is restricted to disperse media. The single scatterer functions u_s are sums over Hankel functions of the second kind $H_n^{(2)}(k_0 r)$ for cylindrical scatterers or spherical Hankel functions of the second kind $h_n^{(2)}(k_0 r) = \sqrt{\pi/(2k_0 r)}\; H_{n+1/2}^{(2)}(k_0 r)$ for spherical scatterers.

It is a further assumption in REICHE's experiment that receiving points for the transmitted and reflected fields are chosen at large distances, so that $k_0\,|x| \gg 1$. Then the scattered far field can be written as a product of a factor $\mathfrak{R}(k_0 r)$ with only a radial variation, and an angular factor $g(\mathbf{o}, \mathbf{i})$ which contains the angle between the direction $\mathbf{o}$ to the field point with the direction $\mathbf{i}$ of incidence on the scatterer. Replacing the summation over the index s of the scatterers by an integration and taking into account the symmetry of the problem around the axis of propagation, one can write for the scattered fields outside the layer (at large distances of it):

$$U_>(x) = \Phi_e(k_0 x) \cdot C \int_0^D e^{jk_0\xi} \cdot G(\xi, \mathbf{i})\, d\xi \quad ; \quad x > D,$$

$$U_<(x) = \Phi_e(-k_0 x) \cdot C \int_0^D e^{-jk_0\xi} \cdot G(\xi, -\mathbf{i})\, d\xi \quad ; \quad x < 0 \tag{6}$$

and inside the layer:

$$\Phi(x) = \Phi_e(k_0 x) \cdot \left[1 + C \int_0^x e^{jk_0\xi} \cdot G(\xi, \mathbf{i})\, d\xi \right] + \Phi_e(-k_0 x) \cdot C \int_x^D e^{-jk_0\xi} \cdot G(\xi, -\mathbf{i})\, d\xi, \tag{7}$$

where C is a constant factor (depending on the far field decomposition) which will be given below, and

$$G(\xi, o) = g(o, i) \cdot \Phi_+(0, \xi) + g(o, -i) \cdot \Phi_-(\xi, D),$$

(8)

$$G(\xi, \pm i) = g(\pm i, i) \cdot \Phi_+(0, \xi) + g(\pm i, -i) \cdot \Phi_-(\xi, D),$$

($\pm i$ represent forward or backward direction, in or against the x direction) with

$$\Phi(x) = \Phi_+(0, x) + \Phi_-(x, D),$$

$$\Phi_+(0, x) = e^{-jk_0 x} \cdot \left[1 + C \int_0^x e^{jk_0 \xi} \cdot G(\xi, i)\, d\xi \right],$$

(9)

$$\Phi_-(x, D) = e^{+jk_0 x} \cdot C \int_x^D e^{-jk_0 \xi} \cdot G(\xi, -i)\, d\xi .$$

We introduce here four symbols corresponding to the four possible combinations of forward and backward directions (and include, for simplicity, the constant C):

$$S_+ = C\, g(i, i) \quad ; \quad S_- = C\, g(-i, -i),$$

(10)

$$R_+ = C\, g(i, -i) \quad ; \quad R_- = C\, g(-i, i).$$

Assume further that the scatterers have a forward-backward symmetry (as spheres and cylinders); then

$$g(-i, -i) = g(i, i) \quad ; \quad g(-i, i) = g(i, -i),$$

(11)

$$S_+ = S_- = S \quad ; \quad R_+ = R_- = R$$

and two coupled integral equations are obtained:

$$\Phi_+(0, x) = e^{-jk_0 x} \cdot \left[1 + \int_0^x e^{+jk_0 \xi}[S_+\Phi_+(0, \xi) + R_+\Phi_-(\xi, D)]\, d\xi \right],$$

(12)

$$\Phi_-(x, D) = e^{+jk_0 x} \cdot \int_x^D e^{-jk_0 \xi}[R_-\Phi_+(0, \xi) + S_-\Phi_-(\xi, D)]\, d\xi .$$

The essential trick of REICHE's experiment is to use these intgral equations for obtaining the boundary conditions at the layer surfaces as well as a "wave equation". Differentiation of $\Phi_\pm$ with respect to $\times$ gives, for constant $S_\pm, R_\pm,$

$$\Phi'_\pm = \mp jk_0\, \Phi_\pm \pm (S_\pm\, \Phi_\pm + R_\pm\, \Phi_\mp) = \pm T_\pm\, \Phi_\pm \pm R_\pm\, \Phi_\mp,$$

(13)

$$\Phi''_\pm + (T_- - T_+)\, \Phi'_\pm + (R_+R_- - T_+T_-)\, \Phi_\pm = 0,$$

with $T_\pm = -jk_0 + S_\pm$. The differential equation in the second line is interpreted as a wave equation; then the parentheses of the last term contain the square of the effective wave number k_E with $\Gamma = jk_E$:

$$k_E^2 = R_+ R_- - T_+ T_- \xrightarrow[\substack{R_+ = R_- = R \\ S_+ = S_- = S \\ T_+ = T_- = T}]{} R^2 - T^2 = k_0^2 + R^2 - S^2 + 2jk_0 S$$

$$(14)$$

$$k_E^2 / k_0^2 = 1 + \frac{R^2 - S^2}{k_0^2} + \frac{2j}{k_0} S$$

(the last line contains the square of the index of refraction).

If the assumption of symmetrical scatterers cannot be made, formulate a general solution for $\Phi_\pm$:

$$\Phi_\pm = A_\pm \, e^{-jk_{E+}x} + B_\pm \, e^{+jk_{E-}x}. \tag{15}$$

Insert this in the derivatives above to obtain two homogeneous linear systems of equations for the amplitudes $A_\pm, B_\pm$:

$$\begin{pmatrix} (T_+ + jk_{E+}) & R_+ \\ R_- & (T_- - jk_{E+}) \end{pmatrix} \cdot \begin{pmatrix} A_+ \\ A_- \end{pmatrix} = \begin{pmatrix} 0 \\ 0 \end{pmatrix} = \mathbf{M}(k_{E+}) \bullet \mathbf{A},$$

$$(16)$$

$$\begin{pmatrix} (T_+ - jk_{E-}) & R_+ \\ R_- & (T_- + jk_{E-}) \end{pmatrix} \cdot \begin{pmatrix} B_+ \\ B_- \end{pmatrix} = \begin{pmatrix} 0 \\ 0 \end{pmatrix} = \mathbf{M}(k_{E-}) \bullet \mathbf{B}.$$

The condition of zero determinants gives the characteristic equations with solutions:

$$k_{E\pm} = k_{E0} \pm \Delta$$
$$(17)$$
$$k_{E0} = j\sqrt{\frac{1}{4}(T_+ + T_-)^2 - R_+ R_-} \quad ; \quad \Delta = \frac{j}{2}(T_+ - T_-).$$

The wave impedance is determined from the following boundary conditions:

$$\Phi_+(0,0) = A_+ + B_+ = 1$$

$$(18)$$

$$\Phi_-(D, D) = A_- \cdot e^{-jk_{E+}D} + B_- \cdot e^{+jk_{E-}D} = 0$$

which, together with the above systems of equations, give an inhomogeneous system of equations whose solutions are, with $k_{E+} + k_{E-} = 2k_{E0}$,

$$A_+ = [1 - QQ' \, e^{-2jk_{E0}D}]^{-1} =: F \quad ; \quad A_- = -Q \, A_+ ,$$

$$(19)$$

$$B_- = Q \, e^{-2jk_{E0}D} \cdot F \qquad\qquad ; \quad B_+ = -Q' \, B_- ,$$

with the abbreviations (besides of F)

$$Q = R_-/(T_- - jk_{E+}) \quad ; \quad Q' = R_+/(T_+ - jk_{E-}). \tag{20}$$

The sound field inside the layer thus becomes:

$$\Phi_I(x) = e^{-j\Delta \cdot x} \cdot \frac{1 - Q}{1 - QQ' \, e^{-2jk_{E0}D}} \cdot \left(e^{-jk_{E0}x} - Q \, \frac{1 - Q'}{1 - Q} \, e^{+jk_{E0}(x-2D)} \right). \tag{21}$$

In the special case of symmetrical scatterers

$$S_+ = S_- = S \quad ; \quad R_+ = R_- = R \quad ; \quad T_+ = T_- = T$$

$$\Delta = 0 \quad ; \quad k_{E+} = k_{E-} = k_{E0} = k_E \quad ; \quad Q' = Q \quad ; \quad F = \frac{1}{1 - Q^2 \, e^{-2jk_E D}} \tag{22}$$

and

$$\Phi_I(x) = \frac{1 - Q}{1 - Q^2 \, e^{-2jk_E D}} \cdot (e^{-jk_E x} - Q \, e^{+jk_E(x-2D)}). \tag{23}$$

This can be made completely analogous to the field in a homogeneous medium layer by the equivalencies $Q \leftrightarrow \underline{r}_a$; $jk_E \leftrightarrow \Gamma$, from which follows the wave impedance of the layer material:

$$\frac{Z_i}{Z_0} = \frac{1 - Q}{1 + Q}. \tag{24}$$

The reflected field in front of the layer and the transmitted field behind the layer are

$$\Phi_r(x) = U_<(x) = -Q \, (1 - e^{-2jk_E D}) \, F \cdot e^{jk_0 x} \quad ; \quad x \le 0,$$

$$\Phi_t(x) = U_>(x) = (1 - QQ') \, e^{-2jk_E D} \, F \cdot e^{-jk_0 x} \quad ; \quad x \ge D. \tag{25}$$

Thus the characteristic values of the composite material and the sound fields are known using this method (and with its restrictive assumptions) if the scattered far field functions $g_> = g(\mathbf{i}, \mathbf{i})$ and $g_< = g(-\mathbf{i}, \mathbf{i})$ are known from single scatterer evaluations, which are the scattered far fields in forward and backward directions. With them the characteristic values can be given other forms, using

$$R = C \, g_< \quad ; \quad T = C \, g_> - jk_0 \quad ; \quad Q = \frac{C \, g_<}{C \, g_> - j \, (k_0 + k_E)} \tag{26}$$

and

$$\frac{k_E}{k_0} = \sqrt{\frac{\rho_{eff}}{\rho_0} \cdot \frac{C_{eff}}{C_0}} \quad ; \quad \frac{Z_i}{Z_0} = \sqrt{\frac{\rho_{eff}}{\rho_0} \Big/ \frac{C_{eff}}{C_0}}, \tag{27}$$

$$\frac{\rho_{eff}}{\rho_0} = 1 + j\frac{C}{k_0} \, (g_> - g_<) \quad ; \quad \frac{C_{eff}}{C_0} = 1 + j\frac{C}{k_0} \, (g_> + g_<). \tag{28}$$

For low scatterer number density $N \to 0$ will be $|jC \cdot g/k_0| \ll 1$, and therefore

$$\frac{k_E^2}{k_0^2} \approx 1 + 2j\frac{C}{k_0} \cdot g_> \quad ; \quad \frac{Z_i^2}{Z_0^2} \approx 1 + 2j\frac{C}{k_0} \cdot g_< . \tag{29}$$

In this approximation the wave number only depends on the forward scattering and the wave impedance only on the backward scattering. With the extinction cross section Q_e of a single scatterer

$$Q_e = -2C \cdot \text{Re}\{g_>\} \quad ; \quad C = \begin{cases} 2/k_0 & \text{Cylinder ,} \\ 2\pi/k_0^2 & \text{Sphere ,} \end{cases} \tag{30}$$

one finds the plausible result for the attenuation (in the present approximation):

$$-2\,\text{Im}\{k_E\} \approx N \cdot Q_e, \tag{31}$$

i.e. the attenuation is proportional to the number density of the scatterers and to their extinction cross section.

E.12   Function Tables for Monotype Scattering

This section gives tables of functions for monotype scattering to be applied in the general scheme of the previous ❯ *Sect. E.11*, i.e. incident and scattered waves are of the same type, to say, density waves.

It is not necessary to use potential functions Φ for the field with monotype scattering; therefore the field function here will be the sound pressure p. The time factor is, as usual, $e^{j\omega t}$. The incident plane wave has a unit amplitude.

The first table compiles radial functions $R_n(r)$ and azimuthal functions $T_n(\vartheta)$ for cylindrical and spherical scatterers. $Z_n(z)$ stands for a Bessel, Neumann or Hankel function; $K_n(z)$ stands for a spherical Bessel, Neumann or Hankel function. Because Hankel functions only are of the second kind, the upper index [(2)] will be dropped (for ease of writing). The second table gives formulations of the incident plane wave and of the scattered wave for both geometries of the scatterer. The third table collects modal amplitudes and mode admittances (normalised with Z_0) for both locally reacting and bulk reacting scatterers. Bulk reacting scatterers are supposed to be of an isotropic, homogeneous material having the characteristic propagation constant Γ_σ and wave impedance Z_σ; thus this type of scatterer can represent also fluids with losses. Hard and soft cylinders and spheres are treated as special cases of locally reacting scatterers. a is the radius of the scatterer; N is the number density of scatterers (number of scatterers per unit volume); µ is the massivity, i.e. the ratio of space occupied by the scatterers. The argument in radial functions is dropped if it is k_0a .

Some of the contents of these tables may be found also in ❯ *Sects. E.1 and E.2*, but the tables here have been completed with terms required in the previous ❯ *Sect. E.11*.

Table 1 Radial and polar functions for cylindrical and spherical co-ordinates

	Quantity	Cylinder	Sphere
1	**Radial functions** $R_n(z)$	$Z_n(z) = \{J_n(z), Y_n(z), H_n(z)\}$ $H_n(z) = J_n(z) - j\,Y_n(z)$	$K_n(z) = \{j_n(z), y_n(z), h_n(z)\}$ $K_n(z) = \sqrt{\pi/(2z)} \cdot Z_{n+1/2}(z)$ $h_n(z) = j_n(z) - j\,y_n(z)$
2	$R'_n(z)$	$Z'_n(z) = \dfrac{n}{z}\,Z_n(z) - Z_{n+1}(z)$ $= Z_{n-1}(z) - \dfrac{n}{z}\,Z_n(z)$	$K'_n(z) = \dfrac{n}{z}\,K_n(z) - K_{n+1}(z)$ $= K_{n-1}(z) - \dfrac{n}{z}\,K_n(z)$
3	$J_n(z) \xrightarrow[\,|z| \ll 1\,]{}$ $j_n(z) \xrightarrow[\,|z| \ll 1\,]{}$	$\dfrac{(z/2)^n}{n!}$	$\dfrac{z^n}{1 \cdot 2 \cdot 3 \cdot \ldots \cdot (2n+1)}$
4	$J_n(z) \xrightarrow[\,|z| \gg 1\,]{}$ $j_n(z) \xrightarrow[\,|z| \gg 1\,]{}$	$\sqrt{\dfrac{2}{\pi z}} \cdot \cos\left(z - n\dfrac{\pi}{2} - \dfrac{\pi}{4}\right)$	$\dfrac{1}{z} \cdot \cos\left(z - n\dfrac{\pi}{2}\right)$
5	$Y_n(z) \xrightarrow[\,|z| \ll 1\,]{}$ $y_n(z) \xrightarrow[\,|z| \ll 1\,]{}$	$Y_0(z) \to \dfrac{2}{\pi}\,\ln z$ $Y_n(z) \to -\dfrac{(n-1)!}{\pi\,(z/2)^n}$; $n > 0$	$-\dfrac{1 \cdot 3 \cdot 5 \cdot \ldots \cdot (2n-1)}{z^{n+1}}$
6	$Y_n(z) \xrightarrow[\,|z| \gg 1\,]{}$ $y_n(z) \xrightarrow[\,|z| \gg 1\,]{}$	$\sqrt{\dfrac{2}{\pi z}} \cdot \sin\left(z - n\dfrac{\pi}{2} - \dfrac{\pi}{4}\right)$	$\dfrac{1}{z} \cdot \sin\left(z - n\dfrac{\pi}{2}\right)$
7	$H_n(z) \xrightarrow[\,|z| \ll 1\,]{}$ $h_n(z) \xrightarrow[\,|z| \ll 1\,]{}$	$H_0(z) \to -\dfrac{2j}{\pi}\,\ln z$ $H_n(z) \to \dfrac{j(n-1)!}{\pi\,(z/2)^n}$; $n > 0$	$j\,\dfrac{1 \cdot 3 \cdot 5 \cdot \ldots \cdot (2n-1)}{z^{n+1}}$
8	$H_n(z) \xrightarrow[\,|z| \gg 1\,]{}$ $h_n(z) \xrightarrow[\,|z| \gg 1\,]{}$	$\sqrt{\dfrac{2}{\pi z}} \cdot e^{-j(z - n\pi/2 - \pi/4)}$ $= \dfrac{j^n}{\sqrt{\pi/2}} \cdot \dfrac{e^{-jz}}{\sqrt{-jz}}$	$\dfrac{j}{z} \cdot e^{-j(z - n\pi/2)}$ $= j^n \cdot \dfrac{e^{-jz}}{(-jz)}$
9	$J_{n+1}(z)Y_n(z)$ $-Y_{n+1}(z)J_n(z)$	$2/(\pi z)$	$1/z^2$
10	**Polar functions** $T_n(\vartheta)$	$\cos(n\vartheta)$	$P_n(\cos\vartheta)$
11	$T_0(\vartheta)$	1	1
12	$T_n(0)$	1	1
13	$T_n(\pi)$	$(-1)^n$	$(-1)^n$

Table 2 Incident and scattered waves

	Quantity	Cylinder	Sphere
1	**Incident wave**	$p_e(r, \vartheta) = e^{-jk_0 r \cdot \cos \vartheta}$	
	$p_e(r, \vartheta) =$	$\sum\limits_{n=0}^{\infty} \delta_n \cdot (-j)^n \cdot T_n(\vartheta) \cdot R_{en}(r)$	
2	$\delta_n =$	$\begin{cases} 1 \,;\, n = 0 \\ 2 \,;\, n > 0 \end{cases}$	$2n + 1$
3	$T_n(\vartheta) =$	$\cos(n\vartheta)$	$P_n(\cos \vartheta)$
4	$R_{en}(r) =$	$J_n(k_0 r)$	$j_n(k_0 r)$
5	**Scattered wave** $p_s(r, \vartheta) =$	$\sum\limits_{n=0}^{\infty} \delta_n \cdot (-j)^n \cdot D_n \cdot T_n(\vartheta) \cdot R_{sn}(r)$	
6	$R_{sn}(r) =$	$H_n(k_0 r)$	$h_n(k_0 r)$
7	$p_s(r, \vartheta) \xrightarrow[k_0 r \gg 1]{}$	$\Re(r) \cdot \Theta(\vartheta)$	
8	$\Re(r) =$	$\sqrt{\dfrac{2j}{\pi}} \dfrac{e^{-jk_0 r}}{\sqrt{k_0 r}}$	$j \dfrac{e^{-jk_0 r}}{k_0 r}$
9	$\Theta(\vartheta) = g(\mathbf{o}, \mathbf{i}) =$	$\sum\limits_{n=0}^{\infty} \delta_n \, D_n \, T_n(\vartheta)$	$\sum\limits_{n=0}^{\infty} \delta_n \, D_n \, T_n(\vartheta)$
10	$\Theta(0) = g(\mathbf{i}, \mathbf{i}) =$	$\sum\limits_{n=0}^{\infty} \delta_n \, D_n \, T_n(0) = \sum\limits_{n=0}^{\infty} \delta_n \, D_n$	$\sum\limits_{n=0}^{\infty} \delta_n \, D_n \, T_n(0) = \sum\limits_{n=0}^{\infty} \delta_n \, D_n$
11	$\Theta(\pi) = g(-\mathbf{i}, \mathbf{i}) =$	$\sum\limits_{n=0}^{\infty} (-1)^n \, \delta_n \, D_n$	$\sum\limits_{n=0}^{\infty} (-1)^n \, \delta_n \, D_n$
12	$C =$	$\dfrac{2N}{k_0}$	$\dfrac{2\pi N}{k_0^2}$
13	Massivity $\mu =$	$N \cdot \pi a^2$	$N \cdot \dfrac{4}{3}\pi a^3$
14	$\dfrac{C}{k_0} =$	$\dfrac{2\mu}{\pi \, (k_0 a)^2}$	$\dfrac{3\mu}{2(k_0 a)^3}$

Table 3 Modal admittances G (normalised) and amplitudes D

	Quantity	Cylinder	Sphere
1	**Locally reacting** $G =$	$-Z_0 \cdot v_r(a)/p(a) = G = $ fix	
2	$D_n =$	$-\dfrac{\left(\dfrac{n}{k_0 a} - jG\right) J_n - J_{n+1}}{\left(\dfrac{n}{k_0 a} - jG\right) H_n - H_{n+1}}$	$-\dfrac{\left(\dfrac{n}{k_0 a} - jG\right) j_n - j_{n+1}}{\left(\dfrac{n}{k_0 a} - jG\right) h_n - h_{n+1}}$
3	**Bulk reacting** $G_n =$	$\dfrac{j}{Z_\sigma/Z_0} \dfrac{J'_n\left(j\Gamma_\sigma a\right)}{J_n\left(j\Gamma_\sigma a\right)}$	$\dfrac{j}{Z_\sigma/Z_0} \dfrac{j'_n\left(j\Gamma_\sigma a\right)}{j_n\left(j\Gamma_\sigma a\right)}$
4	$D_n =$	$-\dfrac{\left(\dfrac{n}{k_0 a} - jG_n\right) J_n - J_{n+1}}{\left(\dfrac{n}{k_0 a} - jG_n\right) H_n - H_{n+1}}$	$-\dfrac{\left(\dfrac{n}{k_0 a} - jG_n\right) j_n - j_{n+1}}{\left(\dfrac{n}{k_0 a} - jG_n\right) h_n - h_{n+1}}$

The hard, immovable scatterer is a special case, $G = 0$, of a locally reacting scatterer:

$$D_n = \begin{cases} -\dfrac{J'_n(k_0 a)}{H'_n(k_0 a)} & \text{Cylinder,} \\[3mm] -\dfrac{j'_n(k_0 a)}{h'_n(k_0 a)} & \text{Sphere.} \end{cases} \tag{1}$$

The soft, immovable scatterer is a special case, $|G| = \infty$, of a locally reacting scatterer:

$$D_n = \begin{cases} -\dfrac{J(k_0 a)}{H(k_0 a)} & \text{Cylinder,} \\[3mm] -\dfrac{j(k_0 a)}{h(k_0 a)} & \text{Sphere.} \end{cases} \tag{2}$$

The bulk reacting scatterers of a homogeneous material are movable under the force of the sound field by formulation; the movement mainly is described by the mode $n = 1$. A hard, freely movable scatterer can be obtained from a bulk reacting scatterer by setting the compressibility of its material to $C_\sigma = 0$ but with a finite density ρ_σ. This produces $\Gamma_\sigma \to 0$ and $Z_\sigma \to \infty$ so that a finite $Z_\sigma \cdot \Gamma_\sigma \to j\omega\rho_\sigma$ is obtained. The modal admittances for cylinders can be written (similarly for spheres)

$$G_n = \frac{n}{jk_0 a} \frac{\rho_0}{\rho_\sigma} - \frac{j}{Z_\sigma/Z_0} \frac{J_{n+1}(j\Gamma_\sigma a)}{J_n(j\Gamma_\sigma a)}. \tag{3}$$

The ratio of the Bessel functions is $j\Gamma_\sigma a/(2n + 2)$ for cylinders and $j\Gamma_\sigma a/(2n + 3)$ for spheres. So for $\Gamma_\sigma \to 0$ the second term can be neglected, and in the first term the replacement $n \to n + 1/2$ takes place for spheres.

E.13 Sound Attenuation in a Forest

The previous ⬗ *Sect. E.12* is used for the evaluation of the attenuation of sound in a forest.

First, the forest is modelled as a random arrangement of trunks with average radius a. The escape of sound in the upward direction is neglected. The propagation constant $\Gamma = jk_E$ of the sound wave in the model forest is evaluated from

$$\frac{\Gamma}{k_0} = j\sqrt{\frac{\rho_{eff}}{\rho_0} \cdot \frac{C_{eff}}{C_0}} \tag{1}$$

with

$$\frac{\rho_{eff}}{\rho_0} = 1 + j\frac{8\mu}{\pi(k_0 a)^2}\sum_{n=1,3,5...}D_n,$$

$$\frac{C_{eff}}{C_0} = 1 + j\frac{8\mu}{\pi(k_0 a)^2}\cdot\left[0.5\,D_0 + \sum_{n=2,4,6...}D_n\right], \tag{2}$$

where μ is the massivity of the trunk arrangement and D_n are the scattered mode amplitudes for hard cylinders from the previous section. The attenuation as level decrease per free field wave length λ_0 is

$$(-\Delta L)_{\lambda_0} = 8.686\cdot\text{Re}\{\Gamma/k_0\} = \frac{8.686}{2\pi}\,\text{Re}\{\Gamma\}\,\lambda_0\quad[\text{dB}]. \tag{3}$$

Re $\{\Gamma/k_0\}$ is plotted below over $k_0 a$ for $\mu = (2a/2R)^2$, where 2R is the average mutual distance of the trunks; up to $n_{max} = 8$ scattered modes were used.
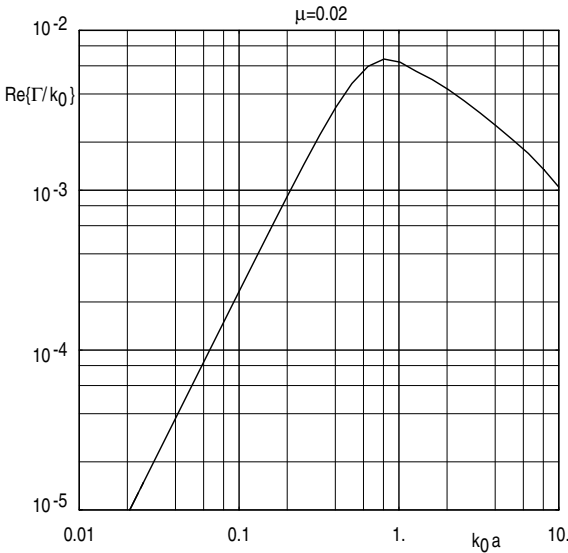
Attenuation constant in a model forest of hard cylindrical trunks with average radius a forming a massivity μ

More instructive is the level decrease ΔL of sound penetrating a strip of forest of width D, with the front side and back side reflections at the forest borders included:

$$(-\Delta L)_D = -20 \cdot \log |t| = -20 \cdot (\log |t_e| + \log |t_a|) + 8.68 \, \mathrm{Re}\{\Gamma\}D \quad [\mathrm{dB}]. \tag{4}$$

This transmission loss $-\Delta L$ is plotted below for $D = 100$ [m] and some trunk diameters. Leaves with a presumably circular shape and average leave radius a_0 will have an effective leaf radius $a = a_0/3^{1/3} = 0.693 \cdot a_0$ normal to the direction of sound because of their random orientation. The leaves are modelled with hard spheres of this effective radius. In C_{eff}/C_0 of the previous ⟩ *Sect. E.12* the mode $n = 0$ with mode amplitude D_0 dominates for small k_0a. The static compressibility of the composite model medium is reduced by $1 \rightarrow 1 - \mu$; therefore one corrects $D_0 \rightarrow D_0/(1 - \mu)$. In ρ_{eff}/ρ_0 the mode $n = 1$ with the mode amplitude D_1 dominates. ρ_{eff} is corrected with the ratio of the oscillating mass of a free disk to that of a sphere. Thus

$$D_0 \rightarrow D_0 \cdot \frac{1}{1 - \mu} \quad ; \quad D_1 \rightarrow D_1 \cdot \frac{1 + \dfrac{2}{\pi}\mu}{1 + \dfrac{3}{2}\mu}. \tag{5}$$

Higher-order mode amplitudes D_n remain unchanged.

The curves in the diagram below show that the transmission loss for a parameter set a, μ, D can be evaluated from the transmission loss for a parameter set a_0, μ_0, D_0 by the transformation

$$\Delta L(f, a, \mu, D) = \frac{a_0 \mu D}{a \, \mu_0 D_0} \cdot \Delta L \left(\frac{a}{a_0} f, a_0, \mu_0, D_0 \right). \tag{6}$$
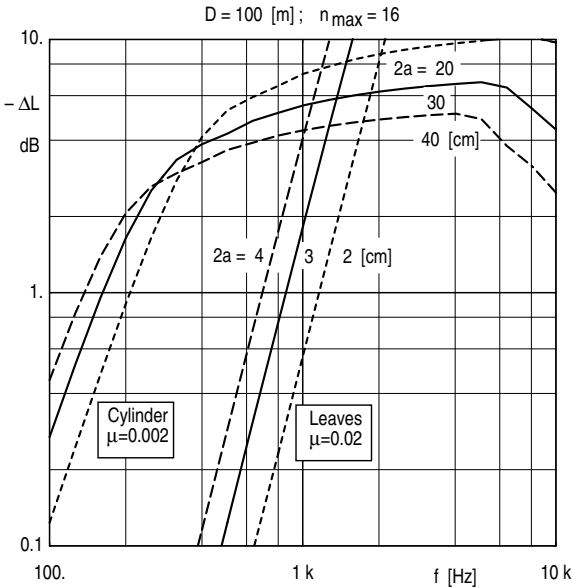
Transmission loss through a model forest, $D = 100$ [m] wide.
The left-hand curves only consider cylindrical, hard trunks; the right-hand curves only consider the leaves, which are modelled as scattering spheres

E.14   Mixed Monotype Scattering in Random Media

The fundamentals of this section are presented in ❯ *Sect. E.11*. The difference in this section with respect to ❯ *Sects. E.11–E.13*, all dealing with monotype scattering, lies in the fact that there not only is the exciting wave of the same type as the scattered wave (density wave), but also their free field wave numbers are supposed to agree with each other. For not too low scatterer densities N, however, the wave which excites a reference scatterer deep in the layer of the composite material will have characteristic values different from those of the wave in free space. This section still makes the assumption that nearby neighbouring scatterers (to the reference scatterer) placed in the forward direction are not shadowed by the reference scatterer with respect to nearby neighbouring scatterers in the backward direction (in front of the scatterer). This condition implies that

$$
\frac{N\,Q_s}{k_0} =
\begin{cases}
\dfrac{2\mu}{\pi\,k_0 a}\,\dfrac{Q_s}{S} \\[2ex]
\dfrac{3\mu}{4\,k_0 a}\,\dfrac{Q_s}{S}
\end{cases}
\approx
\begin{cases}
\dfrac{3\pi}{4}\,\mu\,(k_0 a)^2 \\[2ex]
\dfrac{1}{3}\,\mu\,(k_0 a)^3
\end{cases}
\overset{!}{\ll} 1 \quad ;
\begin{cases}
\text{Cylinder,} \\[2ex]
\text{Sphere.}
\end{cases}
\tag{1}
$$

At the theoretically possible upper limit $\mu = 1$ (which, however, would be in conflict with conditions for the application of monotype scattering), the limits above give $k_0 a \ll 0.65$ for the cylinder and $k_0 a \ll 1.44$ for the sphere.

N	=	number density of scatters;
μ	=	massivity of composite material;
D	=	material layer thickness
Q_S	=	scattering cross section;
a	=	radius of scatterer;
S	=	cross section of scatterer

The effective propagation constant and wave number will be symbolised with $\Gamma = jk_E$, the effective wave impedance with Z_E.

As in ❯ *Sect. E.11*, the scattered far field angular distribution $g(\mathbf{o}, \mathbf{i})$ will be used ($\mathbf{o}$ = outward direction of the scattered field, $\mathbf{i}$ = inward direction of the exciting wave); but the different wave numbers k_0, k_E in both directions will also be indicated; and because only the forward and backward directions (parallel and antiparallel to the incident wave) will be relevant, one changes: $g(\mathbf{o}, \mathbf{i}) \rightarrow g(\pm k_0, \pm k_E)$.

The sound field in the material layer is $\Phi(x) = A\,e^{-jk_E x} + B\,e^{+jk_E x}$ (2)

with the relations between the amplitudes as follows (> *Sect. E.11*):

$$A\, e^{-jk_E x} = e^{-jk_0 x} \cdot \left[1 + \int_0^x e^{jk_0\xi} \cdot (A \cdot S_+\, e^{-jk_E\xi} + B \cdot R_+\, e^{+jk_E\xi})\, d\xi \right],$$

(3)

$$B\, e^{+jk_E x} = e^{+jk_0 x} \cdot \int_x^D e^{-jk_0\xi} \cdot (A \cdot R_-\, e^{-jk_E\xi} + B \cdot S_-\, e^{+jk_E\xi})\, d\xi,$$

where the following abbreviations are used:

$$S_+ = C\, g(k_0,\, k_E) \quad ; \quad S_- = C\, g(-k_0,\, -k_E),$$

(4)

$$R_+ = C\, g(k_0,\, -k_E) \quad ; \quad R_- = C\, g(-k_0,\, k_E).$$

The constant factor C can be taken from Table 5 in > *Sect. E.12*. Integration yields the following system of equations:

$$\frac{S_+}{k_E - k_0} - \frac{R_-}{k_E + k_0} = -j \quad ; \quad \frac{S_-}{k_E - k_0} - \frac{R_+}{k_E + k_0} = -j$$

(5)

$$\frac{A \cdot S_+}{k_E - k_0} - \frac{B \cdot R_-}{k_E + k_0} = -j \quad ; \quad \frac{B \cdot S_- \cdot e^{+jk_E D}}{k_E - k_0} - \frac{A \cdot R_- \cdot e^{-jk_E D}}{k_E + k_0} = 0$$

and the solutions of the last two equations:

$$A = (1 - Q) \cdot F \quad ; \quad B = (1 - Q')\, Q\, e^{-2jk_E D} \cdot F,$$

(6)

where (as in > *Sect. E.11*) the following auxiliary quantities are used:

$$F = [1 - Q\, Q'\, e^{-2jk_E D}]^{-1} \quad ; \quad Q = \frac{R_-}{S_+} \frac{k_E - k_0}{k_E + k_0} \quad ; \quad Q' = \frac{R_+}{S_-} \frac{k_E - k_0}{k_E + k_0}.$$

(7)

For scatterers with front-to-back symmetry (in the statistical average) simplifications are

$$g(k_0,\, k_E) = g(-k_0,\, -k_E) \quad ; \quad g(-k_0,\, k_E) = g(k_0,\, -k_E),$$

$$S_+ = S_- = S \quad ; \quad R_+ = R_- = R \quad ; \quad Q = Q',$$

(8)

$$F = \frac{1}{1 - Q^2\, e^{-2jk_E D}}.$$

For such scatterers the field inside the layer is:

$$\Phi_I(x) = \frac{1 - Q}{1 - Q^2\, e^{-2jk_E D}} \cdot \left(e^{-jk_E x} - Q\, e^{+jk_E(x-2D)} \right) \quad ; \quad 0 \le x \le D;$$

(9)

the reflected field in front of the layer is:

$$\Phi_r(x) = -Q\, (1 - e^{-2jk_E D})\, F \cdot e^{+jk_0 x} \quad ; \quad x \le 0;$$

(10)

the transmitted field behind the layer is:

$$\Phi_t(x) = (1 - Q^2) \, e^{-2j \, k_E D} \, F \cdot e^{-j \, k_0 x} \quad ; \quad x \geq D. \tag{11}$$

The analogy with a homogeneous layer gives the correspondences $Q \leftrightarrow \underline{r}_a; j \, k_E \leftrightarrow \Gamma$, where $\underline{r}_a$ is the reflection factor of the internal plane wave at the back side of the material layer (⊘ Sect. E.11).

Despite the close analogy to the results of ⊘ Sect. E.11 (with pure monotype scattering) there are differences in the $g(\pm k_0, \pm k_E)$ [as compared to $g(\pm \mathbf{o}, \pm \mathbf{i})$; see below for values] and in the definition of Q. For ease of writing (and in close analogy to ⊘ Sect. E.11) the values of the scattered far field angular distribution are defined (for symmetrical scatterers) as

$$g_>(k_0, \ k_E) = g(+k_0, \ +k_E) = g(-k_0, \ -k_E),$$

$$g_<(k_0, \ k_E) = g(-k_0, \ +k_E) = g(+k_0, \ -k_E), \tag{12}$$

with which the wave impedance of the effective wave is,

$$\frac{Z_E}{Z_0} = \frac{1 - Q}{1 + Q} = \frac{\dfrac{k_E}{k_0} \, (g_> - g_<) + (g_> + g_<)}{\dfrac{k_E}{k_0} \, (g_> + g_<) + (g_> - g_<)}, \tag{13}$$

and a square equation holds for the wave number:

$$\frac{k_E^2}{k_0^2} - \frac{k_E}{k_0} \cdot j \frac{C}{k_0} \, (g_> - g_<) - \left(1 + j \frac{C}{k_0} \, (g_> + g_<)\right) = 0. \tag{14}$$

Since both $g_>$ and $g_<$ contain k_E, Z_E, the equation for k_E must be solved numerically, in general.

The still sought $g_>$ and $g_<$ follow from the solution of the scattering task at a single scatterer. The scatterer shall consist of a homogeneous material with a characteristic propagation constant $\Gamma_\sigma = j k_\sigma$ and a characteristic wave impedance Z_σ. The scattered field is formulated as in ⊘ Sect. E.11, i.e. with the scattered mode amplitudes D_n, except for the substitution $k_0 \rightarrow k_E$. The interior field is formulated as

$$p_\sigma(r, \vartheta) = \sum_{n=0}^{\infty} \delta_n \, (-j)^n \, E_n \, T_n(\vartheta) \, R_{\sigma n}(r) \tag{15}$$

with δ_n and the azimuthal functions $T_n(\vartheta)$ taken from Table 2 of ⊘ Sect. E.12, and the radial functions

$$R_{\sigma n}(r) = \begin{cases} J_n(k_\sigma r) \quad ; \quad \text{Cylinder,} \\[12pt] j_n(k_\sigma r) \quad ; \quad \text{Sphere.} \end{cases} \tag{16}$$

The boundary conditions at the surface give for the scattered mode amplitudes D_n and the interior mode amplitudes E_n (below for a cylinder, similarly for a sphere):

$$D_n = \frac{1}{X} \left[\frac{1}{Z_\sigma/Z_0} J_n(k_E a) J_n'(k_\sigma a) - \frac{1}{Z_E/Z_0} J_n(k_\sigma a) J_n'(k_E a) \right],$$

$$E_n = \frac{1}{X} \left[J_n(k_E a) H_n'^{(2)}(k_0 a) - \frac{1}{Z_E/Z_0} H_n^{(2)}(k_0 a) J_n'(k_E a) \right]$$

(17)

with the abbreviation

$$X = J_n(k_\sigma a) H_n'^{(2)}(k_0 a) - \frac{1}{Z_\sigma/Z_0} H_n^{(2)}(k_0 a) J_n'(k_\sigma a)$$

(18)

(a prime indicates the derivative with respect to the argument). With the modal (normalised) admittances G_n the scattered mode amplitudes can be written as:

$$G_n = \frac{j}{Z_\sigma/Z_0} \frac{J_n'(j \Gamma_\sigma a)}{J_n(j \Gamma_\sigma a)},$$

$$D_n = \frac{-1}{Z_E/Z_0} \frac{\left(\frac{n}{k_E a} - j \frac{Z_E}{Z_0} G_n \right) \cdot J_n(k_E a) - J_{n+1}(k_E a)}{\left(\frac{n}{k_0 a} - j G_n \right) \cdot H_n^{(2)}(k_0 a) - H_{n+1}^{(2)}(k_0 a)}.$$

(19)

A locally reacting scatterer with a (normalised) surface admittance G is obtained by the substitution $G_n \to G$.

The usual representation of the characteristic values k_E, Z_E of the composite medium

$$\frac{k_E}{k_0} = \sqrt{\frac{\rho_{eff}}{\rho_0} \cdot \frac{C_{eff}}{C_0}} \quad ; \quad \frac{Z_E}{Z_0} = \sqrt{\frac{\rho_{eff}}{\rho_0} \Big/ \frac{C_{eff}}{C_0}}$$

(20)

with the effective density ρ_{eff} and compressibility C_{eff} is possible with

$$\frac{\rho_{eff}}{\rho_0} = \frac{1}{1 - \frac{k_0}{k_E} \cdot j \frac{C}{k_0} (g_> - g_<)} \quad ; \quad \frac{C_{eff}}{C_0} = 1 + j \frac{C}{k_0} (g_> + g_<).$$

(21)

In the special case of a composite medium consisting of hard, parallel cylinders with radius a, and the plane wave incident normally on the cylinders (a forest of trunks, see ▶ Sect. E.13), the expressions needed in the equations for the characteristic values are

$$g_>(k_0, k_E) + g_<(k_0, k_E) = D_0(k_0, k_E) + 2 \sum_{n=2, 4, \ldots}^{n_{max}} \delta_n D_n(k_0, k_E),$$

$$g_>(k_0, k_E) - g_<(k_0, k_E) = 2 \sum_{n=1, 3, 5, \ldots}^{n_{max}} \delta_n D_n(k_0, k_E).$$

(22)

The diagram shows the attenuation coefficient $\text{Re}\{\Gamma_E/k_0\}$ in such a medium where the scatterers have a massivity $\mu = 0.02$ (cf. ▶ Sect. E.13).
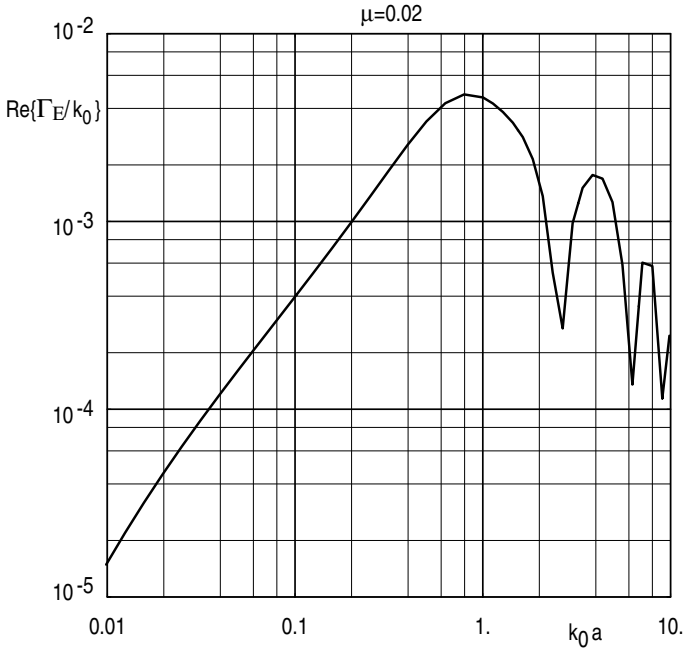
Attenuation coefficient in a composite medium of parallel, hard cylinders of radius a, forming a massivity $\mu = 0.02$, evaluated with the method of mixed monotype scattering

E.15 Multiple Triple-Type Scattering in Random Media

See ▶ *Sect. E.11* for general distinctions and notations. The sections about sound in capillaries in the chapter "Duct Acoustics" contain fundamentals about sound fields with thermal and viscous losses.

A sound wave with a scalar potential function Φ_e is incident on a scatterer in the composite medium. If the mutual distances of the scatterers are larger than the thickness of the shear boundary layer at a scatterer, it will be a density wave; otherwise it will be an "effective" wave Φ_E (i.e. influenced by the three wave types). The scatterer produces a scattered density wave Φ_ρ, a temperature wave Φ_α and a viscous wave $\vec{\Psi}$. $\Phi_\text{ß}$; ß = e, ρ, α are scalar potentials with particle velocities $\vec{v}_\text{ß} = -\text{grad } \Phi_\text{ß}$, and $\vec{\Psi}$ is a vector potential, so that the total particle velocity is

$$\vec{v} = -\sum_\text{ß} \text{grad } \Phi_\text{ß} + \text{rot } \vec{\Psi}. \tag{1}$$

The component fields obey the wave equations

$$(\Delta + k_\text{ß}^2)\,\Phi_\text{ß} = 0 \qquad ; \qquad (\Delta + k_v^2)\,\vec{\Psi} = 0 \tag{2}$$

with characteristic wave numbers (given as squares)

$$k_\rho^2 \approx k_0^2 = \left(\frac{\omega}{c_0}\right)^2 \quad ; \quad k_\nu^2 = -j\frac{\omega}{\nu} \quad ;$$
$$k_\alpha^2 \approx k_{\alpha 0}^2 = -j\frac{\kappa\omega}{\alpha} = \kappa\,\mathrm{Pr}\cdot k_\nu^2 \ . \tag{3}$$

---

c_0 = adiabatic sound velocity;

ρ_0 = air density;

C_0 = air compressibility;

ν = η/ρ = kinematic viscosity;

η = dynamic viscosity;

α = $\Lambda/(\rho_0 c_p)$ = temperature conductivity;

Λ = heat conductivity;

c_p = specific heat at constant pressure;

P_r = ν/α = Prandtl number;

ω = angular frequency;

p_0 = atmospheric pressure

The sound pressure p in the scattered field is

$$p = p_0\Pi_\rho \cdot \Phi_\rho + p_0\Pi_\alpha \cdot \Phi_\alpha. \tag{4}$$

The coefficients $\Pi_ß$ are given in the mentioned sections about capillaries. The ratio Π_E/Π_ρ for an effective wave Φ_E can be expressed by the effective density ρ_{eff} of the composite medium:

$$p_0\Pi_E = jk_E\,Z_E = j\omega\,\rho_{eff} \quad ; \quad \frac{p_0\Pi_E}{p_0\Pi_\rho} = \frac{k_E}{k_0}\,\frac{Z_i}{Z_0} = \frac{\rho_{eff}}{\rho_0}. \tag{5}$$

If the composite medium is statistically homogeneous, the scattered vector potentials $\vec{\Psi}$ compensate each other in the forward and backward directions of scattering; thus the scattered far field angular distributions $g(\mathbf{o},\mathbf{i})$ do not contain the viscous wave in those directions. A similar compensation for the thermal wave Φ_α does not exist; it can be neglected in the propagating wave Φ_e only if the immediate neighbours of a reference scatterer are outside the boundary layer.

The scatterer is assumed below to be either a cylinder or a sphere of a fluid with thermal and viscous losses (hard, soft or locally reacting scatterers can be treated as special cases of this general assumption). Field quantities and material parameters inside the scatterer are marked with a prime. Only Hankel functions of the second kind will appear; the upper index [2] therefore will be dropped (for ease of writing). The exciting wave Φ_e is supposed to have unit amplitude:

$$\Phi_e = e^{-jk_e x} = e^{-jk_e r\,\cos\vartheta}. \tag{6}$$

The particle velocities are:

$$\vec{v} = -\text{grad} \sum_{\text{ß}=e,\rho,\alpha} \Phi_{\text{ß}} + \text{rot}\,\Psi_{\nu} \quad ; \quad \text{outside,}$$

$$\vec{v}' = -\text{grad} \sum_{\text{ß}'=\rho',\alpha'} \Phi_{\text{ß}'} + \text{rot}\,\Psi_{\nu'} \quad ; \quad \text{inside.} \tag{7}$$
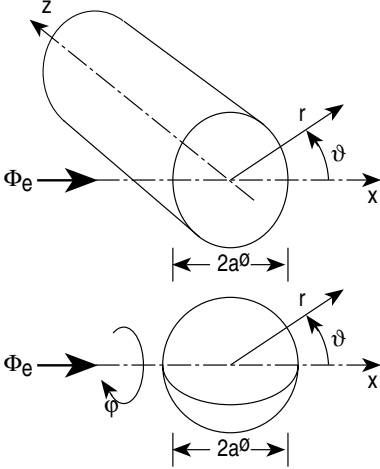
The vector potential of the viscous wave has the components

$$\Psi_{\text{ß}} = \begin{cases} \{0,\,0,\,\Psi_{\text{ß}z}\} & ; \quad \text{Cylinder} \\[2mm] \{0,\,0,\,\Psi_{\text{ß}\varphi}\} & ; \quad \text{Sphere} \end{cases} \quad ; \quad \text{ß} = \nu,\,\nu'. \tag{8}$$

The boundary conditions are:

$$\text{(a):} \quad v_r = v_r' \qquad ; \qquad \text{(b):} \quad v_\vartheta = v_\vartheta' \,;$$

$$\text{(c):} \quad T = T' \qquad ; \qquad \text{(d):} \quad \Lambda \cdot \partial T/\partial r = \Lambda' \cdot \partial T'/\partial r\,; \tag{9}$$

$$\text{(e):} \quad p_{rr} = p_{rr}' \qquad ; \qquad \text{(f):} \quad p_{r\vartheta} = p_{r\vartheta}' \,.$$

(a),(b) fit the radial and tangential particle velocities; (c),(d) fit the (alternating) temperature and heat flow; (e),(f) fit the radial and tangential tensions, which are (i, j standing for co-ordinates; η = dynamic viscosity):

$$p_{ii} = p + 2\eta \cdot \frac{\partial v_i}{\partial x_i} \quad ; \quad p_{ij} = \eta \cdot \left(\frac{\partial v_j}{\partial x_i} + \frac{\partial v_i}{\partial x_j} \right) \quad ; \quad i \neq j. \tag{10}$$

The pressure field is (p_0 = atmospheric pressure):

$$p = p_0 \cdot \sum_{\text{ß}} \Pi_{\text{ß}}\ \Phi_{\text{ß}} \quad ; \quad \text{ß} = \begin{cases} e,\ \rho,\ \alpha & \text{outside,} \\ \\ \rho',\ \alpha' & \text{inside.} \end{cases} \tag{11}$$

The following tables give:
- Strain velocities in cylindrical and spherical co-ordinates;
- Vector components of grad and rot in both systems;
- Field formulations of the incident wave, the scattered wave, and the wave inside the scatterer;
- Terms appearing in the boundary conditions.

Table 3 contains
- $P_n(z)$ Legendre polynomials,
- $P_n^1(z)$ associate Legendre functions, with the useful relations:

$$P_n^1(z) \qquad\qquad = \quad -\sqrt{1-z^2}\ \frac{dP_n(z)}{dz} = -\sqrt{1-z^2}\ P_n'(z)\ ,$$

$$P_n^1(\cos\vartheta) = -\sin\vartheta\ P_n'(\cos\vartheta) \quad = \quad \frac{d}{d\vartheta}\ P_n(\cos\vartheta)\ , \tag{12}$$

$$\frac{1}{\sin\vartheta}\ \frac{d}{d\vartheta}(\sin\vartheta \cdot P_n^1(\cos\vartheta)) \quad = \quad \sin^2\vartheta \cdot P_n''(\cos\vartheta) - 2\cos\vartheta \cdot P_n'(\cos\vartheta)$$

$$\tag{13}$$

$$= \quad -n(n+1) \cdot P_n(\cos\vartheta)$$

and the recursive evaluation

$$P_{n+1}(z) = \frac{1}{n+1}[(2n+1)\ z\ P_n(z) - n\ P_{n-1}(z)] \quad ; \quad P_0(z) = 1 \quad ; \quad P_1(z) = z, \tag{14}$$

from which can be evaluated:

$$P_n^1(\cos\vartheta) = \frac{n}{\sin\vartheta}\ [\cos\vartheta\ P_n(\cos\vartheta) - P_{n-1}(\cos\vartheta)]\ . \tag{15}$$

Table 1 Components of the strain velocity in cylindrical and spherical co-ordinates

	Cylinder	Sphere
1	$\dot{s}_{rr} = \dfrac{\partial v_r}{\partial r}$	$\dot{s}_{rr} = \dfrac{\partial v_r}{\partial r}$
2	$\dot{s}_{\vartheta\vartheta} = \dfrac{1}{r}\left(v_r + \dfrac{\partial v_\vartheta}{\partial \vartheta}\right)$	$\dot{s}_{\vartheta\vartheta} = \dfrac{1}{r}\left(v_r + \dfrac{\partial v_\vartheta}{\partial \vartheta}\right)$
3	$\dot{s}_{zz} = \dfrac{\partial v_z}{\partial z}$	$\dot{s}_{\varphi\varphi} = \dfrac{1}{\sin\vartheta}\left[v_r \sin\vartheta + v_\vartheta \cos\vartheta + \dfrac{\partial v_\varphi}{\partial\varphi}\right]$
4	$\dot{s}_{r\vartheta} = \dot{s}_{\vartheta r}$ $= \dfrac{1}{2}\left[\dfrac{\partial v_\vartheta}{\partial r} - \dfrac{v_\vartheta}{r} + \dfrac{1}{r}\dfrac{\partial v_r}{\partial\vartheta}\right]$	$\dot{s}_{r\vartheta} = \dot{s}_{\vartheta r}$ $= \dfrac{1}{2r}\left[r\dfrac{\partial v_\vartheta}{\partial r} - v_\vartheta + \dfrac{\partial v_r}{\partial\vartheta}\right]$
5	$\dot{s}_{z\vartheta} = \dot{s}_{\vartheta z} = \dfrac{1}{2}\left[\dfrac{1}{r}\dfrac{\partial v_z}{\partial\vartheta} + \dfrac{\partial v_\vartheta}{\partial z}\right]$	$\dot{s}_{r\varphi} = \dot{s}_{\varphi r}$ $= \dfrac{1}{2r\sin\vartheta}\left[\dfrac{\partial v_r}{\partial\varphi} + r\dfrac{\partial v_\varphi}{\partial r}\sin\vartheta - v_\varphi\sin\vartheta\right]$
6	$\dot{s}_{zr} = \dot{s}_{rz} = \dfrac{1}{2}\left[\dfrac{\partial v_r}{\partial z} + \dfrac{\partial v_z}{\partial r}\right]$	$\dot{s}_{\vartheta\varphi} = \dot{s}_{\varphi\vartheta}$ $= \dfrac{1}{2r\sin\vartheta}\left[\dfrac{\partial v_\varphi}{\partial\vartheta}\sin\vartheta - v_\varphi\cos\vartheta + \dfrac{\partial v_\vartheta}{\partial\varphi}\right]$

Table 2 Components of grad and rot in cylindrical and spherical co-ordinates

	Component	Cylinder	Sphere
1		grad U	
2	r	$\dfrac{\partial U}{\partial r}$	$\dfrac{\partial U}{\partial r}$
3	ϑ	$\dfrac{1}{r}\dfrac{\partial U}{\partial\vartheta}$	$\dfrac{1}{r}\dfrac{\partial U}{\partial\vartheta}$
4	z, φ	$\dfrac{\partial U}{\partial z}$	$\dfrac{1}{r\sin\varphi}\dfrac{\partial U}{\partial\varphi}$
5		rot **V**	
6	r	$\dfrac{1}{r}\dfrac{\partial V_z}{\partial\vartheta} - \dfrac{\partial V_\vartheta}{\partial z}$	$\dfrac{1}{r\sin\vartheta}\left(\dfrac{\partial}{\partial\vartheta}(\sin\vartheta\, V_\varphi) - \dfrac{\partial V_\vartheta}{\partial\varphi}\right)$
7	ϑ	$\dfrac{\partial V_r}{\partial z} - \dfrac{\partial V_z}{\partial r}$	$\dfrac{1}{r\sin\vartheta}\left(\dfrac{\partial V_r}{\partial\varphi} - \dfrac{1}{r}\dfrac{\partial}{\partial r}(rV_\varphi)\right)$
8	z, φ	$\dfrac{1}{r}\left(\dfrac{\partial(rV_\vartheta)}{\partial r} - \dfrac{\partial V_r}{\partial\vartheta}\right)$	$\dfrac{1}{r}\dfrac{\partial}{\partial r}(rV_\vartheta) - \dfrac{1}{r}\dfrac{\partial V_r}{\partial\vartheta}$

Table 3 Field formulations of the incident wave, the scattered wave and the interior wave

	Quantity	Cylinder	Sphere
1	**Incident wave** $\Phi_e(r, \vartheta) =$	$\Phi_e(r, \vartheta) = e^{-jk_e r \cdot \cos\vartheta}$ $\sum_{n=0}^{\infty} \delta_n \cdot (-j)^n \cdot T_n(\vartheta) \cdot R_{en}(r)$	
2	$\delta_n =$	$\begin{cases} 1 \; ; \; n = 0 \\ 2 \; ; \; n > 0 \end{cases}$	$2n + 1$
3	$T_n(\vartheta) =$	$\cos(n\vartheta)$	$P_n(\cos\vartheta)$
4	$R_{en}(r) =$	$J_n(k_e r)$	$j_n(k_e r)$
5	**Scattered wave** $\Phi_\beta(r, \vartheta) =$	$\sum_{n=0}^{\infty} \delta_n \cdot (-j)^n \cdot A_{\beta n} \cdot T_n(\vartheta) \cdot R_{an}(r)$	
6	$T_n(\vartheta) =$	$\cos(n\vartheta)$	$P_n(\cos\vartheta)$
7	$\Psi_{vz(\varphi)}(r, \vartheta) =$	$\sum_{n=0}^{\infty} \delta_n \cdot (-j)^n \cdot A_{vn} \cdot T_n^1(\vartheta) \cdot R_{an}(r) \quad ; \quad A_{v0} = 0$	
8	$T_n^1(\vartheta) =$	$\sin(n\varphi)$	$P_n^1(\cos\vartheta)$
9	$R_{an}(r) =$	$H_n(k_\beta r) \quad ; \quad \beta = \rho, \alpha, v$	$h_n(k_\beta r) \quad ; \quad \beta = \rho, \alpha, v$
10	**Interior wave** $\Phi_{\beta'}(r, \vartheta) =$	$\sum_{n=0}^{\infty} \delta_n \cdot (-j)^n \cdot A_{\beta' n} \cdot T_n(\vartheta) \cdot R_{in}(r)$	
11	$T_n(\vartheta) =$	$\cos(n\vartheta)$	$P_n(\cos\vartheta)$
12	$\Psi_{v'z(\varphi)}(r, \vartheta) =$	$\sum_{n=0}^{\infty} \delta_n \cdot (-j)^n \cdot A_{v'n} \cdot T_n^1(\vartheta) \cdot R_{in}(r) \quad ; \quad A_{v'0} = 0$	
13	$T_n^1(\vartheta) =$	$\sin(n\varphi)$	$P_n^1(\cos\vartheta)$
14	$R_{in}(r) =$	$J_n(k_{\beta'} r) \quad ; \quad \beta' = \rho', \alpha', v'$	$j_n(k_{\beta'} r) \quad ; \quad \beta' = \rho', \alpha', v'$

Table 4 Terms in the boundary conditions

	Quantity	Cylinder	Sphere
1	$v_r =$	$-\dfrac{\partial}{\partial r}\sum\limits_{\beta}\Phi_\beta + \dfrac{1}{r}\dfrac{\partial\Psi_z}{\partial\vartheta}$	$-\dfrac{\partial}{\partial r}\sum\limits_{\beta}\Phi_\beta + \dfrac{1}{r\sin\vartheta}\dfrac{\partial}{\partial\vartheta}(\sin\vartheta\Psi_\varphi)$
2	$v_\vartheta =$	$-\dfrac{1}{r}\dfrac{\partial}{\partial\vartheta}\sum\limits_{\beta}\Phi_\beta - \dfrac{\partial\Psi_z}{\partial r}$	$-\dfrac{1}{r}\dfrac{\partial}{\partial\vartheta}\sum\limits_{\beta}\Phi_\beta - \dfrac{\Psi_\varphi}{r} - \dfrac{\partial\Psi_z}{\partial r}$
3	$\dfrac{T}{T_0} =$	$\sum\limits_{\beta}\Theta_\beta\Phi_\beta$	$\sum\limits_{\beta}\Theta_\beta\Phi_\beta$
4	$\dfrac{\partial}{\partial r}\dfrac{T}{T_0} =$	$\sum\limits_{\beta}\Theta_\beta\dfrac{\partial\Phi_\beta}{\partial r}$	$\sum\limits_{\beta}\Theta_\beta\dfrac{\partial\Phi_\beta}{\partial r}$
5	$P_{rr} =$	$p_0\sum\limits_{\beta}\Pi_\beta\Phi_\beta$ $+2\eta\left[-\sum\limits_{\beta}\dfrac{\partial^2\Phi_\beta}{\partial r^2}\right.$ $\left.+\dfrac{\partial}{\partial\vartheta}\left(-\dfrac{\Psi_z}{r^2}+\dfrac{1}{r}\dfrac{\partial\Psi_z}{\partial r}\right)\right]$	$p_0\sum\limits_{\beta}\Pi_\beta\Phi_\beta$ $+2\eta\left\{-\sum\limits_{\beta}\dfrac{\partial^2\Phi_\beta}{\partial r^2}\right.$ $\left.+\dfrac{1}{\sin\vartheta}\dfrac{\partial}{\partial\vartheta}\left[\sin\vartheta\left(-\dfrac{\Psi_\varphi}{r^2}+\dfrac{1}{r}\dfrac{\partial\Psi_\varphi}{\partial r}\right)\right]\right\}$
6	$P_{r\vartheta} =$	$\eta\left[-2\sum\limits_{\beta}\dfrac{\partial}{\partial\vartheta}\left(\dfrac{1}{r}\dfrac{\partial\Phi_\beta}{\partial r}-\dfrac{\Phi_\beta}{r^2}\right)\right.$ $\left.-\left(\dfrac{\partial^2\Psi_z}{\partial r^2}-\dfrac{1}{r}\dfrac{\partial\Psi_z}{\partial r}\right)+\dfrac{1}{r^2}\dfrac{\partial^2\Psi_z}{\partial\vartheta^2}\right]$	$\eta\left\{-2\sum\limits_{\beta}\dfrac{\partial}{\partial\vartheta}\left(\dfrac{1}{r}\dfrac{\partial\Phi_\beta}{\partial r}-\dfrac{\Phi_\beta}{r^2}\right)\right.$ $-\left(\dfrac{\partial^2\Psi_\varphi}{\partial r^2}-\dfrac{2}{r^2}\Psi_\varphi\right)$ $\left.+\dfrac{1}{r^2}\dfrac{\partial}{\partial\vartheta}\left[\dfrac{1}{\sin\vartheta}\dfrac{\partial}{\partial\vartheta}(\sin\vartheta\Psi_\varphi)\right]\right\}$

The following Table 5 contains the equations of the boundary conditions with the above field formulations. Use was made of the derivatives of the radial functions:

$$z\cdot R_n'(z) = n\cdot R_n(z) - z\cdot R_{n+1}(z) \tag{16}$$

and for the second derivatives of the cylindrical radial functions $Z_n(z)$ and spherical radial functions $K_n(z)$:

$$z^2\cdot Z_n''(z) = (n^2 - n - z^2)\cdot Z_n(z) + z\cdot Z_{n+1}(z),$$

$$z^2\cdot K_n''(z) = (n^2 - n - z^2)\cdot K_n(z) + 2z\cdot K_{n+1}(z). \tag{17}$$

The following terms, appearing in the table, can be simplified as:

$$\frac{p_0 a^2\Pi_\rho}{\eta} = -(k_v a)^2\frac{k_\rho^2}{k_0^2}\frac{1-(k_\rho/k_{\alpha 0})^2}{1-\kappa(k_\rho/k_{\alpha 0})^2} \approx -(k_v a)^2,$$

$$\frac{p_0 a^2\Pi_\alpha}{\eta} \approx -(k_v a)^2\left(1-\frac{4}{3}\kappa\ \mathrm{Pr}\right) \quad ; \quad \frac{p_0 a^2\Pi_E}{\eta} = -(k_v a)^2\frac{\rho_{\mathrm{eff}}}{\rho_0}. \tag{18}$$

Table 5a Equations for cylinder

Bound cond.	Equations for cylinder
$v_r = v_r'$	$nJ_n(k_e a) - k_e a J_{n+1}(k_e a) + \sum\limits_{\beta=\rho,\alpha} A_{\beta n}[nH_n(k_\beta a) - k_\beta a H_{n+1}(k_\beta a)] - A_{vn} n H_n(k_v a)$ $= \sum\limits_{\beta'=\rho',\alpha'} A_{\beta' n}[nJ_n(k_{\beta'} a) - k_{\beta'} a J_{n+1}(k_{\beta'} a)] - A_{v'n} n J_n(k_{v'} a)$
$v_\vartheta = v_\vartheta'$	$nJ_n(k_e a) + \sum\limits_{\beta=\rho,\alpha} A_{\beta n} n H_n(k_\beta a) - A_{vn}[nH_n(k_v a) - k_v a H_{n+1}(k_v a)]$ $= \sum\limits_{\beta'=\rho',\alpha'} A_{\beta' n} n J_n(k_{\beta'} a) - A_{v'n}[nJ_n(k_{v'} a) - k_{v'} a J_{n+1}(k_{v'} a)]$
$\dfrac{T}{T_0} = \dfrac{T'}{T_0}$	$\Theta_e J_n(k_e a) + \sum\limits_{\beta=\rho,\alpha} A_{\beta n} \Theta_\beta H_n(k_\beta a) = \sum\limits_{\beta'=\rho',\alpha'} A_{\beta' n} \Theta_{\beta'} J_n(k_{\beta'} a)$
$\Lambda \dfrac{\partial}{\partial r} \dfrac{T}{T_0} =$ $\Lambda' \dfrac{\partial}{\partial r} \dfrac{T'}{T_0}$	$\Lambda \left[\Theta_e \left[n\, J_n(k_e a) - k_e a\, J_{n+1}(k_e a) \right] + \sum\limits_{\beta=\rho,\alpha} A_{\beta n}\, \Theta_\beta \left[n\, H_n(k_\beta a) - k_\beta a\, H_{n+1}(k_\beta a) \right] \right]$ $= \Lambda' \left[\sum\limits_{\beta'=\rho',\alpha'} A_{\beta' n}\, \Theta_{\beta'} \left[n\, J_n(k_{\beta'} a) - k_{\beta'} a\, J_{n+1}(k_{\beta'} a) \right] \right]$
$p_{rr} = p_{rr}'$	$\eta\left[\left[\dfrac{\rho_0 a^2}{\eta}\Pi_e + 2(n - n^2 + (k_e a)^2) \right]J_n(k_e a) - 2k_e a J_{n+1}(k_e a) \right.$ $+ \sum\limits_{\beta=\rho,\alpha} A_{\beta n}\left(\left[\dfrac{\rho_0 a^2}{\eta}\Pi_\beta + 2(n - n^2 + (k_\beta a)^2) \right]H_n(k_\beta a) - 2k_\beta a H_{n+1}(k_\beta a)\right)$ $\left. + A_{vn} 2n[(n-1)H_n(k_v a) - k_v a H_{n+1}(k_v a)] \right]$ $= \eta'\left[A_{v'n} 2n[(n-1)J_n(k_{v'} a) - k_{v'} a J_{n+1}(k_{v'} a)] \right.$ $\left. + \sum\limits_{\beta'=\rho',\alpha'} A_{\beta' n}\left(\left[\dfrac{\rho_0 a^2}{\eta'}\Pi_{\beta'} + 2(n - n^2 + (k_{\beta'} a)^2) \right]J_n(k_{\beta'} a) - 2k_{\beta'} a J_{n+1}(k_{\beta'} a)\right) \right]$
$p_{r\vartheta} = p_{r\vartheta}'$	$\eta\left[2n[(n-1)J_n(k_e a) - k_e a J_{n+1}(k_e a)] \right.$ $+ 2n \sum\limits_{\beta=\rho,\alpha} A_{\beta n}[(n-1)H_n(k_\beta a) - k_\beta a H_{n+1}(k_\beta a)]$ $\left. - A_{vn}[(2n(n-1) - (k_v a)^2)H_n(k_v a) + 2k_v a H_{n+1}(k_v a)] \right]$ $= \eta'\left[2n \sum\limits_{\beta'=\rho,\alpha} A_{\beta' n}[(n-1)J_n(k_{\beta'} a) - k_{\beta'} a J_{n+1}(k_{\beta'} a)] \right.$ $\left. - A_{v'n}[(2n(n-1) - (k_{v'} a)^2)J_n(k_{v'} a) + 2k_{v'} a J_{n+1}(k_{v'} a)] \right]$

Table 5b Equations for sphere

Bound. cond.	Equations for Sphere
$v_r = v_r'$	$nj_n(k_ea) - k_ea\,j_{n+1}(k_ea) + \sum\limits_{\beta=\rho,\alpha} A_{\beta n}[nh_n(k_\beta a) + k_\beta a\,h_{n+1}(k_\beta a)] + A_{vn}n(n+1)h_n(k_v a)$ $= \sum\limits_{\beta'=\rho',\alpha'} A_{\beta'n}[nj_n(k_{\beta'}a) - k_{\beta'}a\,j_{n+1}(k_{\beta'}a)] + A_{v'n}n(n+1)j_n(k_{v'}a)$
$v_\vartheta = v_\vartheta'$	$j_n(k_ea) + \sum\limits_{\beta=\rho,\alpha} A_{\beta n}h_n(k_\beta a) + A_{vn}[(n+1)h_n(k_v a) - k_v a\,h_{n+1}(k_v a)]$ $= \sum\limits_{\beta'=\rho',\alpha'} A_{\beta'n}j_n(k_{\beta'}a) + A_{v'n}[(n+1)j_n(k_{v'}a) - k_{v'}a\,j_{n+1}(k_{v'}a)]$
$\dfrac{T}{T_0} = \dfrac{T'}{T_0}$	$\Theta_e j_n(k_ea) + \sum\limits_{\beta=\rho,\alpha} A_{\beta n}\Theta_\beta h_n(k_\beta a) = \sum\limits_{\beta'=\rho',\alpha'} A_{\beta'n}\Theta_{\beta'}j_n(k_{\beta'}a)$
$\Lambda \dfrac{\partial}{\partial r}\dfrac{T}{T_0} =$ $\Lambda' \dfrac{\partial}{\partial r}\dfrac{T'}{T_0}$	$\Lambda\left[\Theta_e\,[n\,j_n(k_ea) - k_ea\,j_{n+1}(k_ea)] + \sum\limits_{\beta=\rho,\alpha} A_{\beta n}\,\Theta_\beta\,[n\,h_n(k_\beta a) - k_\beta a\,h_{n+1}(k_\beta a)]\right]$ $= \Lambda'\left[\sum\limits_{\beta'=\rho',\alpha'} A_{\beta'n}\,\Theta_{\beta'}\,[n\,j_n(k_{\beta'}a) - k_{\beta'}a\,j_{n+1}(k_{\beta'}a)]\right]$
$p_{rr} = p_{rr}'$	$\eta\left[\left[\left[\dfrac{\rho_0 a^2}{\eta}\Pi_e + 2(n - n^2 + (k_ea)^2)\right]j_n(k_ea) - 4k_ea\,j_{n+1}(k_ea)\right.\right.$ $+ \sum\limits_{\beta=\rho,\alpha} A_{\beta n}\left(\left[\dfrac{\rho_0 a^2}{\eta}\Pi_\beta + 2(n - n^2 + (k_\beta a)^2)\right]h_n(k_\beta a) - 4k_\beta a\,h_{n+1}(k_\beta a)\right)$ $\left.- A_{vn}2n(n+1)[(n-1)h_n(k_v a) - k_v a h_{n+1}(k_v a)]\right]$ $= \eta'\left[-A_{v'n}2n(n+1)[(n-1)j_n(k_{v'}a) - k_{v'}a\,j_{n+1}(k_{v'}a)]\right.$ $+ \sum\limits_{\beta'=\rho',\alpha'} A_{\beta'n}\left(\left[\dfrac{\rho_0 a^2}{\eta'}\Pi_{\beta'} + 2(n - n^2 + (k_{\beta'}a)^2)\right]j_n(k_{\beta'}a) - 4k_{\beta'}a\,j_{n+1}(k_{\beta'}a)\right)\right]$
$p_{r\vartheta} = p_{r\vartheta}'$	$\eta\left[2[(n-1)j_n(k_ea) - k_ea\,j_{n+1}(k_ea)]\right.$ $+ 2\sum\limits_{\beta=\rho,\alpha} A_{\beta n}[(n-1)h_n(k_\beta a) - k_\beta a\,h_{n+1}(k_\beta a)]$ $\left.+ A_{vn}[(2(n^2-1) - (k_v a)^2)h_n(k_v a) + 2k_v a\,h_{n+1}(k_v a)]\right]$ $= \eta'\left[2\sum\limits_{\beta'=\rho',\alpha'} A_{\beta'n}[(n-1)j_n(k_{\beta'}a) - k_{\beta'}a\,j_{n+1}(k_{\beta}'a)]\right.$ $\left.+ A_{v'n}[(2(n^2-1) - (k_{v'}a)^2)j_n(k_{v'}a) + 2k_{v'}a\,j_{n+1}(k_{v'}a)]\right]$

Further, the coefficients $\Theta_E, \Theta_\rho, \Theta_\alpha$ can be written as:

$$\Theta_E = \frac{\kappa}{\alpha} \frac{k_E^2}{k_{\alpha 0}^2} \frac{\kappa - 1}{1 - \kappa \cdot k_E^2/k_{\alpha 0}^2} \approx \frac{\kappa(\kappa - 1)}{\alpha} \frac{k_E^2}{k_{\alpha 0}^2},$$

$$\Theta_{\text{ß}} = \frac{\kappa}{\alpha} \frac{k_{\text{ß}}^2}{k_{\alpha 0}^2} \frac{\kappa - 1}{1 - \kappa \cdot k_{\text{ß}}^2/k_{\alpha 0}^2} \approx \begin{cases} \dfrac{\kappa(\kappa - 1)}{\alpha} \dfrac{k_\rho^2}{k_{\alpha 0}^2} & ; \quad \text{ß} = \rho, \\[2mm] \dfrac{-\kappa}{\alpha} & ; \quad \text{ß} = \alpha, \end{cases}$$
(19)

$$\frac{\Theta_{\text{ß}}}{\Theta_\alpha} \approx -(\kappa - 1) \frac{k_{\text{ß}}^2}{k_{\alpha 0}^2} \quad ; \quad \text{ß} = \rho, \; E \quad ; \quad \Lambda\, \Theta_{\text{ß}} \approx \begin{cases} \rho_0\, c_p\, (\kappa - 1) \dfrac{k_{\text{ß}}^2}{k_{\alpha 0}^2} & ; \quad \text{ß} = \rho,\; E, \\[2mm] -\rho_0 c_p & ; \quad \text{ß} = \alpha. \end{cases}$$
(20)

The six boundary equations in the above tables (for each shape of the scatterer) originally contained common factors on both sides; they have been divided out. If these boundary equations are to be used for other types of scatterers besides fluid cylinders or spheres, the factors must be included again before the modification of the equations. These factors are contained in the following Table 6, the first column of which indicates the number of the corresponding row in the above tables and the index letter used above for the boundary conditions.

Table 6 Common factors on both sides of the boundary equations

	Quantity	Factors	
		Cylinder	Sphere
1 (a)	v_r	$-(-j)^n \delta_n \dfrac{\cos(n\vartheta)}{a}$	$-(-j)^n \delta_n \dfrac{P_n(\cos\vartheta)}{a}$
2 (b)	v_ϑ	$(-j)^n \delta_n \dfrac{\sin(n\vartheta)}{a}$	$-(-j)^n \delta_n \dfrac{dP_n(\cos\vartheta)/d\vartheta}{a}$
3 (c)	$\dfrac{T_1}{T_0}$	$(-j)^n \delta_n \cos(n\vartheta)$	$(-j)^n \delta_n P_n(\cos\vartheta)$
4 (d)	$\Lambda \dfrac{\partial}{\partial r} \dfrac{T_1}{T_0}$	$(-j)^n \delta_n \dfrac{\cos(n\vartheta)}{a}$	$(-j)^n \delta_n \dfrac{P_n(\cos\vartheta)}{a}$
5 (e)	p_{rr}	$(-j)^n \delta_n \dfrac{\cos(n\vartheta)}{a^2}$	$(-j)^n \delta_n \dfrac{P_n(\cos\vartheta)}{a^2}$
6 (f)	$p_{r\vartheta}$	$(-j)^n \delta_n \dfrac{\sin(n\vartheta)}{a^2}$	$-(-j)^n \delta_n \dfrac{dP_n(\cos\vartheta)/d\vartheta}{a^2}$

Special types of scatterers

Elastic scatterers:
Replace the dynamic viscosity η' with the shear modulus G' or the Lamé constant μ' and the sound velocity c_0' with the compression modulus K' or the second Lamé constant λ' according to

$$\eta' \to \mu'/j\omega = G'/j\omega,$$

$$c_0' \to \sqrt{K'/\rho_0'} \quad ; \quad K' = \lambda' + \frac{2}{3}\mu'. \tag{21}$$

Rigid scatterer at rest:

Set $v_r' = v_\vartheta' = 0 \quad ; \quad k_{\rho'} = k_{\alpha'} \to 0 \quad ; \quad R_{n>0}(k_{\text{ß}'}a) = 0 \quad ; \quad R_0(k_{\text{ß}'}a) = 1.$ \tag{22}

Delete the boundary conditions (e), (f); in (a)–(d) delete on the right-hand sides all interior wave terms except the temperature wave term. In the special case of an isothermal surface delete (d) and set the right-hand side in (c) to zero. In this special case only a set of amplitudes $A_{\text{ß}n}$ with $\text{ß} = \rho, \alpha, \nu$ must be determined.

Porous scatterers:

Mostly $|k_\rho a|^2$, $|k_E a|^2 \ll 1$ and $|k_\rho/k_\text{ß}|^2 \ll 1$; $\text{ß} = \alpha, \nu$. Then the radial functions $R_n(k_\rho a)$ can be approximated with the first term of their power series, and terms with $\Theta_\rho/\Theta_\alpha$ and Π_α/Π_ρ can be neglected.

Isothermal, freely oscillating hard scatterer:

This case will be fully formulated here. The oscillation is in the x direction ($\delta_1 = 2$ is retained from the general formulations):

$$\Phi_x = (-j)^1 \delta_1 \cdot A_x \frac{x}{a} = (-j)^1 \delta_1 \cdot A_x \frac{r}{a} \cos\vartheta,$$

$$v_x = j\delta_1 \frac{A_x}{a} \quad ; \quad v_r = j\delta_1 A_x \frac{\cos\vartheta}{a} \quad ; \quad v_\vartheta = -j\delta_1 A_x \frac{\sin\vartheta}{a}. \tag{23}$$

On the right-hand sides of the boundary conditions (a), (b) all terms with $n \neq 1$ vanish; and for $n = 1$ there will appear A_x. The right-hand side of the boundary condition (c) disappears, and also the complete boundary condition (d). The two last boundary conditions (e), (f) are replaced by an equation for the balance of force K_x (which is the integral of the stresses in the x direction over the scatterer surface):

$$K_x = \oint (p_{rr} \cos\vartheta - p_{r\vartheta} \sin\vartheta) \cdot dA \overset{!}{=} j\omega M \cdot v_x = j\omega M \cdot j\delta_1 \frac{A_x}{a}, \tag{24}$$

Table 7 Boundary conditions for an isothermal, hard, freely movable scatterer

Bound. cond.	Equations
Cylinder	
$v_r =$ $v_x \cos \vartheta$	$\displaystyle\sum_{\beta=\rho,\alpha} A_{\beta n}[nH_n(k_\beta a) - k_\beta a\, H_{n+1}(k_\beta a)] - A_{vn} nH_n(k_v a) - A_x \delta_{1,n}$ $\qquad = -[nJ_n(k_e a) - k_e a J_{n+1}(k_e a)]$
$v_\vartheta =$ $-v_x \sin \vartheta$	$\displaystyle\sum_{\beta=\rho,\alpha} A_{\beta n} nH_n(k_\beta a) - A_{vn}[nH_n(k_v a) - k_v a H_{n+1}(k_v a)] - A_x \delta_{1,n}$ $\qquad = -nJ_n(k_e a)$
$\dfrac{T}{T_0} = 0$	$\displaystyle\sum_{\beta=\rho,\alpha} A_{\beta n} \Theta_\beta H_n(k_\beta a) = -\Theta_e J_n(k_e a)$
$K_x =$ $j\omega M v_x$	$\displaystyle\sum_{\beta=\rho,\alpha} A_{\beta 1}\left[\frac{\rho_0 a^2}{\eta}\Pi_\beta + 2(k_\beta a)^2\right] H_1(k_\beta a)$ $- A_{v1}(k_v a)^2 H_1(k_v a) - A_x(k_v a)^2 \dfrac{\rho_0'}{\rho_0}$ $\qquad = -\left[\frac{\rho_0 a^2}{\eta}\Pi_e + 2(k_e a)^2\right] J_1(k_e a)$
Sphere	
$v_r =$ $v_x \cos \vartheta$	$\displaystyle\sum_{\beta=\rho,\alpha} A_{\beta n}[nh_n(k_\beta a) - k_\beta a\, h_{n+1}(k_\beta a)] + A_{vn} n(n+1)h_n(k_v a) - A_x \delta_{1,n}$ $\qquad = -[nj_n(k_e a) - k_e a\, j_{n+1}(k_e a)]$
$v_\vartheta =$ $-v_x \sin \vartheta$	$\displaystyle\sum_{\beta=\rho,\alpha} A_{\beta n} h_n(k_\beta a) + A_{vn}[(n+1)h_n(k_v a) - k_v a\, h_{n+1}(k_v a)] - A_x \delta_{1,n}$ $\qquad = -j_n(k_e a)$
$\dfrac{T}{T_0} = 0$	$\displaystyle\sum_{\beta=\rho,\alpha} A_{\beta n} \Theta_\beta h_n(k_\beta a) = -\Theta_e j_n(k_e a)$
$K_x =$ $j\omega M v_x$	$\displaystyle\sum_{\beta=\rho,\alpha} A_{\beta 1}\left[\frac{\rho_0 a^2}{\eta}\Pi_\beta + 2(k_\beta a)^2\right] h_1(k_\beta a)$ $+ A_{v1} 2(k_v a)^2 h_1(k_v a) - A_x(k_v a)^2 \dfrac{\rho_0'}{\rho_0}$ $\qquad = -\left[\frac{\rho_0 a^2}{\eta}\Pi_e + 2(k_e a)^2\right] j_1(k_e a)$

where $M = \rho_0' V_0$ is the scatterer's mass (per unit length of the cylinder). The integrals over the terms with p_{rr}, $p_{r\vartheta}$ lead respectively to

$$I_{rr} = \int_0^\pi P_n(\cos\vartheta) \ \cos\vartheta \ \sin\vartheta \ d\vartheta = \int_{-1}^{+1} y \cdot P_n(y) \ dy = \frac{2}{3} \delta_{1,n},$$

(25)

$$I_{r\vartheta} = \int_0^\pi \frac{\partial}{\partial\vartheta}(P_n(\cos\vartheta)) \ \sin^2\vartheta \ d\vartheta = -2 \ I_{rr} = -\frac{4}{3} \delta_{1,n}$$

with the Kronecker symbol $\delta_{m,n}$.

The boundary equations for an isothermal, movable, hard scatterer are given in Table 7.

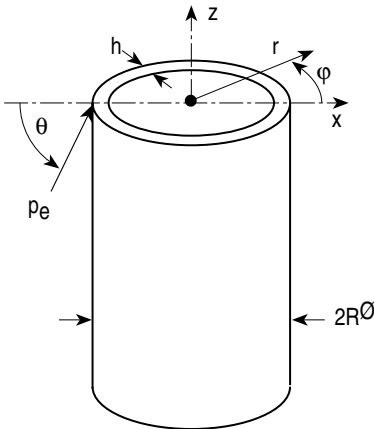## E.16   Plane Wave Scattering at Elastic Cylindrical Shell

▶ *See also:* Paniklenko/Rybak (1984)

A plane wave p_e is incident (under an angle θ with the radius) on a cylindrical shell with radius R and thickness h.

The exterior sound field is written as

$p = p_e + p_r + p_s$

with p_r the scattered field from a hard cylinder and p_s additional scattering due to elasticity.

Parameters of the surrounding medium: ρ_0, c_0, k_0, Z_0 = density, sound speed, free field wave number, free field wave impedance.

Parameters of the shell:
ρ, σ, E η = density, Poisson ratio, Young's modulus, loss factor;
c_D, k_D = speed and wave number of the dilatational wave in a plate of thickness h;
$\underline{E} = E \cdot (1 + j \cdot \eta)$ = complex Young's modulus.

Abbreviations:

$$\Omega_0 = k_0 R; \quad \Omega = k_D R; \quad \xi = k_0 r \cdot \cos \theta; \quad \delta_0 = 1; \quad \delta_{n>0} = 2. \tag{1}$$

Field component formulations:

$$p_e(r, \varphi) = e^{-j(k_0 r \cdot \cos \theta \cdot \cos \varphi + k_0 z \cdot \sin \theta)},$$

$$p_r(r, \varphi) = \sum_{n \geq 0} \frac{J_n'(\xi)}{H_n^{(2)}(\xi)}, \tag{2}$$

$$p_s(r, \varphi) = \frac{-2 Z_0}{\pi \Omega_0 \cos \theta} e^{-j k_0 z \cdot \sin \theta} \sum_{n \geq 0} \frac{\delta_n (-j)^n H_n^{(2)}(\xi) \cdot \cos(n\varphi)}{\left(H_n'^{(2)}(\Omega_0 \cos \theta)\right)^2 (Z_{mn} + Z_{sn})}$$

with radiation impedance Z_{sn} of the n-th mode of the shell:

$$Z_{sn} = \frac{-j Z_0}{\cos \theta} \frac{H_n^{(2)}(\Omega_0 \cos \theta)}{H_n'^{(2)}(\Omega_0 \cos \theta)} \tag{3}$$

and the mechanical impedance Z_{mn} of the n-th shell mode:

$$Z_{mn} = \frac{-j \rho h}{\Omega^2} \frac{D}{D_1} \quad ; \quad D = \text{Det}\{A_{ik}\} \quad ; \quad D_1 = A_{11} \cdot A_{22} - A_{12} \cdot A_{21} \quad ; \quad i, k = 1, \ldots, 3 \tag{4}$$

with matrix coefficients

$$A_{11} = \Omega^2 - (\Omega_0 \sin \theta)^2 - (1 - \sigma) n^2/2 \quad ; \quad A_{12} = -A_{21} = -j(1 + \sigma) \Omega_0 \sin(n\theta/2),$$

$$A_{13} = -A_{31} = -j \sigma \Omega_0 \sin \theta,$$

$$A_{22} = \Omega^2 - (1 - \sigma)\frac{(\Omega_0 \sin \theta)^2}{2} - n^2 \quad ; \quad A_{23} = A_{32} = -n, \tag{5}$$

$$A_{33} = \Omega^2 - h^2 \left((\Omega_0 \sin \theta)^2 + n^2\right)/12 - 1.$$

Asymptotic form of p_s (for $k_0 r \gg 1$):

$$p_s \approx \sqrt{\frac{-2j}{\pi \xi}} e^{-j(k_0 \xi + k_0 z \cdot \sin \theta)} \cdot \Phi_s(\Omega_0, \varphi, \theta),$$

$$\Phi_s(\Omega_0, \varphi, \theta) = \sum_{n \geq 0} \Phi_n = \frac{-2 Z_0}{\pi \Omega_0 \cos \theta} \sum_{n \geq 0} \frac{\delta_n \cdot \cos(n\varphi)}{\left(H_n^{(2)}(\Omega_0 \cos \theta)\right)^2 (Z_{mn} + Z_{sn})}. \tag{6}$$

Shell resonances without shell losses:

Resonance condition: $\text{Im}\{Z_{mn} + Z_{sn}\} = 0.$ \hfill (7)

For $n \geq 2$ the resonances with fluid load are about at the resonances of the shell without fluid load.

Approximation for low frequencies $\Omega_0 \ll 2n + 1$:

$$Z_{sn} \approx \frac{Z_0}{\cos\theta}\left[\frac{4\pi}{(n!)^2}\left(\frac{\Omega_0\cos\theta}{2}\right)^{2n+1} + j\,\frac{\Omega_0\cos\theta}{n}\right]. \tag{8}$$

Far field angular distribution of radiating mode in resonance:

$$\Phi_n^{res}(\varphi) \approx -\delta_n\,\cos(n\varphi). \tag{9}$$

Scattered far field of the n-th mode in resonance:

$$p_s \approx -\sqrt{\frac{-2j}{\pi\xi}}\,e^{-j\,(k_0\xi + k_0 z \cdot \sin\theta)} \cdot \delta_n\,\cos(n\varphi). \tag{10}$$

Scattering cross section in resonance:

$$Q_s = \frac{2\,\delta_n^2}{\pi\,k_0\cos\theta}\int_0^{2\pi}\cos^2(n\varphi)\,d\varphi = \frac{8}{k_0\cos\theta}. \tag{11}$$

Quality factor q_n of the resonance of the n-th mode (without shell losses):

$$q_n = \frac{\text{Im}\{Z_{sn}\} + \rho h}{\text{Re}\{Z_{sn}\}} = \frac{(n!)^2}{2\pi\,n}\left(\frac{2}{\Omega_0}\right)^{2n}\left(1 + \frac{\rho h}{\rho_0 R}n\right). \tag{12}$$

Shell resonances with shell losses:

With $\quad E \to E \cdot (1 + j\eta); \quad c_D^2 \to c_D^2(1 + j\eta).$ \hfill (13)

Mechanical shell mode impedance:

$$Z_{mn} = j\,\omega\rho h\left[1 - (n^2 - 1)^2\frac{h^2}{12\,R^2}\left(\frac{c_D}{c_0}\right)^2\frac{1}{\Omega_0^2}\right]. \tag{14}$$

Resonances at

$$\Omega_{0,res}^2(n) = \frac{n\,B_n}{1 + n\dfrac{\rho h}{\rho_0 R}} \quad;\quad B_n := \frac{\rho h}{\rho_0 R}\left(\frac{c_D}{c_0}\right)^2\frac{h^2}{12\,R^2}(n^2 - 1)^2. \tag{15}$$

For $n \geq 2$, with losses $Z_{mn,\eta}$, without losses $Z_{mn,0}$:

$$Z_{mn,\eta} \approx Z_{mn,0} + \frac{\eta Z_0 B_n}{\Omega_0}. \tag{16}$$

Ratio of radiation loss to internal loss:

$$\frac{\text{Re}\{Z_{sn}\}}{\text{Re}\{Z_{mn}\}} = \frac{8\pi}{\eta\,(n!)^2}\frac{1}{B_n}\left(\frac{\Omega_0}{2}\right)^{2n+1}. \tag{17}$$

Far field angular distribution in resonance with losses and $\theta = 0$ for $\Omega_{0,res} \ll 1$:

$$\Phi_n^{res} \approx \frac{-2\,\delta_n\,\cos\varphi}{\pi\,(n!/2)^2(2/\Omega_0)^{2(n+1)}\,\eta\,B_n}. \tag{18}$$

Relation to far field angular distribution Φ_{nh} of a hard cylinder:

$$\frac{\Phi_n^{res}}{\Phi_{nh}} = \frac{2}{\eta\left(1 + n\dfrac{\rho h}{\rho_0 R}\right)}. \tag{19}$$

E.17   Plane Wave Backscattering by a Liquid Sphere

▶ *See also:* Johnson (1977)

Consider a fluid sphere with radius a and ρ_1, c_1, k_1 for density, sound speed, free field wave number, respectively, of the sphere fluid in an outer medium with ρ_0, c_0, k_0, respectively. Ratios of densities: $g = \rho_1/\rho_0$; of sound velocities $\gamma = c_1/c_0$.

The backscattering cross section σ for an incident plane wave is:

$$\frac{\sigma}{\pi a^2} = \frac{2}{k_0 a} \left| \sum_{m \geq 0} \frac{(-1)^m (2m+1)}{1 + j \cdot C_m} \right| ,$$

$$C_m = \frac{\dfrac{\alpha'_m}{\alpha_m} \dfrac{y_m(k_0 a)}{j_m(k_1 a)} - \dfrac{\ss_m}{\alpha_m} g\gamma}{\dfrac{\alpha'_m}{\alpha_m} \dfrac{j_m(k_0 a)}{j_m(k_1 a)} - g\gamma} , \qquad (1)$$

$$\alpha_m = m \cdot j_m(k_0 a) - (m+1) \cdot j_{m+1}(k_0 a) \; ; \; \alpha'_m = m \cdot j_m(k_1 a) - (m+1) \cdot j_{m+1}(k_1 a) ,$$

$$\ss_m = m \cdot y_m(k_0 a) - (m+1) \cdot y_{m+1}(k_0 a) \; ; \; \ss'_m = m \cdot y_m(k_1 a) - (m+1) \cdot y_{m+1}(k_1 a)$$
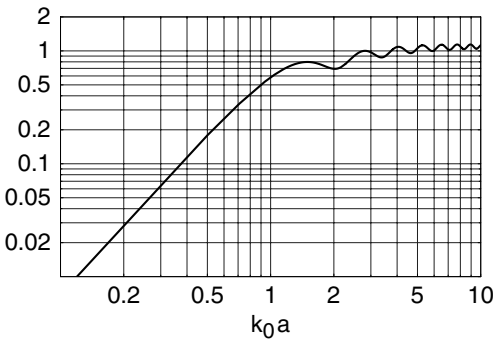
with $j_m(z)$ spherical Bessel functions, $y_m(z)$ spherical Neumann functions.

Approximation for $k_0 a \ll 1$:
$$\frac{\sigma}{\pi a^2} \approx 4 (k_0 a)^4 \left[\frac{1 - g\gamma^2}{3 g\gamma^2} + \frac{1 - g}{1 + 2g} \right]^2 . \qquad (2)$$

Special case: air bubble in water:

$$\frac{\sigma}{\pi a^2} \approx 4 \Big/ \left\{ \left[(f_0/f)^2 - 1 \right]^2 + \delta^2 \right\} \; ; \; f_0 = \frac{1}{2\pi a} \sqrt{3 \kappa P / \rho_0} \qquad (3)$$

with f_0 the first bubble resonance frequency, κ = adiabatic exponent of air, P = static pressure, $\delta \approx 1/5$ an attenuation exponent of the bubble oscillation.


Normalised backscatter cross section $\sigma/(\pi a^2)$ for an air bubble in water (exact form)

E.18   Spherical Wave Scattering at a Perfectly Absorbing Wedge

▶ *See also:* Rawlins (1975)

Attention: The time factor here is $e^{-i\omega t}$. A point source at $Q = \{r_q, \Phi_q, z_q\}$ sends a spherical wave onto a wedge with half wedge angle Ω.

The object treated is an idealised model for an absorbing wedge; the scattered field is half the sum of the fields for a hard and a soft wedge. Thus the wedge here is perfectly absorbing for all directions of incident sound.
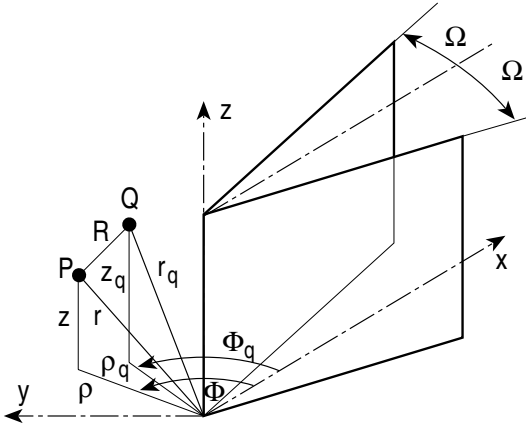
Field composition: $p(\rho, \Phi, z) = p_i(\rho, \Phi, z) + p_s(\rho, \Phi, z)$ (1)

with incident wave $p_i = \dfrac{e^{i k_0 R}}{k_0 R}.$

General solution:

$$p = \frac{1}{2\pi i \nu} \int_{C_1+C_2} \frac{e^{i k_0 R(\alpha)}}{k_0 R(\alpha)} \cdot \cot \frac{\pi - \alpha - \Phi - \Phi_q}{2\nu} \, d\alpha,$$
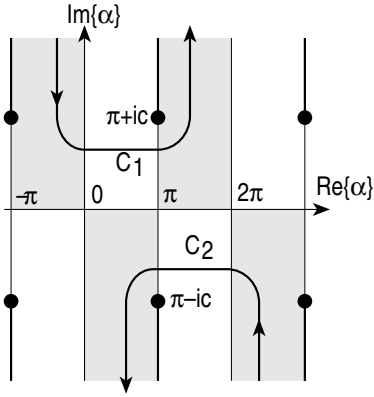
$$R = \sqrt{\rho^2 + \rho_q^2 - 2\rho \rho_q \cos(\Phi - \Phi_q) + (z - z_q)^2},$$

$$R(\alpha) = \sqrt{\rho^2 + \rho_q^2 + 2\rho \rho_q \cos \alpha + (z - z_q)^2},$$

$$\nu = 2(\pi - \Omega)/\pi.$$

(2)

The path of integration circumvents the branch points at $\pi \pm ic$ with

$$c = 2 \cosh^{-1} \frac{R}{2\sqrt{\rho \rho_q}}.$$

(3)

Near field:

$$p = \frac{1}{\nu} \sum_{n \geq 0} \delta_n \cdot \cos \frac{n\,(\Phi - \Phi_q)}{\nu} \cdot S_{n/\nu} \quad ; \quad \delta_0 = 1 \quad ; \quad \delta_{n>0} = 2,$$

$$S_\tau = \frac{i}{2k_0} \int_{-\infty}^{+\infty} e^{i\,t(z-z_q)} \cdot \begin{cases} J_\tau\left(\sqrt{k_0^2 - t^2}\right) \\ H_\tau^{(1)}\left(\sqrt{k_0^2 - t^2}\right) \end{cases} dt \quad ; \quad \begin{cases} \rho < \sqrt{k_0^2 - t^2} \\ \rho > \sqrt{k_0^2 - t^2} \end{cases} \tag{4}$$

with $J_\tau(z)$ = Bessel function; $H_\tau^{(1)}(z)$ = Hankel function of the first kind.
Approximation for $k_0\rho \ll 1$:

$$p \approx \frac{i}{\nu} h_0^{(1)}\left(k_0\sqrt{\rho^2 + \rho_q^2 + (z - z_q)^2}\right)$$

$$+ \frac{2i}{\Gamma(1/\nu)} \left(k_0\rho\rho_q/2\right)^{1/\nu} \cdot \frac{h_{1/\nu}^{(1)}\left(k_0\sqrt{\rho^2 + \rho_q^2 + (z - z_q)^2}\right)}{\left(\rho^2 + \rho_q^2 + (z - z_q)^2\right)^{1/(2\nu)}} \cdot \cos\frac{\Phi - \Phi_q}{\nu} \tag{5}$$

$$+ O\left((k_0\rho)^{\min(2/\nu, 2)}\right)$$

with $h_n^{(1)}(z)$ = spherical Hankel function of the first kind; $\Gamma(z)$ = Gamma function.
Far field, $k_0\rho\rho_q/R_1 \gg 1$:

$$p \approx \sum_{n,m} \frac{e^{i\,k_0 R(\alpha_{nm})}}{k_0 R(\alpha_{nm})} + \left\{V(-\pi - \Phi + \Phi_q) - V(\pi - \Phi + \Phi_q)\right\} \tag{6}$$

with summation over all n, m with $|\Phi - \Phi_q + 2nm\pi\nu| < \pi$, and

$$\alpha_{nm} = \pi - \Phi + \Phi_q - 2nm\pi\nu \quad ; \quad R_1 = \sqrt{(\rho + \rho_q)^2 + (z - z_q)^2},$$

$$V(\text{ß}) = \frac{1}{2\pi\nu} \int_0^\infty \frac{e^{i\,k_0 R(it)}}{k_0 R(it)} \frac{\sin(\text{ß}/\nu)}{\cosh(t/\nu) - \cos(\text{ß}/\nu)} \, dt. \tag{7}$$

Approximation for the scattered far field:

$$p_s \approx \frac{e^{i(k_0 R_1 + \pi/4)}}{\sqrt{2\pi k_0 R_1}} \frac{1}{k_0 \sqrt{\rho \rho_q}} \frac{1}{\nu} \frac{\sin(\pi/\nu)}{\cos(\pi/\nu) - \cos((\Phi - \Phi_q)/\nu)}. \tag{8}$$

E.19 Impulsive Spherical Wave Scattering at a Hard Wedge

▶ *See also:* Biot/Tolstoy (1957), Ouis (1997)

❯ *Sects. E.5 and E.6.* This section will give exact solutions in the time domain for an impulsive point source and approximations for a point source with harmonic signal.

A hard wedge has its apex line on the z axis of a cylindrical co-ordinate system (r, ϑ, z) and its flanks at $\vartheta = 0, \vartheta = \Theta_0$. The wedge may be convex ($\Theta_0 > \pi$) or concave ($\Theta_0 < \pi$).

A point source Q with volume flow q is at $(r_q, \vartheta_q, 0)$; the observer point P is in (r, ϑ, z).
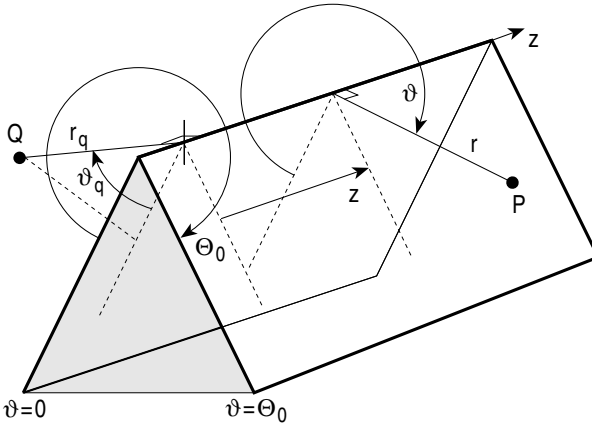
The point source sends a delta pulse $\quad p_q(r') = \frac{\rho_0 q}{4\pi r'} \cdot \delta(t - r'/c_0), \tag{1}$

where t is time; r′ the distance from Q; and $\delta(z)$ is the Dirac delta function.

Composition of the field: $\qquad p = p_q(R_q) + \sum_s p_s(R_s) + p_d, \tag{2}$

where p_q = direct source contribution; p_s = mirror source contribution; p_d = diffracted wave. Some or all of the contributions may vanish, depending on the time interval and the geometrical situation.

In $t < t_0$; $t_0 = R_0/c_0$; $R_0 = \sqrt{(r - r_q)^2 + z^2}$, no signal is received, and $p = 0$.

In $t_0 < t < \tau_0$; $\tau_0 = R_a/c_0$; $R_a = \sqrt{(r + r_q)^2 + z^2}$ the shortest distance between Q and P passing the apex line, only $p_q(R_q)$ and (possibly) mirror source contributions $p_s(R_s)$ are received. $p_q(R_q)$ is obtained by the substitution

$$r' \to R_q = \sqrt{r^2 + r_q^2 + z^2 - 2r\, r_q \cos(\vartheta - \vartheta_q)}$$

in $p_q(r')$, and $p_s(R_s)$ is obtained by a similar substitution in $p_q(r')$ with $r_q \to r_s$; $\vartheta_q \to \vartheta_s$, where r_s, ϑ_s are the co-ordinates of the mirror source.

Mirror sources (of different orders) represent specular reflections at the wedge flanks.

The original source Q and a mirror source S produce a new mirror source at one of the flanks only if they are on the "field side" of that flank (which for that decision is extended to infinity). The black dots represent possible image sources, the open circles are excluded. In general there are conditions in which no image source contribution exists.
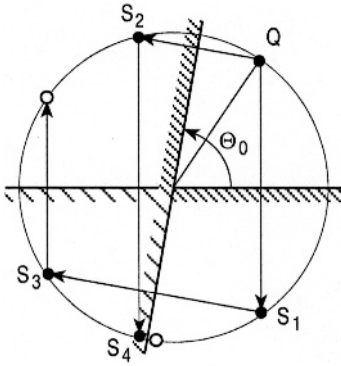
For a contribution $p_s(R_s)$ the condition

$$\arccos \frac{r_s^2 + r_q^2 + z^2 - (c_0 t)^2}{2 r_s r_q} \leq \pi \text{ must hold.} \tag{3}$$

The diffracted wave p_d *in time:*

The diffracted wave is received for $t > \tau_0$. It vanishes if the wedge angle is an integer fraction of π: $\Theta_0 = \pi/m$. Its time function is

$$p_d(t) = \frac{-q Z_0}{4\pi\Theta_0} \cdot \{ß\} \cdot \frac{e^{-\pi y/\Theta_0}}{r\, r_q \cdot \sinh(y)}, \tag{4}$$

$$y = \arccos h \frac{(c_0 t)^2 - (r^2 + r_q^2 + z^2)}{2 r\, r_q},$$

$$\{ß\} = \frac{\sin\left(\pi(\pi \pm \vartheta \pm \vartheta_q)/\Theta_0\right)}{1 - 2e^{-\pi y/\Theta_0} \sin\left(\pi(\pi \pm \vartheta \pm \vartheta_q)/\Theta_0\right) + e^{-2\pi y/\Theta_0}}, \tag{5}$$

where $\{ß\}$ is the sum of terms with the four possible combinations of signs.

E.20 Spherical Wave Scattering at a Hard Screen

▶ *See also:* Biot/Tolstoy (1957), Ouis (1997)

The hard screen is the special case $\Theta_0 = 2\pi$ of the previous ❯ *Sect. E.19.* The diffracted wave $p_d(t)$ in this case can be given an alternative form, valid for $z = 0$ (see sketch in E.19):

$$p_d(t) = \frac{-q\,\rho_0}{4\pi^2 c_0}\sqrt{\frac{t_+^2 - t_-^2}{t^2 - t_+^2}} \cdot \left\{\!\left\{ \frac{\cos\left((\vartheta \pm \vartheta_q)/2\right)}{t^2 - t_+^2 + (t_+^2 - t_-^2)\cos^2\left((\vartheta \pm \vartheta_q)/2\right)} \right\}\!\right\} ;$$

$$t_\pm = (r \pm r_q)/c_0, \tag{1}$$

where $\{\{\ldots\}\}$ is the abbreviation for the sum of two terms corresponding to different signs in the argument of the trigonometric function. This form is suited for the (approximate) Fourier transformation:

$$p_d(\omega) = \int_{\tau_0}^{\infty} p_d(t) \cdot e^{j\omega t}\,dt \quad ; \quad \tau_0 = \frac{r + r_q}{c_0}. \tag{2}$$

Sound field for a harmonic point source:

The sound field for a harmonic point source with angular frequency $\omega = 2\pi f$ is obtained by a Fourier transformation. The contributions p_q, p_s are the values of the spherical wave

$$p(R) = \frac{j\,k_0^2\,qZ_0}{4\pi}\,\frac{e^{-j\,k_0 R}}{k_0 R}, \tag{3}$$

where q is the volume flow amplitude and $R \to R_q; R \to R_s$, respectively (see ❯ *Sect. E.19*).

Approximations of different orders $p_{di}(f)$ will be given below for the diffracted field $p_d(f)$ in the frequency range.

First order: development of $p_d(\tau)$ for $\tau = t - \tau_0 \ll \tau_0$

$$p_{d1}(\omega) = \frac{-q\,\rho_0}{4\pi^2 c_0}\,\frac{1}{\sqrt{2t_+(t_+^2 - t_-^2)}} \cdot \left\{\!\left\{ \frac{1}{\cos\left((\vartheta \pm \vartheta_q)/2\right)} \right\}\!\right\} \frac{1+j}{2\sqrt{f}} \cdot e^{j\,\omega\tau_0}. \tag{4}$$

Second order: in the range of the first order, but improved:

$$p_{d2}(\omega) = \frac{-q\,\rho_0}{4\pi^2 c_0}\sqrt{\frac{t_+^2 - t_-^2}{2t_+}}\,\frac{\pi e^{j\,\omega\tau_0}}{2t_+}$$

$$\cdot \left\{\!\left\{ \frac{\cos\left((\vartheta \pm \vartheta_q)/2\right) \cdot e^{-j\,\omega\,a_\pm}}{\sqrt{a_\pm}} \cdot \operatorname{erfc}\left(\sqrt{-j\,\omega\,a_\pm}\right) \right\}\!\right\} \tag{5}$$

$$a_\pm = (t_+^2 - t_-^2)\cos^2\left((\vartheta \pm \vartheta_q)/2\right)\big/(2t_+) \geq 0$$

with the complementary error function $\operatorname{erfc}(z)$.

Third order: $\tau^2 + 2t_+\tau \ll (t_+^2 - t_-^2)\cos^2\left((\vartheta \pm \vartheta_q)/2\right)$ (6)

$$p_{d3}(\omega) = \frac{-q\,\rho_0}{4\pi^2 c_0}\frac{e^{j\,\omega(\tau_0 - t_+)}}{\sqrt{t_+^2 - t_-^2}} \cdot \left\{\left\{\frac{1}{\cos\left((\vartheta \pm \vartheta_q)/2\right)}\right\}\right\} \cdot K_0\left(-j\,\omega t_+\right)$$ (7)

with $K_0(z)$ the modified Bessel function of the second kind and order zero.

Fourth order: $\sqrt{\tau(\tau + 2t_+)} \approx \sqrt{2t_+\tau}$ (8)

$$p_{d4}(\omega) = \frac{-q\,\rho_0}{4\pi^2 c_0}\sqrt{\frac{t_+^2 - t_-^2}{2t_+}}\frac{\pi\,e^{j\,\omega\tau_0}}{2}$$

$$\cdot\left\{\left\{\frac{\cos\left((\vartheta \pm \vartheta_q)/2\right)}{\sqrt{\Delta_\pm}}\left[\left[\frac{e^{-j\,\omega\tau_{1,2}}}{\sqrt{\tau_{1,2}}}\mathrm{erfc}\left(\sqrt{-j\,\omega\tau_{1,2}}\right)\right]\right]\right\}\right\}$$ (9)

$$\Delta_\pm = t_+^2 - \left(t_+^2 - t_-^2\right)\cos^2\left((\vartheta \pm \vartheta_q)/2\right) \geq 0 \quad ; \quad \tau_{1,2} = t_+ \mp \sqrt{\Delta_\pm} \geq 0,$$ (10)

where $[[\dots]]$ denotes the difference of the term with index 1 minus term with index 2.

Fifth order: after expansion of

$$\frac{1}{\sqrt{\tau + 2t_+}} = \frac{1}{\sqrt{2t_+}}\sum_{n\geq 0}\begin{pmatrix}-1/2\\n\end{pmatrix}\left(\frac{\tau}{2t_+}\right)^n \quad ; \quad \tau \leq 2t_+$$ (11)

and using three series terms:

$$p_{d5}(\omega) = \frac{-q\,\rho_0}{4\pi^2 c_0}\sqrt{\frac{t_+^2 - t_-^2}{2t_+}}\frac{\pi\,e^{j\,\omega\tau_0}}{2}\cdot\left\{\left\{\frac{\cos\left((\vartheta \pm \vartheta_q)/2\right)}{\sqrt{\Delta_\pm}}\right.\right.$$

$$\cdot\left[\left[\left(\frac{1}{\sqrt{\tau_{1,2}}} + \frac{\sqrt{\tau_{1,2}}}{4\,t_+}\right)\cdot e^{-j\,\omega\tau_{1,2}}\mathrm{erfc}\left(-j\,\omega\tau_{1,2}\right) - \frac{1}{4t_+\sqrt{-j\pi\omega}} + \frac{3}{64\pi}\frac{\tau_{1,2}^{3/2}}{t_+^2}\right.\right.$$ (12)

$$\left.\left.\cdot\left(K_0(-j\,\omega\tau_{1,2}/2) - K_1(-j\,\omega\tau_{1,2}/2)\left(1 + \frac{1}{j\,\omega\tau_{1,2}}\right)\right)\right]\right]\right\}\right\}$$

with more terms:

$$p_{d5}(\omega) = \frac{-q\,\rho_0}{4\pi^2 c_0}\sqrt{\frac{t_+^2 - t_-^2}{2t_+}}\frac{\pi\,e^{j\,\omega\tau_0}}{2}\cdot\left\{\left\{\frac{\cos\left((\vartheta \pm \vartheta_q)/2\right)}{\sqrt{\Delta_\pm}}\right.\right.$$

$$\cdot\left[\left[\frac{e^{-j\,\omega\tau_{1,2}}}{\sqrt{\tau_{1,2}}}\cdot\mathrm{erfc}\left(-j\,\omega\tau_{1,2}\right) + \sum_{n\geq 1}\begin{pmatrix}-1/2\\n\end{pmatrix}\frac{1}{(2t_+)^n}\right.$$ (13)

$$\cdot\left((-1)^n\tau_{1,2}^{n-1/2}e^{-j\,\omega\tau_{1,2}}\cdot\mathrm{erfc}\left(\sqrt{-j\,\omega\tau_{1,2}}\right)\right.$$

$$\left.\left.\left.+ 2^{1-n}\sqrt{\frac{2}{\pi}}(-2j\,\omega)^{1/2-n}\sum_{m=0}^{n-1}(2n - 2m - 3)\,!!\cdot(-2j\,\omega\tau_{1,2})^m\right)\right]\right]\right\}\right\}.$$

Sixth order: with development of the fraction in $\{\{\ldots\}\}$ of $p_d(t)$ and $U(a, b; z) = 1/z^a \cdot {}_2F_0(a, 1 + a - b, -1/z)$ the Tricomi function:

$$p_{d6}(\omega) = \frac{-q\,\rho_0}{4\pi^2 c_0}\,\frac{e^{j\,\omega\tau_0}}{\sqrt{t_+^2 - t_-^2}}\sum_{n\geq 0}(-2t_+)^n\Gamma(n + \tfrac{1}{2})\cdot U(n + \tfrac{1}{2}, n + 1; -2j\,\omega t_+)$$

$$\cdot\left\{\left\{\frac{1}{\cos\left((\vartheta \pm \vartheta_q)/2\right)}\sum_{m=0}^{n}\frac{1}{\tau_1^m \cdot \tau_2^{n-m}}\right\}\right\}. \tag{14}$$

E.21 Spherical Wave Scattering at a Cone

The scattering object is a circular cone, infinitely long, with a hard or soft surface. The cone may be tipped with a hard, soft, or absorbing sphere. The incident sound field comes from a point monopole source Q. Plane wave excitation is obtained by letting Q go an infinite distance, combined with Bessel function asymptotics.
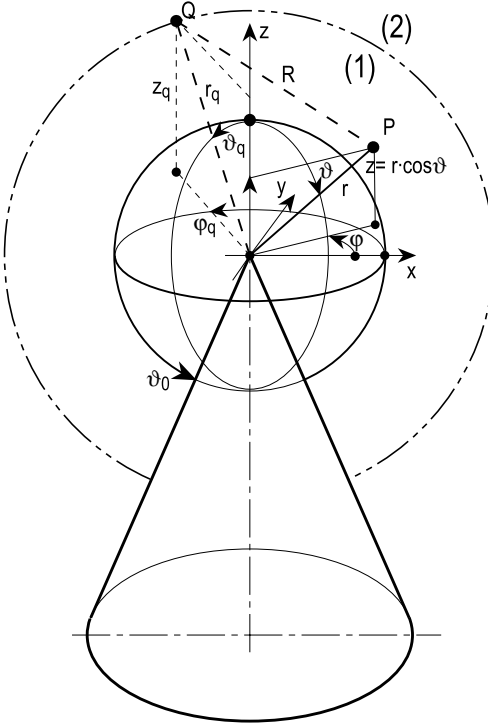
Cone angle $\Theta = \pi - \vartheta_0$. Tipping sphere radius a (≥ 0). Time factor $e^{+j\omega t}$.

Cartesian and spherical co-ordinates of field point $P = (x, y, z) = (r, \varphi, \vartheta)$. Cone tip in origin. Source co-ordinates $Q = (r_q > a, \varphi_q, \vartheta_q \leq \vartheta_0)$.

The sound field is represented by a series of azimuthal and polar modes (eigenfunctions of φ, ϑ; CARSLAW derives an integral representation of the field). Modes of order μ in azimuth φ and order ν in polar angle ϑ are of the form:

$$p_{\mu,\nu}(r, \vartheta, \varphi) = R_\nu(k_0 r) \cdot \Theta_\nu^\mu(\vartheta) \cdot \Phi_\mu(\varphi) \tag{1}$$

The radial factor $R_\nu(k_0 r)$ satisfies the Bessel differential equation and is of the form:

$$\frac{d^2 R_\nu}{dr^2} + \frac{2}{r}\frac{dR_\nu}{dr} + \left(k_0^2 - \frac{\nu(1+\nu)}{r^2}\right) R_\nu = 0 \quad \Rightarrow \quad R_\nu(r) = A \cdot h_\nu^{(1)}(k_0 r) + B \cdot h_\nu^{(2)}(k_0 r) \quad (2)$$

with spherical Hankel functions of the first and second kind: $h_\nu^{(1,2)}(k_0 r) = j_\nu(k_0 r) \pm j \cdot y_\nu(k_0 r)$. The polar factor $\Theta_\nu^\mu(\vartheta)$ satisfies the Legendre differential equation and is of the form:

$$\frac{d^2 \Theta_\nu^\mu}{d\vartheta^2} + \cot\vartheta \frac{d\Theta_\nu^\mu}{d\vartheta} + \left(\nu(1+\nu) - \frac{\mu^2}{\sin^2\vartheta}\right) \Theta_\nu^\mu = 0 \quad \Rightarrow \quad \Theta_\nu^\mu(\vartheta) = P_\nu^\mu(\cos\vartheta) \quad (3)$$

with the associated Legendre functions of the first kind $P_\nu^\mu(\cos\vartheta)$ [the associated Legendre functions of the second kind $Q_\nu^\mu(\cos\vartheta)$ do not appear because they are singular at $\vartheta = 0$]. The identity $P_\nu^\mu(x) = P_{-(\nu+1)}^\mu(x)$ should be noticed. The azimuthal factor $\Phi_\mu(\varphi)$ obeys the differential equation and is of the form:

$$\frac{d^2\Phi}{d\varphi^2} + \mu^2\Phi = 0 \quad \Rightarrow \quad \Phi(\varphi) = A \cdot \cos(\mu\varphi) + B \cdot \sin(\mu\varphi)$$

$$(4)$$

$$= \cos(m(\varphi - \varphi_q)) \ ; \quad m = 0, \pm 1, \pm 2, \ldots.$$

The last form takes into account the field symmetry with respect to $\varphi = \varphi_q$. The mode orders $\mu = m$ are an integer because of the period in φ with $\Delta\varphi = 2\pi$.

The boundary condition at the cone surface for the *hard cone* is zero polar particle velocity v_ϑ at $\vartheta = \vartheta_0$, i.e. with

$$Z_0 v_\vartheta = \frac{j}{k_0} \operatorname{grad}_\vartheta p = \frac{j}{k_0 r}\frac{\partial p}{\partial \vartheta} = j\frac{R_\nu(k_0 r)}{k_0 r}\frac{\partial P_\nu^m(\cos\vartheta)}{\partial\vartheta}$$

$$= -j \sin\vartheta \frac{R_\nu(k_0 r)}{k_0 r}\frac{\partial P_\nu^m(\cos\vartheta)}{\partial(\cos\vartheta)}$$

$$(5)$$

it leads to the *characteristic equation* (mode eigenvalue equation) for eigenvalues ν:

$$P_\nu'^m(\cos\vartheta_0) \xrightarrow[\cos\vartheta_0 \to x_0]{} P_\nu'^m(x_0) \overset{!}{=} 0. \quad (6)$$

The special cases $\vartheta_0 = 0$ and $\vartheta_0 = \pi$ here are irrelevant; a prime indicates the derivative.

In the case of the *soft cone* the condition of zero sound pressure at the cone surface $\vartheta = \vartheta_0$ leads to the following characteristic equation for ν:

$$P_\nu^m(\cos\vartheta_0) \xrightarrow[\cos\vartheta_0 \to x_0]{} P_\nu^m(x_0) \overset{!}{=} 0. \quad (7)$$

Because of $P_0^0(x) = 1$; $P_0^{m>0}(x) \equiv 0$, the value $\nu = 0$ is the trivial solution for the hard cone; it is a forbidden value for the soft cone. Because of the equivalence $\nu \overset{\wedge}{=} -(\nu + 1)$ it is sufficient to consider eigenvalues $\nu > 0$.

The conditions of regularity at $r = 0$, the Sommerfeld far field condition for large r, and the source condition at $r = r_q$ suggest a radial subdivision of the field formulation by

two zones (1) and (2) with their common limit at $r = r_q$ and the field formulations in zone (1):

$$p_1(r, \vartheta, \varphi) = \sum_{\substack{|m| \geq 0 \\ \nu > 0}} A_{\nu m} h_\nu^{(2)}(k_0 r_q) \left[h_\nu^{(1)}(k_0 r) + r_\nu \cdot h_\nu^{(2)}(k_0 r) \right] \tag{8}$$
$$\cdot P_\nu^m(\cos \vartheta) \cos(m(\varphi - \varphi_q)),$$

and in zone (2):

$$p_2(r, \vartheta, \varphi) = \sum_{\substack{|m| \geq 0 \\ \nu > 0}} A_{\nu m} h_\nu^{(2)}(k_0 r) \left[h_\nu^{(1)}(k_0 r_q) + r_\nu \cdot h_\nu^{(2)}(k_0 r_q) \right] \tag{9}$$
$$\cdot P_\nu^m(\cos \vartheta) \cos(m(\varphi - \varphi_q)).$$

The summation index $|m| > 0$ indicates that both signs of $m = \pm 1, \pm 2, \dots$ must be considered although the sign has no influence on the azimuthal factor, but it has an important influence on the polar eigenvalues $\nu(\pm m)$, and therefore on $P_{\nu(\pm m)}^{\pm m}(x)$ (see below).

The factors r_ν in (8) and (9) are the modal reflection factors of the sphere around the cone tip. They are for a sphere surface with admittance G:

$$r_\nu = -\frac{j Z_0 G h_\nu^{(1)}(k_0 a) - h_\nu'^{(1)}(k_0 a)}{j Z_0 G h_\nu^{(2)}(k_0 a) - h_\nu'^{(2)}(k_0 a)}$$
$$= -\frac{\left[j Z_0 G - (\nu/k_0 a) \right] h_\nu^{(1)}(k_0 a) + h_{\nu+1}^{(1)}(k_0 a)}{\left[j Z_0 G - (\nu/k_0 a) \right] h_\nu^{(2)}(k_0 a) + h_{\nu+1}^{(2)}(k_0 a)}. \tag{10}$$

The special cases of a hard sphere, $G = 0$, and of a soft sphere, $|G| = \infty$, lead to:

$$r_\nu \xrightarrow[G \to 0]{} -\frac{h_\nu'^{(1)}(k_0 a)}{h_\nu'^{(2)}(k_0 a)} \quad ; \quad r_\nu \xrightarrow[|G| \to \infty]{} -\frac{h_\nu^{(1)}(k_0 a)}{h_\nu^{(2)}(k_0 a)} \xrightarrow[k_0 a \to 0]{} 1. \tag{11}$$

The modal amplitudes $A_{\nu m}$ in (8) and (9) are determined from the *source condition*, which fits the step of the radial volume flow at $r = r_q$ to the volume flow q of the point source:

$$v_{r2}(r_q + 0) - v_{r1}(r_q - 0) \overset{!}{=} q \cdot \frac{\delta(\vartheta - \vartheta_q)}{h_2} \cdot \frac{\delta(\varphi - \varphi_q)}{h_3} = q \cdot \frac{\delta(\vartheta - \vartheta_q)}{r_q} \cdot \frac{\delta(\varphi - \varphi_q)}{r_q \cdot \sin \vartheta_q} \tag{12}$$

with the Dirac delta functions $\delta(\dots)$ and the scale factors $h_2 = r_q$; $h_3 = r_q \sin \vartheta_q$ of the transformation betwen the Cartesian and the spherical co-ordinates. The factors on the right-hand side will be expanded in polar and in azimuthal modes, respectively:

$$\frac{\delta(\varphi - \varphi_q)}{r_q \cdot \sin \vartheta_q} = \sum_{m \geq 0} c_m \cos(m(\varphi - \varphi_q)) \quad ; \quad \frac{\delta(\vartheta - \vartheta_q)}{r_q} = \sum_{\nu > 0} b_\nu P_\nu^m(\cos \vartheta). \tag{13}$$

The coefficients are:
$$c_m = \frac{1}{M_m \, r_q \, \sin \vartheta_q} \tag{14}$$

with the azimuthal mode norms

$$M_m = \int_0^{2\pi} \cos^2(m(\varphi - \varphi_q)) \, d\varphi = \frac{2\pi}{\delta_m} \; ; \; \delta_m = \begin{cases} 1 \; ; \; m = 0 \\ 2 \; ; \; |m| > 0 \end{cases} \tag{15}$$

from the orthogonal integrals

$$\int_0^{2\pi} \cos(m(\varphi - \varphi_q)) \cdot \cos(m'(\varphi - \varphi_q)) \, d\varphi = \begin{cases} 0 \; ; \; m \neq m' \text{ integer} \\ M_m \; ; \; m = m' \text{ integer} \end{cases} \tag{16}$$

and
$$b_\nu = \frac{\sin \vartheta_q}{N_\nu^m \, r_q} P_\nu^m(\cos \vartheta_q) \tag{17}$$

with the polar mode norms N_ν^m from the integrals

$$\int_0^{\vartheta_0} P_\nu^m(\cos \vartheta) \cdot P_{\nu'}^m(\cos \vartheta) \, \sin \vartheta \, d\vartheta$$

$$\xrightarrow[\substack{dx = -\sin \vartheta \, d\vartheta \\ x_0 = \cos \vartheta_0}]{x = \cos \vartheta} \quad - \int_1^{x_0} P_\nu^m(x) \cdot P_{\nu'}^m(x) \, dx = \begin{cases} 0 \; ; \; \nu \neq \nu' \\ N_\nu^m \; ; \; \nu = \nu' \end{cases}. \tag{18}$$

The source condition (12), when applied term-wise, gives:

$$j \, A_{\nu m} \left\{ h_\nu^{(1)}(k_0 r_q) \, h_\nu'^{(2)}(k_0 r_q) - h_\nu'^{(1)}(k_0 r_q) \, h_\nu^{(2)}(k_0 r_q) \right\} = \frac{Z_0 q}{N_\nu^m \cdot M_m \, r_q^2} P_\nu^m(\cos \vartheta_q), \tag{19}$$

where the brackets $\{\dots\}$ contain the Wronski determinant of the spherical Hankel functions:

$$W\left(h_\nu^{(1)}(k_0 r_q), \, h_\nu^{(2)}(k_0 r_q)\right) = \frac{-2j}{(k_0 r_q)^2}. \tag{20}$$

Thus, the amplitudes $A_{\nu m}$ in (8) and (9) will become:

$$A_{\nu m} = \frac{k_0^2 Z_0 \, q}{2 \, N_\nu^m \cdot M_m} P_\nu^m(\cos \vartheta_q) = \frac{k_0^2 Z_0 \, q}{4\pi} \frac{\delta_m}{N_\nu^m} P_\nu^m(\cos \vartheta_q). \tag{21}$$

A useful modification of field formulations (8) and (9) is obtained by the identical substitutions of r_ν with C_ν:

$$r_\nu = 1 + (r_\nu - 1) = 1 - 2C_\nu \quad \Rightarrow \quad 2C_\nu = 1 - r_\nu, \tag{22}$$

together with the relations between spherical Hankel and Bessel and Neumann functions: $h_\nu^{(1,\,2)}(z) = j_\nu(z) \pm j \cdot y_\nu(z)$, giving the intermediate result:

$$
2C_\nu = \frac{j\,Z_0G\,h_\nu^{(2)}(k_0a) - h_\nu'^{(2)}(k_0a) + j\,Z_0G\,h_\nu^{(1)}(k_0a) - h_\nu'^{(1)}(k_0a)}{j\,Z_0G\,h_\nu^{(2)}(k_0a) - h_\nu'^{(2)}(k_0a)}
$$

$$
= 2\frac{j\,Z_0G\,j_\nu(k_0a) - j_\nu'(k_0a)}{j\,Z_0G\,h_\nu^{(2)}(k_0a) - h_\nu'^{(2)}(k_0a)},
$$

(23)

from which follow the special cases:

$$
C_\nu \xrightarrow[G\to 0]{} \frac{j_\nu'^{(1)}(k_0a)}{h_\nu'^{(2)}(k_0a)} \quad ; \quad C_\nu \xrightarrow[|G|\to\infty]{} \frac{j_\nu^{(1)}(k_0a)}{h_\nu^{(2)}(k_0a)} \quad ; \quad C_\nu \xrightarrow[k_0a\to 0]{} 0.
$$

(24)

With these amplitudes and $r_\nu = 1 - 2C_\nu$, the sound fields in (1) and (2) finally are

$$
p_1(r, \vartheta, \varphi) = \frac{k_0^2 Z_0\,q}{2\pi} \sum_{\substack{|m| \geq 0 \\ \nu > 0}} \frac{\delta_m}{N_\nu^m} h_\nu^{(2)}(k_0r_q) \left[j_\nu(k_0r) - C_\nu \cdot h_\nu^{(2)}(k_0r) \right]
$$

$$
\cdot P_\nu^m(\cos \vartheta_q)\, P_\nu^m(\cos \vartheta)\, \cos(m(\varphi - \varphi_q)) = p_{1,\,\text{cone}} + p_{1,\,\text{sphere}};
$$

(25)

$$
p_2(r, \vartheta, \varphi) = \frac{k_0^2 Z_0\,q}{2\pi} \sum_{\substack{|m| \geq 0 \\ \nu > 0}} \frac{\delta_m}{N_\nu^m} h_\nu^{(2)}(k_0r) \left[j_\nu(k_0r_q) - C_\nu \cdot h_\nu^{(2)}(k_0r_q) \right]
$$

$$
\cdot P_\nu^m(\cos \vartheta_q)\, P_\nu^m(\cos \vartheta)\, \cos(m(\varphi - \varphi_q)) = p_{2,\,\text{cone}} + p_{2,\,\text{sphere}}.
$$

(26)

The first terms in the brackets […] describe the sound fields in each zone including the scattered field from the cone. The second terms describe the additional scattering by the tip sphere; they vanish when the sphere disappears, $k_0a \to 0$ [see (24)]. The amplitude factor in front of the sum supposes a point source with a volume flow q.

Results (25) and (26) and their derivation so far are quite normal. The problems begin with the numerical application by difficulties in the *determination of the polar eigenvalues ν* (because modes of associated Legendre functions have a steady transition to useless trivial solutions for positive integer azimuthal mode numbers m) and continue in the *evaluation of the polar mode norms N_ν^m* by numerical integrations of (18) because of the extremely large variation with m of the order of magnitude of the oscillating associated Legendre functions $P_\nu^m(x)$.

An analytical description of the polar mode norm

$$
N_\nu^m = - \int_1^{\cos \vartheta_0} \left(P_\nu^m(x) \right)^2 dx
$$

(27)

follows from the orthogonal integral:

$$
\int_\alpha^\beta P_\nu^\mu(x) \cdot P_\sigma^\mu(x)\, dx = \frac{\left[(1 - x^2) \left(P_\nu^\mu(x) \cdot P_\sigma'^\mu(x) - P_\nu'^\mu(x) \cdot P_\sigma^\mu(x) \right) \right]_\alpha^\beta}{(\nu - \sigma)(1 + \nu + \sigma)},
$$

(28)

which with mode solutions obeying the boundary conditions of eq. (6) or (7) vanishes for different mode numbers ν, σ. For equal mode numbers $\nu = \sigma$ in the norm integral it is evaluated as a limit ($x_0 = \cos \vartheta_0$, a prime for the derivative):

$$N_\nu^m = -(1 - x_0^2) \lim_{\sigma \to \nu} \frac{P_\nu^m(x_0) \cdot P_\sigma'^m(x_0) - P_\nu'^m(x_0) \cdot P_\sigma^m(x_0)}{(\nu - \sigma)(1 + \nu + \sigma)} \qquad (29)$$

or, with the recursion for the derivative:

$$-(1 - x^2)P_\nu'^\mu(x) = \mu x P_\nu^\mu(x) + \sqrt{1 - x^2}P_\nu^{\mu+1}(x), \qquad (30)$$

one gets a limit representation:

$$N_\nu^m = \sqrt{1 - x_0^2} \lim_{\sigma \to \nu} \frac{P_\nu^m(x_0) \cdot P_\sigma^{m+1}(x_0) - P_\nu^{m+1}(x_0) \cdot P_\sigma^m(x_0)}{(\nu - \sigma)(1 + \nu + \sigma)}. \qquad (31)$$
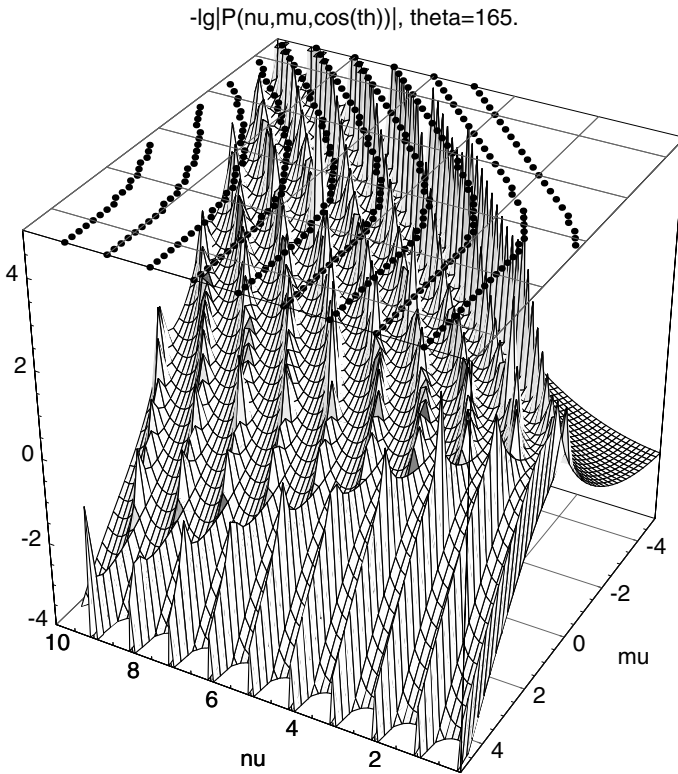
Numerical application of (29) and (31) requires the availability of precisely computing programs for associated Legendre functions.

E.22   Polar Mode Numbers at a Soft Cone

The characteristic equation for polar mode numbers ν at a cone with soft surface at polar angle $\vartheta = \vartheta_0$ (see ▶ *Sect. E.21*) is:

$$P_\nu^m(\cos \vartheta_0) \xrightarrow[\cos \vartheta_0 \to x_0]{} P_\nu^m(x_0) \overset{!}{=} 0 \quad \text{with integer m} = 0, \pm 1, \pm 2, \ldots \qquad (1)$$

The difficulties with the evaluation of polar mode numbers ν may be illuminated by the fact that for positive integers m and n the associated Legendre functions are identically zero, $P_n^m(x) \equiv 0$ for $m > n$, and they are constant for $m = n$. When $m > n$, eq. (1) holds, but $P_n^m(x)$ then does not represent a mode since it is a trivial solution. Because there are no other solutions ν for $m > 0$ and $\nu < m$, the transition between modes and trivial solutions is steady.

-lg|P(nu,mu,cos(th))|, theta=165.

$-\lg\left|P_\nu^\mu(\cos\vartheta)\right|$ over ν and μ, for $\vartheta = 165°$. Equivalences in the plot labels:
nu $\to \nu$; mu $\to \mu$; theta $\to \vartheta$;   P(nu, mu, cos(th)) $\to P_\nu^\mu(\cos\vartheta)$

For getting an overall view of the space μ, ν of mode solutions the magnitude $|P_\nu^\mu(\cos\vartheta)|$ is 3D-plotted over μ, ν for constant values of ϑ (indeed, the negative common logarithm $-\lg|P_\nu^\mu(\cos\vartheta)|$ is plotted, so that zeros are visible as crests). The mesh points of the crests (i.e. the solutions) are collected in the roof plane of the enclosing cube of the 3D-plot. The diagram above is an example for $\vartheta = 165°$. The large variation of the order of magnitude with μ and the change of the structure of the function for $\nu > \mu$ are clearly visible.

The next plot combines points of mode solutions $\nu(\mu)$ from the level plot with straight approximation lines suited for the evaluation of approximations as starters to Muller's numerical solution method for the characteristic equation (see ❯ *Sect. J.4* "Lined ducts, general").

nu(mu), soft; theta=165.
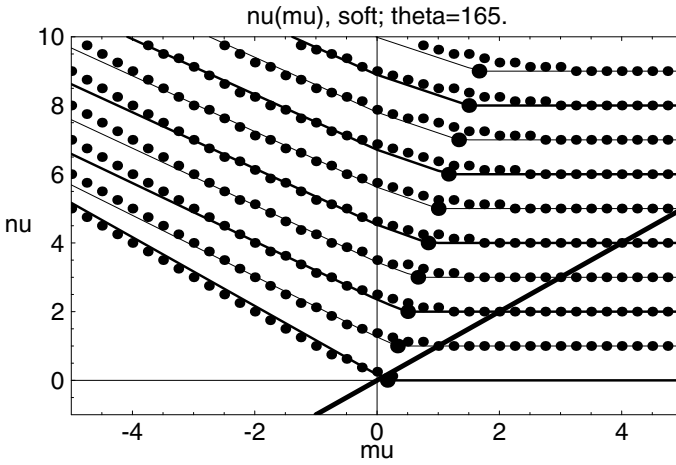
Points of solutions (μ, ν) from the 3D-level plot for $\vartheta = 165°$, and straight lines of approximation (see below). The thick points mark the values for which the solutions approach $\nu(\mu) \approx \mu$; the thick inclined line through the origin represents $\nu = \mu$

The solution point curves will be enumerated with $k = 0, 1, 2, \ldots$ from low to high; $k = 0$ belongs to the lowest curve ending near $(\mu, \nu) = (0, 0)$. The approximations are composed of three line sections in the ranges $\mu \leq 0, 0 < \mu \leq \mu_2, \mu > \mu_2$, respectively, where μ_2 belongs to the "thick points" in the plot. The approximations are evaluated according to the following table:

ϑ_0	$\mu \leq 0$	$0 < \mu \leq \mu_2$	$\mu > \mu_2$
$90° < \vartheta_0 \leq 145°$	$\nu_{ap}(\mu)$	$\nu_{ap}(\mu)$	$\nu(\mu) = k$
$145° < \vartheta_0 \leq 170°$	$\left(\nu_{ap}(\mu) + \nu_{ap_1}(\mu)\right)/2$	$\nu_{ap}(\mu)$	$\nu(\mu) = k$
$170° \leq \vartheta_0$	$\nu_{ap_1}(\mu)$	$\nu_{ap}(\mu)$	$\nu(\mu) = k$

with the endpoints (μ_1, ν_1) on the axis $\mu = 0$, and (μ_2, ν_2) marking the transition to constant values $\nu \approx k$ ("thick points"):

- Endpoint on the axis $\mu = 0$:

$$
\begin{cases}
\mu_1 = 0 \\
\nu_1 = k \cdot \pi/\vartheta_0 - \mu_1 + 2(1 - \vartheta_0/\pi)
\end{cases}
\xrightarrow[\mu_1 \to \mu]{} \nu_{ap1}(\mu);
\tag{2}
$$

- Transition point to $\nu_{ap2}(\mu) = k = \text{const.}; k = 0, 1, 2, \ldots$

$$
\begin{cases}
\mu_2 = 2(1 - \vartheta_0/\pi)(1 + k) \\
\nu_2 = k
\end{cases}
\xrightarrow[\mu > \mu_2]{} \nu_{ap2}(\mu) = k;
\tag{3}
$$

- Connection of the points (μ_1, ν_1) and (μ_2, ν_2):

$$\nu_{ap}(\mu) = \nu_2 + (\nu_1 - \nu_2) \cdot (\mu - \mu_2)/(\mu_1 - \mu_2). \tag{4}$$

These approximations are safe starters to Muller's procedure for a set of mode solutions (in contrast to approximations published in the literature or produced by widely distributed mathematical computer applications) if the (small) increments applied to them for the second and third Muller starters are taken in directions for partial compensation for the deviations to solution points for which the plot above is typical.

Analytical approximations to mode solutions for a soft cone, usable as start solutions in Muller's procedure, are obtained from the series representation of the associated Legendre functions in (1) for $\mu \to m$, integer:

$$P_\nu^m(x) = \frac{(-1)^m}{2^m\, m!} \frac{\Gamma(\nu + m + 1)}{\Gamma(\nu - m + 1)} (1 - x^2)^{m/2} \,_2F_1\, (m + \nu + 1 \, , \; m - \nu; \; m + 1; \; (1 - x)/2) \tag{5}$$

with the hypergeometric function $\quad _2F_1\,(a_1, \; a_2; \; b_1; \; z) = \sum_{k=0}^{\infty} \frac{(a_1)_k \cdot (a_2)_k}{k!\,(b_1)_k}\, z^k \tag{6}$

containing the recursively evaluated Pochhammer symbols (k, n = integers; a = real):

$$(a)_0 = 1 \; : \; (a)_k = a \cdot (a + 1) \cdot \ldots \cdot (a + k - 1)$$

$$= (a)_{k-1} \cdot (a + k - 1) = \Gamma(a + k)/\Gamma(a) \; ; \; k \geq 1, \tag{7}$$

$$(n)_k = \frac{(n + k - 1)!}{(n - 1)!} \xrightarrow[n \to 2]{} (1 + k)!.$$

For negative integer orders $\mu \to -m$ holds:

$$P_\nu^{-m}(\cos \vartheta) = (-1)^m \frac{\Gamma(\nu - m + 1)}{\Gamma(\nu + m + 1)} P_\nu^m(\cos \vartheta) = 0, \tag{8}$$

and therefore, with (5), the characteristic equation for eigenvalues ν of soft cones then is:

$$P_\nu^{-m}(\cos \vartheta) = \frac{(1 - x^2)^{m/2}}{2^m\, m!} \,_2F_1\, (m + \nu + 1 \, , \; m - \nu; \; m + 1; \; (1 - x)/2) \,. \tag{9}$$

Truncation of the series returns a polynomial in ν whose solutions may be used as approximations to mode numbers ν. Some of the polynomial solutions may appear several times, while others may be complex; they should be excluded from application as starters of Muller's procedure.

An important decision is the limit μ up to which azimuthal mode numbers $\mu = m > 0$ can be used in a modal field synthesis so that trivial solutions are avoided in the field series. From numerical investigations one can derive the recommendation for a soft cone:

$$\mu \leq Min(k, \mu_2) = Min(k, 2(1 + k)(1 - \vartheta_0/\pi)). \tag{10}$$

E.23   Polar Mode Numbers at a Hard Cone

The characteristic equation for mode eigenvalues ν is:

$$P_\nu'^{\,m}(\cos \vartheta_0) = 0 \ ; \quad \nu > 0 \ ; \quad m = 0, \pm 1, \pm 2, \dots . \tag{1}$$
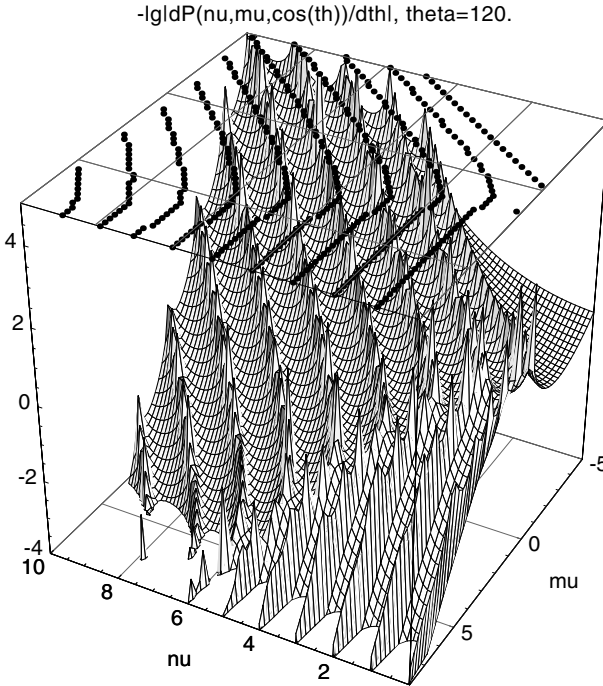
The derivative may be evaluated with the recursion

$$\frac{d\, P_\nu^\mu(\cos \vartheta)}{d\vartheta} = P_\nu^{\mu+1}(\cos \vartheta) + \mu \, \cot \vartheta \, P_\nu^\mu(\cos \vartheta), \tag{2a}$$

$$\frac{d\, P_\nu^\mu(x)}{dx} = -\frac{1}{\sqrt{1 - x^2}} P_\nu^{\mu+1}(x) - \mu \frac{x}{1 - x^2} P_\nu^\mu(x). \tag{2b}$$

Reliable starters for Muller's equation solver procedure can be obtained from 3D-survey plots of $-\lg \left| \partial P_\nu^\mu(\cos \vartheta)/\partial\vartheta \right|$ over ν and μ for a fixed parameter ϑ. Solutions therein are marked by maxima which arrange in crests. These solutions (μ, ν) are collected as points in the roof plane of the enclosing cube of the 3D-plot. The following example is for $\vartheta = 120°$.

Equivalences in the plot labels: nu $\to \nu$; mu $\to \mu$; theta $\to \vartheta$;

$$P(\text{nu, mu, } \cos(\text{th})) \to P_\nu^\mu(\cos \vartheta).$$

-lg|dP(nu,mu,cos(th))/dth|, theta=120.

$-\lg \left| \partial P_\nu^\mu(\cos \vartheta)/\partial\vartheta \right|$ over ν and μ for $\vartheta = 120°$

The next plot combines points of mode solutions $\nu(\mu)$ from the level plot with straight approximation lines suited for the evaluation of approximations as starters to Muller's

numerical solution method for the characteristic equation (see ❯ *Sect. J.4*, "Lined ducts, general").

nu(mu), hard; theta=120.
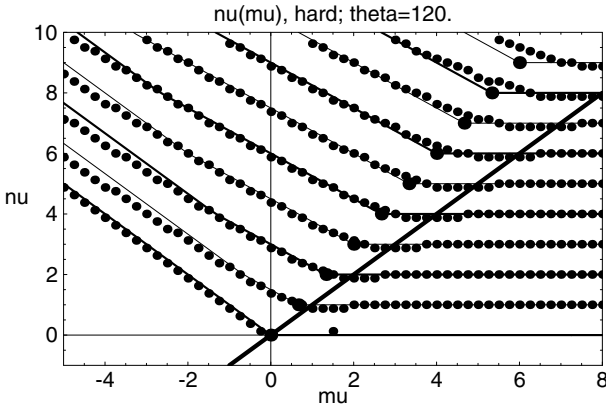
Points of solution (μ, ν) from the 3D-plot for $\vartheta = 120°$ of a hard cone, and straight lines of approximation

The structure of the approximations is shown in the next graph. The sequences (curves) of the solution points are enumerated from low to high with $k = 0, 1, 2, \ldots$. The approximation lines are composed of line sections (a), (b), (c), (d) through endpoints (0), (1), (2).
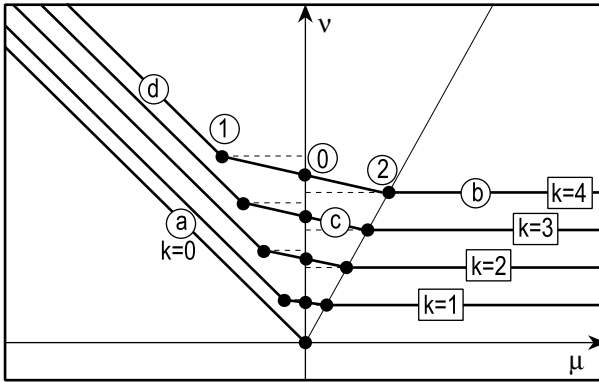
Construction of the straight approximations to the moden solutions $\nu(\mu)$ for a hard cone

<u>Points:</u>

(0): Value of ν_{ap1} at $\mu = 0$: $\nu_{ap1}(0) = k \cdot \pi/\vartheta$: $(\mu_0, \nu_0) = (0, k \cdot \pi/\vartheta)$

(2): $(\mu_2, \nu_2) = (2k(1 - \vartheta/\pi), k)$ (3)

(1): Extension of the line $(\mu_2, \nu_2) \rightarrow (\mu_0, \nu_0)$ to $\mu = -\mu_2$:

$$\left(\mu_1, \nu_1\right) = \left(-\mu_2, \ \left(k + \mu_2/2\right) \cdot \pi/\vartheta\right)$$

Sections:

(a): $\nu(\mu) = \nu_{ap1} = k \cdot \pi/\vartheta - \mu \xrightarrow[k=0]{} -\mu \ ; \ k = 0 \ ; \ \mu < 0$

(b): $\nu(\mu) = \nu_{ap2} = k; \quad k = 1, 2, 3, \ldots \ ; \ \mu \geq \mu_2$

(c): Connection between (1) & (2); $\mu_1 \leq \mu \leq \mu_2$:

$$\nu(\mu) = \nu_{ap} = \nu_0 + (\nu_2 - \nu_0) \frac{\mu - \mu_0}{\mu_2 - \mu_0} = \left(k - \mu/2\right) \cdot \pi/\vartheta \tag{4}$$

(d): Straight line through (1) with slope of ν_{ap1}; $\quad \mu < \mu_1$:

$$\nu(\mu) = \nu_{ap3} = \nu_1 - \left(\mu - \mu_1\right)$$

Special case $\mu = m = 0$ for a hard cone:

Then the characteristic equation:

$$\begin{aligned}
\frac{d\,P_\nu(x_0)}{dx} &= \frac{1}{2}(\nu + 1)\,\nu\,{}_2F_1\left(2 + \nu,\ 1 - \nu;\ 2;\ (1 - x_0)/2\right) \\[4pt]
&= \frac{1}{2}(\nu + 1)\,\nu \sum_{k=0}^{\infty} \frac{(2 + \nu)_k \cdot (1 - \nu)_k}{2^k k!\,(1 + k)!}\,(1 - x_0)^k \stackrel{!}{=} 0
\end{aligned} \tag{5}$$

can be formulated with the hypergeometric function

$$_2F_1\left(a_1,\ a_2;\ b_1;\ z\right) = \sum_{k=0}^{\infty} \frac{(a_1)_k \cdot (a_2)_k}{k!\,(b_1)_k}\,z^k \tag{6a}$$

containing Pochhammer's symbols:

$$(a)_0 = 1 \ : \ (a)_k = a \cdot (a+1) \cdot \ldots \cdot (a+k-1) = (a)_{k-1} \cdot (a+k-1) = \Gamma(a+k)/\Gamma(a) \ ; \ k \geq 1. \tag{6b}$$

Truncation of the series will return a polynomial equation in ν. The factor $(\nu + 1)\nu$ in front of the polynomial produces the solution $\nu = 0$ and the equivalent solution $-(1 + \nu) = -1$. Expansion up to the fourth degree gives the following approximations (of moderate precision; $x_0 = \cos\vartheta_0$):

$$\nu \approx -\frac{(1 - x_0) \pm \sqrt{(1 - x_0)^2 + 4(1 - x_0)\left(10 - 4x_0 \pm 2\sqrt{4 - 8x_0 + x_0^2}\right)}}{2\,(1 - x_0)}. \tag{7}$$

As the upper limit $\mu = m > 0$ up to which azimuthal mode numbers m can be used in a modal field synthesis so that trivial solutions are avoided in the field series one can recommend for a hard cone:

$$\mu \leq \text{Min}(k, \mu_2) = \text{Min}(k, 2k(1 - \vartheta_0/\pi)). \tag{8}$$

The next 3D-plot shows φ-orbits (thick) for the sound pressure magnitude $|p(r, \vartheta, \varphi)/p_Q(0)|$ with fixed $\vartheta = \vartheta_0 = 145°$, i.e. immediately on the hard cone surface, for some values of k_0r. The sound pressure is plotted as radial distance from the orbit circle (thin). The point source Q (thick point) is placed at the height of the cone tip ($\vartheta_q = 90°$) at a radial distance $k_0r_q = 12$. (Naming equivalences in the plot label: $|p(phi)/pQ(0)| \rightarrow |p(r, \vartheta, \varphi)/p_Q(0)|$; tha0 $\rightarrow \vartheta_0$; k0rq $\rightarrow k_0r_q$; thaq $\rightarrow \vartheta_q$).
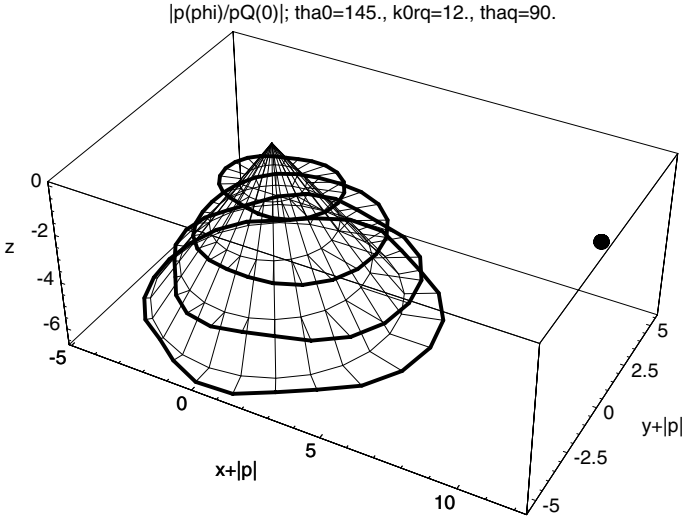
$|p(\varphi)/pQ(0)|$ on φ-orbit for point source Q at $(k_0r_q, \vartheta_q, \varphi_q = 0)$ near a hard cone with $\vartheta_0 = 145°$; field point $P = (k_0r, \vartheta, \varphi)$ parameter values: $\vartheta_0 = 145.°$; $k_0r = 2. \& 4. \& 6. \& 8.$; $\vartheta = 145.°$; $k_0r_q = 12.$; $\vartheta_q = 90.°$; $\varphi_q = 0.$; $k_{hi} = 6$; $\mu_{lo} = -8$; $\Delta\varphi = 15.°$
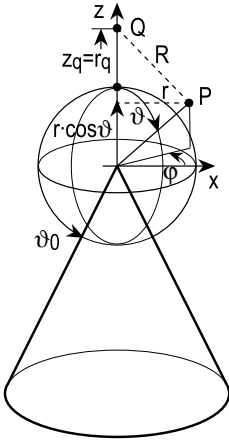
E.24   Scattering at a Cone with Axial Sound Incidence

This section treats a special case with axial sound incidence, $\vartheta_q = 0$, $\varphi_q = 0$, of the preceding sections on sound scattering at a cone (see those sections for definitions of symbols). This special case avoids some analytical and numerical difficulties of the more general task. The associated Legendre functions go over to the Legendre functions, $P_\nu^\mu(x) \xrightarrow[\mu=0]{} P_\nu(x)$; $P_\nu(1) = 1$.

Mode series for the sound field in zones (1) and (2) with common boundary at the radius $r = r_q$ of the point source with its strength defined by volume flow q ($k_0 = \omega/c_0$; $Z_0 = \rho_0c_0$):

$$p_1(r, \vartheta, \varphi) = \frac{k_0^2 Z_0\, q}{2\pi} \sum_{\nu>0} \frac{1}{N_\nu}\, h_\nu^{(2)}(k_0r_q) \left[j_\nu(k_0r) - C_\nu \cdot h_\nu^{(2)}(k_0r)\right] \cdot P_\nu(\cos\vartheta),$$

$$p_2(r, \vartheta, \varphi) = \frac{k_0^2 Z_0\, q}{2\pi} \sum_{\nu>0} \frac{1}{N_\nu}\, h_\nu^{(2)}(k_0r) \left[j_\nu(k_0r_q) - C_\nu \cdot h_\nu^{(2)}(k_0r_q)\right] \cdot P_\nu(\cos\vartheta),$$

(1a)

and with reference to the source free field pressure $p_Q(0)$ at the origin:

$$\frac{p_1(r, \vartheta, \varphi)}{p_Q(0)} = \frac{2}{h_0^{(2)}(k_0 r_q)} \sum_{v>0} \frac{1}{N_v} h_v^{(2)}(k_0 r_q) \left[j_v(k_0 r) - C_v \cdot h_v^{(2)}(k_0 r) \right] \cdot P_v(\cos \vartheta),$$

$$\frac{p_2(r, \vartheta, \varphi)}{p_Q(0)} = \frac{2}{h_0^{(2)}(k_0 r_q)} \sum_{v>0} \frac{1}{N_v} h_v^{(2)}(k_0 r) \left[j_v(k_0 r_q) - C_v \cdot h_v^{(2)}(k_0 r_q) \right] \cdot P_v(\cos \vartheta). \tag{1b}$$

Eigenvalues (mode numbers) v of the polar modes are solutions of the characteristic equations $P_v(x_0) = 0$ with a soft cone, and $dP_v(x_0)/dx = 0$ with a hard cone; $x_0 = \cos \vartheta_0$ for a cone half-angle ϑ_0. The terms with the factors C_v in the brackets represent the scattered field generated additionally by a sphere of radius a and surface admittance G around the cone tip; they will be dropped if there is no sphere.

$$C_v = \frac{j Z_0 G j_v(k_0 a) - j'_v(k_0 a)}{j Z_0 G h_v^{(2)}(k_0 a) - h'^{(2)}_v(k_0 a)} \tag{2}$$

with special values:

$$C_v \xrightarrow[G \to 0]{} \frac{j'^{(1)}_v(k_0 a)}{h'^{(2)}_v(k_0 a)} \quad ; \quad C_v \xrightarrow[|G| \to \infty]{} \frac{j^{(1)}_v(k_0 a)}{h_v^{(2)}(k_0 a)} \quad ; \quad C_v \xrightarrow[k_0 a \to 0]{} 0. \tag{3}$$

The N_v are the mode norms N_v^m for $m = 0$. One gets by partial integration:

$$N_v = -\int_1^{x_0} (P_v(t))^2 \, dt = \frac{x_0 \cdot (P_v(x_0))^2}{1 + 2v} + \frac{P_{v-1}(x_0) \cdot P_v(x_0)}{1 + 2v}$$

$$+ \frac{v}{1 + 2v} \left[P_v(x_0) \left(\partial P_y(x_0)/\partial y \right)_{y=v-1} - P_{v-1}(x_0) \cdot \left(\partial P_y(x_0)/\partial y \right)_{y=v} \right]. \tag{4}$$

This simplifies in the *case of a soft cone*, because of $P_v(x_0) = 0$, to:

$$N_v = -\int_1^{x_0} (P_v(t))^2 \, dt = \frac{-v}{1 + 2v} P_{v-1}(x_0) \cdot \left(\partial P_y(x_0)/\partial y \right)_{y=v}. \tag{5}$$

Alternatively, evaluation of the mode norm by integration of the product of the series for the Legendre function:

$$P_\nu(x) = {}_2F_1\left(-\nu,\ 1+\nu;\ 1;\ (1-x)/2\right) = \sum_{k\geq 0} \frac{(-\nu)_k\,(1+\nu)_k}{2^k\,(k!)^2}(1-x)^k \tag{6a}$$

will return:

$$N_\nu = -\int_1^{x_0} (P_\nu(x))^2\ dx = \sum_{k,\,\kappa\geq 0} \frac{(-\nu)_k\,(1+\nu)_k}{2^k\,(k!)^2}\,\frac{(-\nu)_\kappa\,(1+\nu)_\kappa}{2^\kappa\,(\kappa!)^2}\,\frac{(1-x_0)^{1+k+\kappa}}{1+k+\kappa}. \tag{6b}$$

The upper summation limits for k and κ must be definitely higher than ν. The convergence becomes slow for $\vartheta_0 \approx \pi$.

Analytical approximations to mode numbers (eigenvalues) ν for a *soft cone* can be obtained by truncation of the series in the characteristic equation:

$$P_\nu(x_0) = P_\nu^0(x_0) = {}_2F_1\left(-\nu,\ 1+\nu;\ 1;\ (1-x_0)/2\right) = \sum_{k\geq 0} \frac{(-\nu)_k\,(1+\nu)_k}{2^k\,(k!)^2}(1-x_0)^k \overset{!}{=} 0, \tag{7}$$

and for a *hard cone* by truncation of:

$$\frac{d\,P_\nu(x_0)}{dx} = \frac{1}{2}(\nu+1)\,\nu\,{}_2F_1\left(2+\nu,\ 1-\nu;\ 2;\ (1-x_0)/2\right)$$

$$= \frac{1}{2}(\nu+1)\,\nu\sum_{k=0}^{\infty} \frac{(2+\nu)_k\cdot(1-\nu)_k}{2^k k!\,(1+k)!}(1-x_0)^k \overset{!}{=} 0. \tag{8}$$

The summation over k must go rather high, because a number of the polynomial solutions ν must be excluded from the application as starters in Muller's procedure, due to multiple solutions, negative values, complex values, or too large magnitudes of the characteristic equations at the polynomial solutions. A "more economic" construction of starters makes use of the construction rules given in ⊙ *Sects. 22 or 23*.

The sound field for axial incidence of a plane wave is obtained by starting with the field in zone (1) from eq. (1b) in the limit $r_q \to \infty$ with asymptotic approximations for the Hankel functions with argument $z = k_0 r_q \to \infty$:

$$H_\sigma^{(2)}(z) \sim \sqrt{2/\pi z}\ e^{-j\,(z-\sigma\pi/2-\pi/4)}; \qquad h_\nu^{(2)}(z) = \sqrt{\pi/2z}\ H_{\nu+1/2}^{(2)}(z) \sim \frac{1}{z}e^{-j\,(z-\nu\pi/2-\pi/2)} \tag{9}$$

$$h_\nu^{(2)}(k_0 r_q)/h_0^{(2)}(k_0 r_q) \sim e^{+j\,\nu\pi/2}$$

leading to [$p_Q(0)$ is the plane wave pressure in the origin]:

$$\frac{p(r,\vartheta,\varphi)}{p_Q(0)} = 2\sum_{\nu>0} \frac{e^{+j\,\nu\pi/2}}{N_\nu}\left[j_\nu(k_0 r) - C_\nu\cdot h_\nu^{(2)}(k_0 r)\right]\cdot P_\nu(\cos\vartheta). \tag{10}$$

References

Biot, M.A.; Tolstoy, I.: Formulation of wave propagation in infinite media by normal coordinates with an application to diffraction. J.Acoust.Soc. Am. **29** 381–391 (1957)

Carslaw, H.S.: The scattering of sound waves by a cone. Math. Annalen **75**, 133–147 (1914)

Johnson, R.K.: J. Acoust. Soc. Amer. **61** 375–377 (1977)

Mechel, F.P.: Schallabsorber, Vol. I, Ch. 6: Cylindrical sound absorbers Hirzel, Stuttgart (1989)

Mechel, F.P. Schallabsorber, Vol. II, Ch. 14: "Characteristic values of composite media" Hirzel, Stuttgart (1995)

Mechel, F.P.: A uniform theory of sound screens and dams. Acta Acustica **83**, 260–283 (1997)

Mechel, F.P.: Mathieu Functions; Formulas, Generation, Use Hirzel, Stuttgart (1997)

Mechel, F.P.: Schallabsorber, Vol. III, Ch. 22: Semicircular absorbing dam on absorbing ground Hirzel, Stuttgart (1998)

Mechel, F.P.: Improvement of corner shielding by an absorbing cylinder. J. Sound Vibr. **219**, 559–579 (1999)

Ouis, D.: Report TVBA-3094, Lund Inst.of Technology Theory and Experiment of the Diffraction by a Hard Half Plane (1997)

Paniklenko, A.P.; Rybak, S.A.: Sov. Phys. Acoust. **30**, 148–151 (1984)

Rawlins: J.Sound Vibr. **41**, 391–393 (1975)